

**FINITE ELEMENT MODELLING OF COMPRESSIVE
BEHAVIOR OF BACK TO BACK LIPPED CHANNEL SECTIONS**

by

Md. Abdul Basit

A thesis submitted to the

Department of Civil Engineering

in partial fulfillment for the degree of

MASTER OF SCIENCE IN CIVIL ENGINEERING (STRUCTURAL)

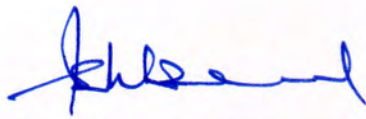


Department of Civil Engineering
Bangladesh University of Engineering and Technology

December 2021

BOARD OF EXAMINERS

The thesis titled “FINITE ELEMENT MODELLING OF COMPRESSIVE BEHAVIOR OF BACK TO BACK LIPPED CHANNEL SECTIONS” submitted by Md. Abdul Basit, Student ID: 0417042301F (Session: April, 2017) has been accepted as satisfactory in partial fulfillment of the requirement for the degree of Master of Science in Civil Engineering (Structural) on 22nd December 2021.



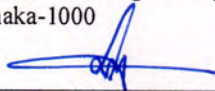
-
1. Dr. Ishtiaque Ahmed
Professor
Department of Civil Engineering
BUET, Dhaka-1000

Chairman
(Supervisor)



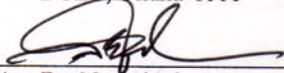
-
2. Dr. Md. Delwar Hossain
Professor and Head
Department of Civil Engineering
BUET, Dhaka-1000

Member
(Ex-Officio)



-
3. Dr. Khan Mahmud Amanat
Professor
Department of Civil Engineering
BUET, Dhaka-1000

Member



-
4. Dr. Nazrul Islam
Associate Professor
Department of Civil Engineering
BUET, Dhaka-1000

Member

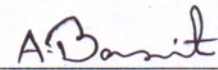


-
5. Dr. Mahmud Ashraf
Associate Professor
School of Engineering
Deakin University
75 Pigdons Road,
Warrn Pond VIC 3216, Australia

Member
(External)

DECLARATION

It is hereby declared that this thesis or any part of it has not been submitted elsewhere for the award of any degree or diploma.



Md. Abdul Basit

Dedicated

to

“My family members”

ACKNOWLEDGEMENTS

The Author sincerely expresses his deepest gratitude to the Almighty Allah.

The Author would like to express sincere gratefulness to Dr. Ishtiaque Ahmed for the guidance, encouragement and numerous hours spent to help in this research work. His contribution as a supervisor is genuinely appreciable. He was also gracious enough in giving enough scope regarding the planning and execution of numerical work. His valuable comments and insights helped to improve the analysis enormously.

The Author conveys the deepest gratitude to Dr. Raquibul Hossain for his unconditional inspiration and supervision to this research at primary stage. His generosity and support will not be forgotten.

Finally, the Author admits the support of Dr. Md. Anwar-Us-Saadat who has helped in this research in many ways.

ABSTRACT

Cold Formed Steel (CFS) as a construction material has many advantages like lightness in weight, no requirement of formwork etc. Because of these reasons use of built-up CFS members are increasing. Although extensive experimental and numerical studies have been carried out by a number of researchers on such sections under compression, limited research work has been reported that investigates the effect of width-to-thickness ratio (b/t) and lip height-to-thickness ratio (c/t) on the strength and stability of such channels under axial compression. Moreover, present design codes like Eurocode (EC), American Iron and Steel Institute (AISI) and the Australian and New Zealand standards (AS/NZ) include limited guidance on the approximation of capacity of built-up CFS columns considering different width-to-thickness ratio and lip height-to-thickness ratio.

This thesis presents a numerical investigation on the behavior of built-up CFS lipped channels considering different width-to-thickness ratios and lip height-to-thickness ratios of different columns. Nonlinear finite element model was developed based on thirty available experimental results considering different material models and geometric imperfections. The axial compression strengths obtained from finite element model shows good agreement with experimental results of previous researchers validating the reliability of the model. A parametric study comprising of total eighty-eight models was then carried out by using the principles of validated model, with various width-to-thickness ratios and lip height-to-thickness ratios for four types of column sections covering a range of lengths (stub, short, intermediate and slender) which has generated sufficient information about the axial strength of such channels. Obtained axial column strengths were compared against the design strengths calculated in accordance with the AISI standard. It was observed that the AISI standard have predicted somewhat higher strength values with respect to finite element results in most of the cases for all four types of columns. A design guideline was proposed through linear regression analysis between FEA and AISI strength and a multiplier of AISI equation for obtaining better strength result is suggested followed by deriving some curves which can be used while predicting the buckling behavior of such channels.

Table of Contents

ABSTRACT	vi
List of Figures	viii
List of Tables	xii
Chapter 1 INTRODUCTION	1
1.1 Background and Motivations	1
1.2 Research Objectives and Overview	2
1.3 Organization of the thesis	2
Chapter 2 LITERATURE REVIEW	4
2.1 Introduction	4
2.2 Advantages of cold-formed steel	5
2.3 Experimental study on axially loaded back to back cold-formed steel channel sections	5
2.4 Numerical research on axially loaded back to back cold-formed steel channel sections	10
2.5 Design guidelines available in different codes	13
2.5.1 BNBC	13
2.5.2 AISI and AS/NZ Standard	13
2.5.3 AISC	15
2.5.4 Eurocode EN 1993-1-3	15
2.5.5 Continuous Strength Method (CSM)	17
Chapter 3 FINITE ELEMENT MODELLING	19
3.1 Introduction	19
3.2 Geometry and material properties	19
3.3 Element type and mesh optimization	23
3.4 Boundary conditions, constraints and load application	25
3.5 Contact modelling	26
3.6 Modelling of local and global geometric imperfections	26
3.7 Verification of finite element model with experimental results	28
Chapter 4 PARAMETRIC STUDY FOR BACK-TO-BACK CFS LIPPED CHANNELS	42
4.1 Introduction	42
4.2 Parametric study	42
4.2.1 Comparison of the FE results with Design Standards	44
4.2.2 Formulation of Design Guideline and Derivation of Design Curves	62
Chapter 5 CONCLUSIONS AND FUTURE WORKS	76
5.1 Conclusions	76
5.2 Recommendations for Future Works	77
REFERENCES	78

List of Figures

Figure 2-1. Different types of Cold-formed steel	4
Figure 2-2. Details of back-to-back built-up cold-formed steel channel-sections	6
Figure 2-3. Variation of strength against modified slenderness	7
Figure 2-4. Typical window framing	9
Figure 2-5. Typical C section	9
Figure 2-6. Built-up batten column section details	11
Figure 2-7. Geometry of a lipped channel section	13
Figure 2-8. Specification of a typical lipped channel	15
Figure 2-9. Reduction factor vs non-dimensional slenderness curve	16
Figure 3-1. Typical cold-formed steel stress-strain curve with definitions of key material parameter	21
Figure 3-2. Full range stress-strain curve for flat and corner zone	23
Figure 3-3. Comparison of FEA strength with experimental strength for different mesh sizes	24
Figure 3-4. Finite element mesh used for verification of the model	24
Figure 3-5. Pin ended boundary condition applied in FE model	25
Figure 3-6. Tied joint and rigid body constraint used in FE model	26
Figure 3-7. Initial imperfection contours for different columns	27
Figure 3-8. Specimen labeling	29
Figure 3-9. Failure pattern of back-to-back built-up lipped channels under axial load	35
Figure 3-10. Comparison of capacity predicted by present model and experimental results for (a) stub column (b) short column (c) intermediate column and (d) slender column	37
Figure 3-11. Comparison of deformed shapes between experimental and FEA	38

Figure 3-12. Comparison of load-displacement curve between experimental and FEA results	38
Figure 3-13. Comparison of capacity vs slenderness ratio curve between experimental and FEA results for (a) stub (b) short (c) intermediate and (d) short column	39
Figure 4-1. Full range stress-strain curve using (a) material 1 (b) material 2	44
Figure 4-2. Von-Mises stress contour at ultimate load for different column	45
Figure 4-3. Comparison of FEA strength with AISI strength for stub column using (a) material 1 (b) material 2	48
Figure 4-4. Comparison of FEA strength with AISI strength for short column using (a) material 1 (b) material 2	52
Figure 4-5. Comparison of FEA strength with AISI strength for intermediate column using (a) material 1 (b) material 2	56
Figure 4-6. Comparison of FEA strength with AISI strength for slender column using (a) material 1 (b) material 2	60
Figure 4-7. Strength vs Slenderness ratio curve for stub (a) material 1 (b) material 2	62
Figure 4-8. Strength vs Slenderness ratio curve for short (a) material 1 (b) material 2	63
Figure 4-9. Strength vs Slenderness ratio curve for intermediate (a) material 1 (b) material 2	64
Figure 4-10. Strength vs Slenderness ratio curve for slender (a) material 1 (b) material 2	65
Figure 4-11. Strength vs Displacement curve for stub column using (a) material 1 (b) material 2	66
Figure 4-12. Strength vs Displacement curve for short column using (a) material 1 (b) material 2	67
Figure 4-13. Strength vs Displacement curve for intermediate column using (a) material 1 (b) material 2	68
Figure 4-14. Strength vs Displacement curve for slender column using (a) material 1 (b) material 2	69
Figure 4-15. Relation between FEA and AISI strength for stub (a) material 1 (b) material 2	72
Figure 4-16. Relation between FEA and AISI strength for short (a) material 1 (b) material 2	73

Figure 4-17. Relation between FEA and AISI strength for intermediate (a) material 1 (b) material 2	74
Figure 4-18. Relation between FEA and AISI strength for slender (a) material 1 (b) material 2	75

List of Tables

Table 3-1. Recommended representative values for strain hardening exponents n and m	21
Table 3-2. Nonlinear material property for flat zone and corner zone	22
Table 3-3. Mesh Convergence Study	24
Table 3-4. Comparison of capacity predicted by present model and experimental results	30
Table 3-5. Representation of P_{EXP}/P_{FE} for all types of imperfections	32
Table 4-1. Types of columns considered in parametric study	43
Table 4-2. Specification of materials used in parametric study	43
Table 4-3. Comparison of Axial Capacity obtained from FE Analysis with AISI Design Guidelines (stub - material 1)	46
Table 4-4. Comparison of Axial Capacity obtained from FE Analysis with AISI Design Guidelines (stub - material 2)	47
Table 4-5. Comparison of Axial Capacity obtained from FE Analysis with AISI Design Guidelines (short - material 1)	50
Table 4-6. Comparison of Axial Capacity obtained from FE Analysis with AISI Design Guidelines (short - material 2)	51
Table 4-7. Comparison of Axial Capacity obtained from FE Analysis with AISI Design Guidelines (intermediate - material 1)	54
Table 4-8. Comparison of Axial Capacity obtained from FE Analysis with AISI Design Guidelines (intermediate - material 2)	55
Table 4-9. Comparison of Axial Capacity obtained from FE Analysis with AISI Design Guidelines (slender - material 1)	58
Table 4-10. Comparison of Axial Capacity obtained from FE Analysis with AISI Design Guidelines (slender - material 2)	59
Table 4-11. Suggested multiplier of AISI design equation	71

Chapter 1

INTRODUCTION

1.1 Background and Motivations

Use of built-up cold-formed steel (CFS) members are significantly increasing in residential as well as commercial buildings because of its light-weight nature and ease of construction to fabricate in a suitable shape as required [1]. Back-to-back built-up CFS lipped channel sections are used as compression member in steel trusses whereas, in portal frames it is used as columns [2]. In this type of cross-sections, fasteners at discrete points along the length prevent the individual channel sections against buckling as like other sections [3]. The design codes include limited guidance on the approximation of capacity of built-up CFS columns [4]. For instance, the American Iron and Steel institute (AISI) S100-16 section 11.2 [5] and Australian and New Zealand Standards (AS/NZ 4600) [6] both necessitate the calculation of axial capacity through revised slenderness ratio approach, which was adopted from hot rolled steel design in AISC 360 (2010) [7].

Some research work has been carried out for such back-to-back screw-fastened built-up cold-formed lipped channels under compression, limited research work has been stated that investigates the effect of width-to-thickness ratio and lip height-to-thickness ratio on the strength and stability of such channels under axial compression [8] which calls for research in this context. To this end, an attempt has been made in this study to investigate the effect of various width-to-thickness (b/t) ratio and lip height-to-thickness (c/t) ratio on axial compressive strength of lipped channel cross-sections covering a wide range of lengths (stub, short, intermediate and slender) by using a validated finite element model. Aims and objectives of the research will be discussed on the upcoming section.

1.2 Research Objectives and Overview

The specific aims of this research are:

a) To conduct a nonlinear numerical analysis considering full elastic-plastic material model for back-to-back lipped channel up to failure subjected to axial compressive load and validate the model with available experimental results [3].

b) To investigate the effects of width-to-thickness ratio and lip height-to-thickness ratio of four different types of columns (stub, short, intermediate and slender) on axial strength of back-to-back lipped channel sections by parametric study.

c) To propose a design guideline along with developing some column curves (capacity vs slenderness ratio and load vs displacement) for back-to-back lipped channel columns based on the result of parametric study.

To achieve the objectives mentioned above a nonlinear finite element model was developed in ABAQUS [9] for cold formed steel considering full range stress-strain curve for back-to-back lipped channel sections subjected to axial compression. Both local and global geometric imperfections were considered. Suitable experimental data was collected from previous research [3] and against these data, the developed model was verified successfully. The results of parametric study were compared with design strengths calculated in accordance with AISI code which is same as in Bangladesh National Building Code (BNBC). Finally, an attempt has been made in this research to propose a design guideline. Design curves have been derived by analyzing the data obtained from parametric study considering effect of width-to-thickness ratio and lip height-to-thickness ratio on buckling behavior of such lipped channels.

1.3 Organization of the thesis

This thesis is comprised of five chapters. A reflection of each chapter is given below.

Chapter 1: Introduction and objective delivers the background and motivations of the research. All the objectives and probable results are also described in this chapter.

Chapter 2: Literature Review presents the related works in the field of finite element modelling with a special focus on back-to-back built up lipped channel sections subjected to axial compression.

Chapter 3: Finite Element Modelling describes the detailed modelling techniques adopted to validate the model with experimental result. It also includes the results regarding validation of finite element model with experimental results.

Chapter 4: Parametric Study for back-to-back CFS lipped channels describes the results regarding parametric study including comparison of numerical results with AISI design code and proposal of a design guideline along with derivation of some design curves including linear regression analysis of FEA strength and AISI strength.

Chapter 5: Conclusions and Future Works summarizes the conclusions and major findings of this research along with recommendations for future research.

Chapter 2

LITERATURE REVIEW

2.1 Introduction

Cold-formed steel (CFS) members are made from structural quality sheet steel that are formed into C-sections and further shapes by roll forming the steel through a series of dies. No heat is essential to construct the shapes hence the name cold-formed steel. A range of steel thicknesses are available for a wide range of structural and non-structural applications [10]. As a uniformly manufactured product, the superiority of CFS is widely accepted. CFS produces less scrap to haul off because there is less waste and is regarded as eco-friendly material. Cold-formed steel, especially in the form of thin gauge sheets, is commonly used in the construction of structural or non-structural objects such as columns, beams, joists, studs, floor decking, built-up sections and other constituents. Cold-formed steel members have been used similarly in bridges, storage racks, grain bins, car bodies, railway coaches, highway products, transmission towers, transmission poles, firearms etc. The varieties of sections are cold-formed from steel sheet, strip, plate or flat bar in roll forming machines, by press brake (machine press) or bending operations [11]. Different shapes of CFS steel sections are shown in Figure 2-1.

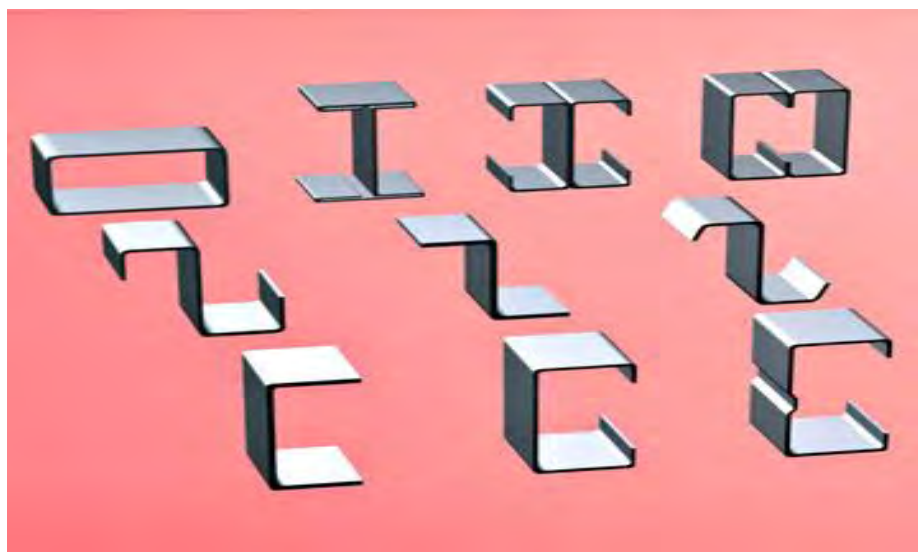


Figure 2-1. Different types of Cold-formed steel [12]

2.2 Advantages of cold-formed steel

CFS as a construction material has many advantages. For example, it is light in weight, no formwork required for it, uniform quality, economy in transportation and handling [11]. CFS does not shrink or split and will not absorb moisture. Its physical properties allow it to be used in a wide range of environments. Some of the notable main properties of cold formed steel are non-combustibility and termite-proof and rot-proof [11]. Its strength and ductility make it perfect for construction in regions subject to high winds or earthquakes. Furthermore, a study, conducted by the National Association of Home Builders (NAHB) research center, showed that the zinc coating on steel framing materials can protect against corrosion for many years [10]. In recent times, cold-formed steel is increasingly used all over the world due to ease of construction and due to its higher strength to self-weight ratio [1,13]. Applications comprise struts in steel trusses and space frames, wall studs in wall frames and columns in portal frames [12].

2.3 Experimental study on axially loaded back to back CFS channel sections

For using back-to-back built-up cold-formed steel channel sections as struts in steel trusses and space frames or as wall studs in wall frames, intermediate fasteners at discrete points along the length are used to prevent the channel sections from buckling independently.

In the literature, limited research is available for back-to-back built-up cold-formed steel channel sections under compression, in the arrangement shown in Figure 2-2. However, some research has been designated for cold-formed steel channel sections under axial compression to understand the buckling behavior of such columns [14-17].

Ting [3] recently conducted an experimental and numerical investigation on the behavior of back-to-back built-up CFS lipped channel sections under axial compression. The results of thirty experimental tests are described as shown in Figure 2-3, performed on back-to-back cold-formed steel channel sections covering stub columns to slender columns. It is stated that the modified slenderness approach is overall conservative but for stub columns it can be un-conservative by around 10%.

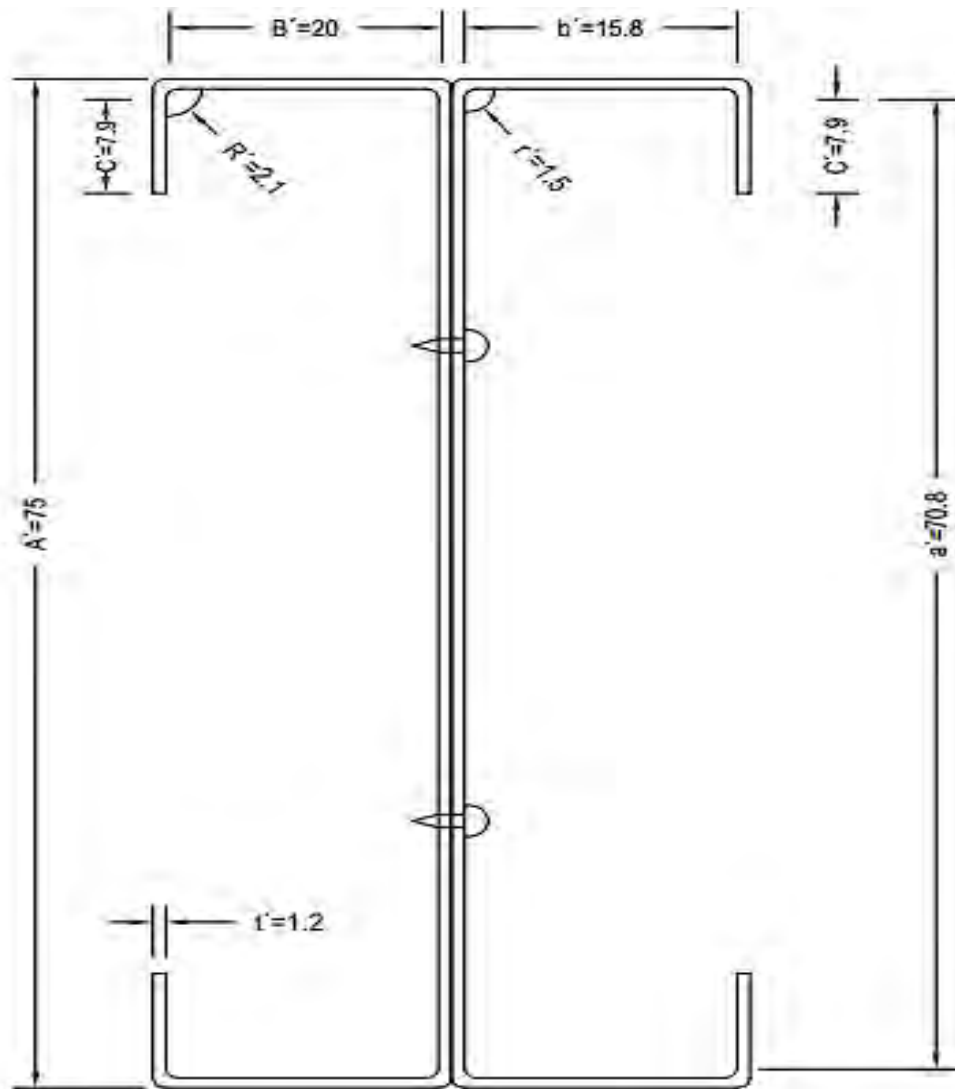


Figure 2-2. Details of back-to-back built-up cold-formed steel channel-sections studied by Ting [3]

In the Figure 2-2,

A' = web height including corner (mm)

a' = web height without corner (mm)

B' = flange width including corner (mm)

b' = flange width without corner (mm)

C' = lip height (mm)

r' = inner corner radius (mm)

R' = outer corner radius (mm)

t' = thickness (mm)

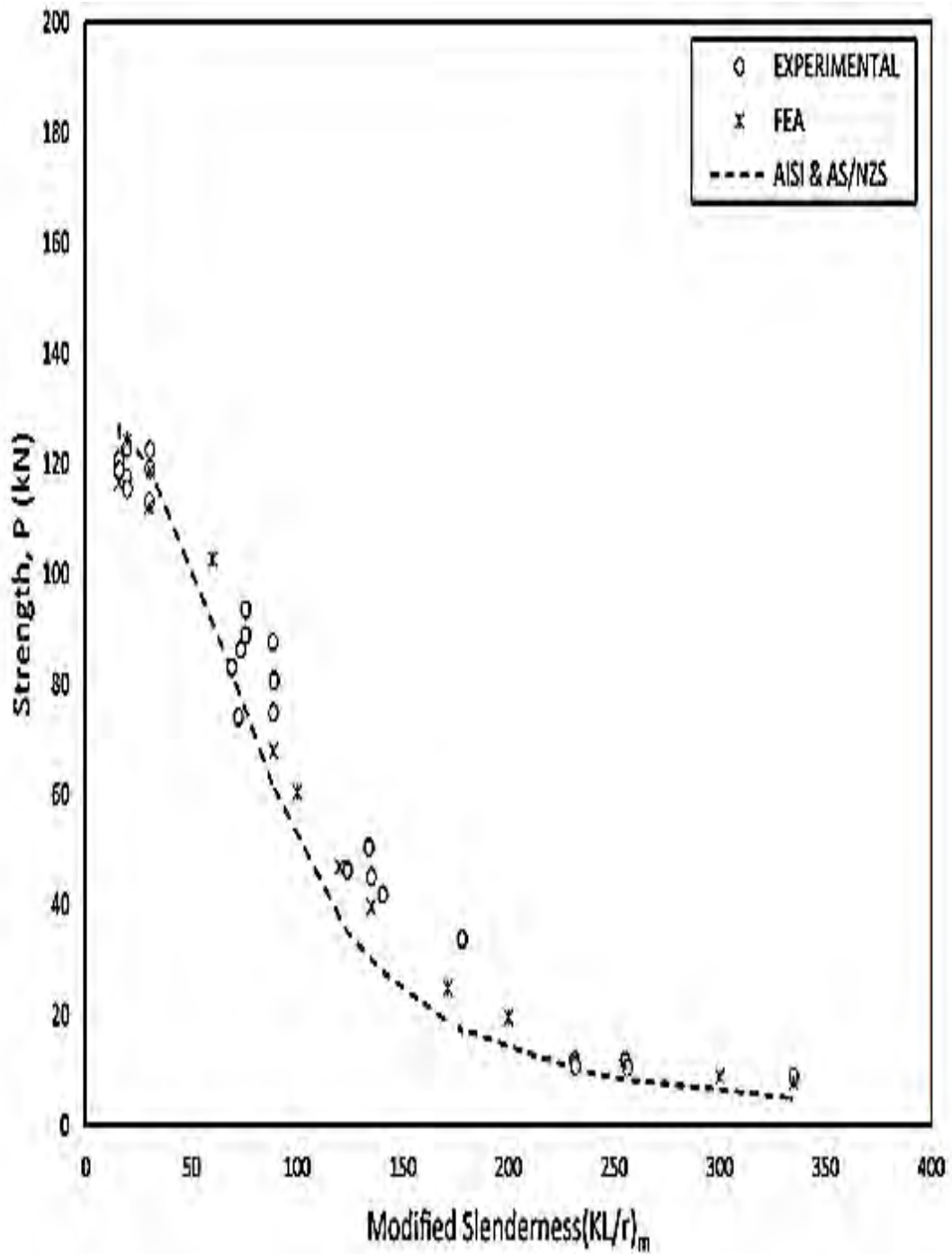


Figure 2-3. Variation of strength against modified slenderness [3]

To extend this work, Roy [18] has examined the effect of thickness on the behavior of back-to-back built-up cold-formed steel lipped channel sections.

Roy [19-20] also has studied experimentally and numerically the axial capacity of back-to-back gapped built-up cold-formed steel lipped channel sections and established

that the current design guidelines by AISI and AS/NZ, can be too conservative while estimating the axial capacity of such columns.

Moreover, Roy [21] conducted experiments in recent times on back to-back built-up CFS channels. These experimental results were used to validate the numerical models using the finite element technique [22].

Roy [8] also investigated the nonlinear behavior of axially loaded back-to-back built up cold-formed stainless steel channel sections and concluded that no previous work in the literature has considered back-to-back built up cold-formed un-lipped channel and specially investigated the effect of screw spacing on axial strength of such un-lipped channels.

Fratamico [23] examined the significance of screw spacing on the behavior of back-to-back built-up lipped channel columns. In his research, thirty columns were modelled under concentric loading condition up to failure. The screw spacing is varied from L to $L/6$, where L is the column length, with and without varying lengths of End Fastener Groups (EFG), which are a prescriptive layout of fasteners at the ends of built-up columns that is required by AISI S100-12 [5]. Results yielded two general types of deformation modes: compatible (where the connected webs conform to the same buckling shape) and isolated stud buckling.

Stone and Laboube [24] considered back-to-back lipped channel-sections but these had stiffened flanges and track sections. The built-up studs consisted of two C-sections oriented back-to-back forming an I-shaped cross-section as shown in Figure 2-4 and Figure 2-5. For each specimen, the studs were connected to each other with two self-drilling screws spaced at a set interval. A cold-formed steel track section was connected running perpendicular to each end of the built-up stud with a single self-drilling screw through each flange of the C-sections to keep the ends of the studs together. As a result of the investigation, the current design requirements were found to be conservative in predicting the ultimate capacity of built-up studs.

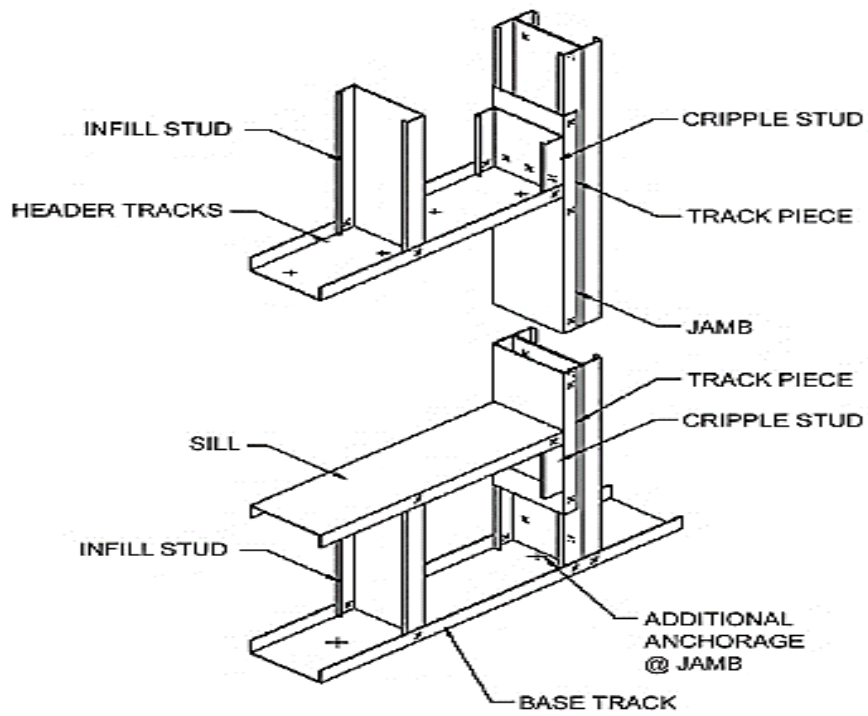


Figure 2-4. Typical window framing [24]

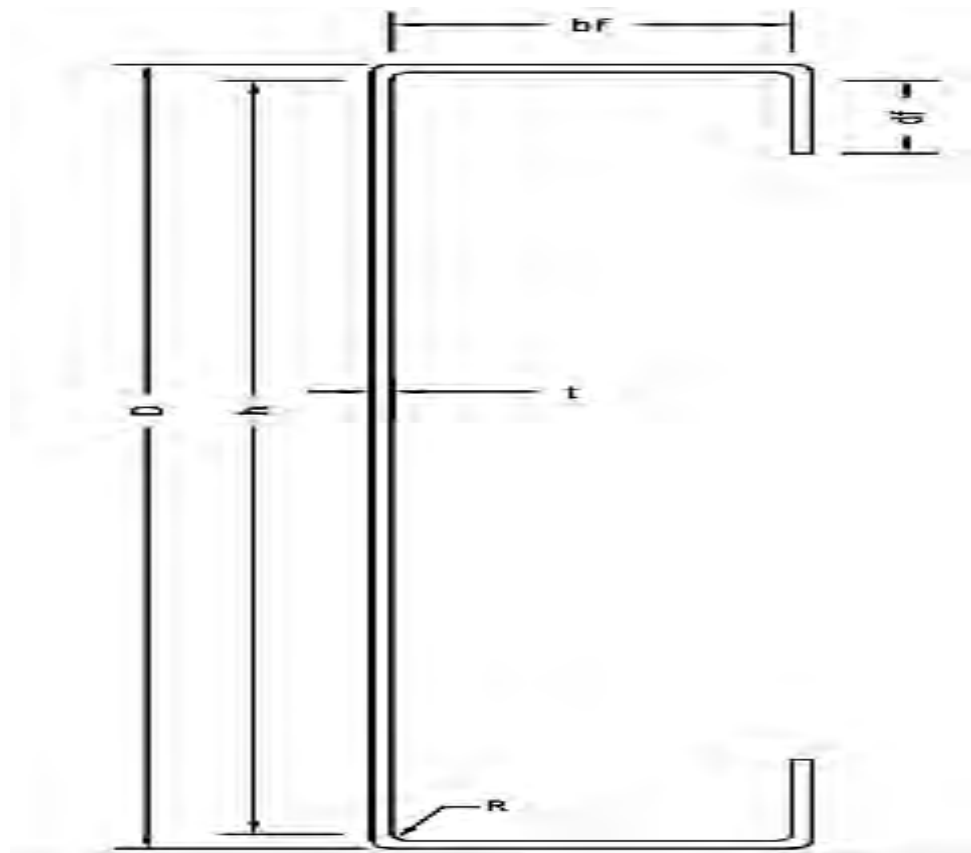


Figure 2-5. Typical C section [24]

In the Figure 2-5,

d_f = lip height (mm)

b_f = flange width (mm)

D = Web height including corner (mm)

h = Web height without corner (mm)

R = corner radius (mm)

t = thickness (mm)

Zhang and Young [25] considered back-to-back built-up lipped channel-sections with an opening. A series of column tests on cold-formed steel I-shaped open sections with edge and web stiffeners has been conducted. The column length of the test specimens varied from 300 to 3200 mm with an increment of approximately 600 mm. The appropriateness of the Direct Strength Method (DSM) in the North American Specification and the AS/NZ Standard [5] for I-shaped open sections with edge and web stiffeners was evaluated. It is concluded that the direct strength method can be used for cold-formed steel I-shaped open sections with edge and web stiffeners.

Cold-formed steel built-up closed sections with intermittent stiffeners were investigated by Young and Chen [26]. A series of column tests on cold-formed steel built-up closed sections with intermediate stiffeners has been conducted. The test strengths are compared with the design strengths calculated using DSM in the North American Specification and the AS/NZ Standard [5] for cold-formed steel structures. It is shown that DSM using single section to obtain the buckling stresses is generally conservative.

2.4 Numerical research on axially loaded back-to-back cold-formed steel channel sections

In this section, the summary of numerical research work on cold-formed steel channel sections under axial compression are presented.

Anbarasu and Ashraf [27] investigated the structural response of cold-formed single lipped channel columns made of lean duplex stainless steel. Verified finite element technique was used to examine 64 lipped channel columns recording local and flexural buckling failure. The recorded strengths were compared against those calculated using the main DSM developed for cold-formed steel sections and modified DSM proposed

by Becque [28] as well. The comparison revealed that both main and modified DSM techniques were extremely conservative in predicting the strengths of the lipped channels.

Anwar and Ashraf [29] numerically studied the performance of stainless steel single lipped channel sections exposed to compression and bending. Nonlinear finite element models were used to analyze 120 lipped channel stub column sections subjected to eccentric compression producing bending about the main axis only. Previously proposed [29] Continuous Strength Method (CSM) interaction equations with four discrete sets of coefficients are examined for their appropriateness in predicting the performance of such sections. Observed variations in predictions are summarized and subsequently used to recommend a new set of coefficients for lipped channel sections.

Anbarasu [30] investigated the behavior and strength of cold-formed steel web stiffened built-up batten columns as shown in Figure 2-6. Three types of web stiffened lipped channel cross section have been chosen for the study, based on the AISI-S100:2007 [5] geometric limitations. The column strength predicted by the finite element analysis is compared with the design column strengths predicted by DSM and finally a recommendation to modify the current DSM, while computing axial strength of such columns has been proposed.

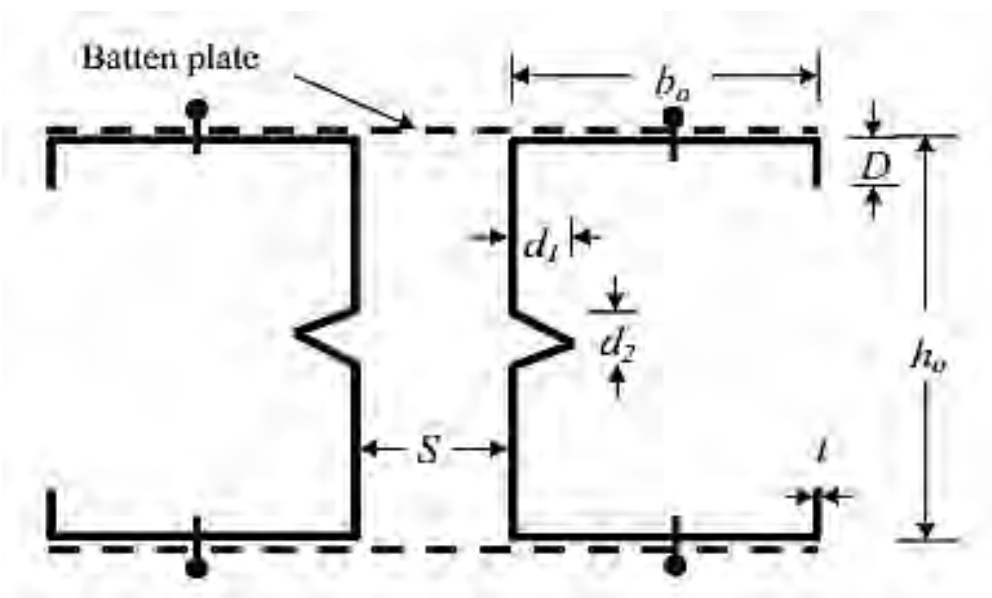


Figure 2-6. Built-up batten column section details [30]

In the Figure 2-6,

d_1 = stiffener width (mm)

b_o = flange width (mm)

D = lip height (mm)

d_2 = stiffener height (mm)

S = spacing between lipped channels (mm)

h_o = web height (mm)

Dabaon [31] investigated built-up battened columns and concluded that AISI and Eurocode provisions were un-conservative when the steel battened columns failed through local buckling, but were conservative when they failed through flexural buckling.

Whittle and Ramseyer [32] considered built up channel sections, but these were welded toe to toe. Over 150 experimental compression tests on closed-section, built-up members formed of intermediately welded C shaped channels were conducted and these experimental values were compared to theoretical buckling capacities based on the AISI –S100 section C4.5 [5] modified slenderness ratio. It is reported that use of the modified slenderness ratio was exceedingly conservative and capacities based on the unmodified slenderness ratio and fastener and spacing provisions were consistently conservative.

Piyawat [33] studied back-to-back welded lipped channel-sections. A numerical parametric study involving a total of 360 different configurations was conducted. To address the issues of an unnecessarily complicated AISI specification [5] for doubly symmetric members subject to distortional buckling, a simple and reliable axial load capacity equation was developed based on a regression analysis of a three-dimensional surface fitting and calibration with the experimental data. That proposed equation exhibited good agreement with the numerically simulated and experimentally measured capacities.

An analytical principle for buckling strength of built-up compression members were studied by Aslani and Goel [34]. Related work was carried out by Reyes and Guzman [35] and the slenderness ratio was estimated in built-up cold formed box sections. On the other hand, Biggs [36] examined the axial strength of rectangular and I-shaped

welded built-up cold formed steel columns under compression and clinched that AISI [5] can be more conservative for thicker members but less conservative for wider members.

From the information presented above it can be said that considerable amount of numerical research work has been carried out for cold-formed steel channel sections to comprehend the compressive behavior of such columns. However, no research has investigated the effect of various width-to-thickness ratio or lip height-to-thickness ratio on compressive strength of such back-to-back channels which can be marked as a research gap in this field.

2.5 Design guidelines available in different codes

2.5.1 Bangladesh National Building Code (BNBC)

According to BNBC 2020 section [37] 10.1.3.1 (e) for cold formed structural steel, AISI standard (AISI/COS/NASPEC 2001) or equivalent may be followed.

2.5.2 American Iron and Steel Institute (AISI) and AS/NZ Standard

The un-factored design strengths determined in accordance with the American Iron and Steel Institute (AISI) specification complies with AS/NZ standard. Effective width area method is used while calculating width-to-thickness ratio (b/t), depth-to-thickness ratio (d/t) and design strengths according to AISI.

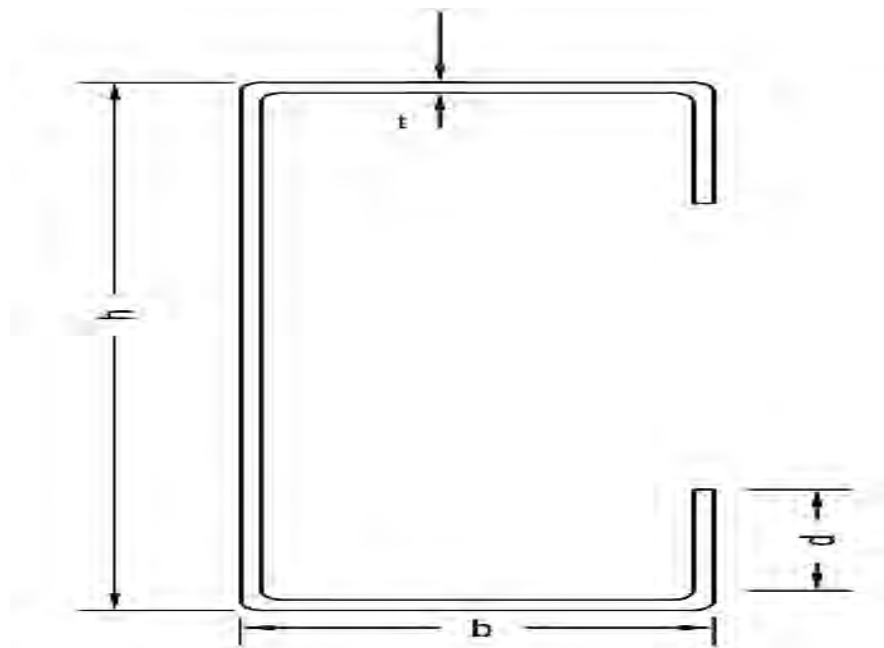


Figure 2-7. Geometry of a lipped channel section

In the Figure 2-7,

b = flange width (mm)

d = lip height (mm)

t = thickness (mm)

h = web height (mm)

$b/t \leq 60$ [Effective width method]

$h/t \leq 300$ [for bearing and intermediate stiffener]

For built-up lipped channel sections, the un-factored design strength of axially loaded columns calculated in line with AISI and AS/NZ standard are as follow

$$P_{AISI \text{ and } AS/NZ} = A_g F_n \text{-----(2.1)}$$

Here A_g = gross area

The critical buckling stress F_n depends on following considerations

For $\lambda_c \leq 1.5$

$$F_n = (0.658^{\lambda_c^2}) F_y \text{-----(2.2)}$$

Where F_y = yield stress

For $\lambda_c > 1.5$

$$F_n = \left(\frac{0.877}{\lambda_c^2}\right) F_y \text{-----(2.3)}$$

Where non dimensional critical slenderness (λ_c) will be calculated as

$$\lambda_c = \sqrt{\frac{F_y}{F_e}} \text{-----(2.4)}$$

$$F_e = \text{Elastic global buckling stress} = \frac{\pi^2 E}{\left(\frac{KL}{r}\right)^2} \text{-----(2.5)}$$

K = effective length factor

L = nominal length of column

For compression members composed of two section in contact modified slenderness ratio was used which is calculated as

$$\left(\frac{KL}{r}\right)_m = \sqrt{\left(\frac{KL}{r}\right)_0^2 + \left(\frac{a}{r_i}\right)^2} \text{-----(2.6)}$$

$\frac{a}{r_i}$ does not exceed one-half of the governing slenderness ratio of the built-up member

Where $\left(\frac{KL}{r}\right)_0$ = overall slenderness ratio of entire section about built-up member axis

a = intermediate fastener or spot weld spacing

r_i = minimum radius of gyration of full unreduced cross sectional area of an individual shape in a built-up member

2.5.3 American Institute of Steel Construction (AISC)

For built-up lipped channel sections, the un-factored design strength of axially loaded columns calculated in line with the American Institute of Steel Construction (AISC) are as follow

$$P_n = A_g F_{cr} \text{-----}(2.7)$$

Here A_g = gross area

The critical buckling stress F_{cr} will depend on following considerations

$$F_{cr} = (0.658^{\frac{F_y}{F_e}}) F_y \left[\frac{L_c}{r} \leq 4.71 \sqrt{\frac{E}{F_y}} \text{ or } \frac{F_y}{F_e} \leq 2.25 \right] \text{-----}(2.8)$$

$$F_{cr} = 0.877 F_e \left[\frac{L_c}{r} > 4.71 \sqrt{\frac{E}{F_y}} \text{ or } \frac{F_y}{F_e} > 2.25 \right] \text{-----}(2.9)$$

Where F_y = yield stress

$$F_e = \text{Elastic global buckling stress} = \frac{\pi^2 E}{\left(\frac{L_c}{r}\right)^2}, \quad L_c = KL \text{-----}(2.10)$$

Provided that $\frac{L_c}{r}$ does not exceed 200

K = effective length factor

L = nominal length of column

2.5.4 Eurocode EN 1993-1-3

EN 1993-1-3 gives [40] design requirements for cold formed members and sheeting.

Thickness tolerance : for sheeting and members : $0.45 \text{ mm} \leq t_{cor} \leq 15 \text{ mm}$

Maximum width to thickness ratio : $\frac{b}{t} \leq 60, \frac{c}{t} \leq 50$

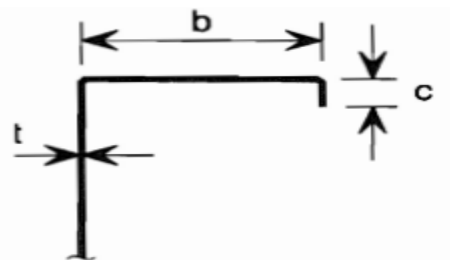


Figure 2-8. Specification of a typical lipped channel

For built-up lipped channel sections, the design strength of axially loaded columns calculated in line with Eurocode 1993 are as follow

$$\text{The design buckling resistance of a column , } N_{b,Rd} = \frac{\chi f_y A}{\gamma_{M1}} \text{-----(2.11)}$$

Here A = Effective cross sectional area

γ_{M1} = Material partial safety factor = 1

f_y = Basic yield strength

χ = Reduction factor, will be obtained from buckling curve.

For built-up lipped channel sections, following buckling curve will be maintained

<u>Buckling about axis</u>	<u>Buckling curve</u>
Y-Y	a
Z-Z	b

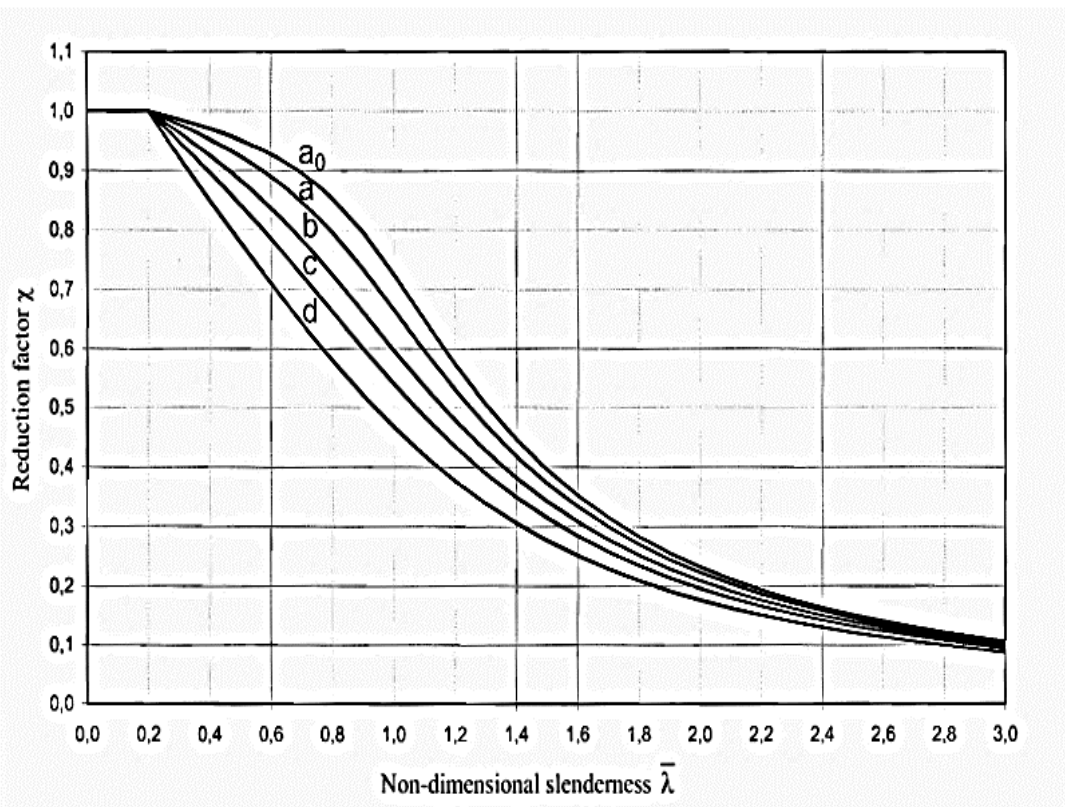


Figure 2-9. Reduction factor vs non-dimensional slenderness curve [18]

$$\text{Non-dimensional slenderness } \lambda = \frac{L_{cr}}{i} \frac{1}{\lambda_1} \text{-----(2.12)}$$

Where L_{cr} = buckling length in buckling plane

i = radius of gyration

$$\lambda_1 = 93.9 \varepsilon \text{ where } \varepsilon = \sqrt{\frac{235}{f_y}} \text{-----(2.13)}$$

2.5.5 Continuous Strength Method (CSM)

Continuous Strength Method (CSM) is a deformation based design approach that is aimed to utilize beneficial strain hardening observed in nonlinear metals [38].

It was worthwhile to note that, CSM is yet to be extended towards open ended CFS cross sections. Thus, existing rules of CSM developed based on stainless steel open sections (I-sections) was described herein to gather idea about the compression resistance. For built-up lipped channel sections, the design strength of axially loaded columns calculated in line with CSM are as follows [39]

$$\text{Cross-section capacity in compression, } N_{c,Rd} = \frac{f_{csm} A_g}{\gamma_{MO}} \text{-----(2.14)}$$

Here A_g = gross cross sectional area

γ_{MO} = Material partial safety factor = 1 [40]

For slender section f_{csm} = the limiting buckling stress = $\epsilon_{e,ev} E$ [$\lambda_p > 0.6$] ---(2.15)

$\epsilon_{e,ev}$ = Equivalent elastic strain at ultimate load = $C \epsilon_{csm}$ [$\lambda_p > 0.68$] -----(2.16)

Where C = constant that depends on cross section slenderness λ_p

Relation between C and λ_p is $C = a\lambda_p^b$ -----(2.17)

Where a and b are two constants that depends on cross-section types. Value of a and b for different cross section types are available in [39-41]. For lipped channel section a = 3.04 and b = 3.15 [39].

Therefore $C = 3.04 \times \lambda_p^{3.15}$

$$\lambda_p = \frac{\sqrt{\sigma_{0.2}}}{\sqrt{\sigma_{cr,cs}}} \text{-----(2.18)}$$

Where $\sigma_{0.2}$ = 0.2% proof stress

$\sigma_{cr,cs}$ = The critical elastic buckling stress corresponds to the lowest local buckling shape of the section for a given load

$$= \frac{\pi^2 E}{\left(\frac{L_c}{r}\right)^2}, L_c = KL \text{-----(2.19)}$$

K = effective length factor

L = nominal length of column

and ϵ_{csm} = Maximum strain that a cross section can sustain, can be calculated from following relationship

$$\frac{\epsilon_{csm}}{\epsilon_y} = \frac{0.25}{\lambda_p^{3.6}} \leq \min\left(0.15, 0.1 \frac{\epsilon_u}{\epsilon_y}\right) \text{-----(2.20)}$$

ϵ_y = Elastic strain at ultimate stress

ε_u = Ultimate strain

It can be summarized that the American Iron and Steel Institute (AISI 2012) and Australian and New Zealand Standard [5] recommends the use of modified slenderness approach to take into account the spacing of screws in built-up sections. It should be noted that this modified slenderness approach has been adapted from design guidance for hot-rolled steel. On the other hand, American Institute of Steel Construction (AISC) standard and Continuous Strength Method (CSM) uses effective length instead of modified slenderness whereas Eurocode considers buckling length in buckling plane.

Chapter 3

FINITE ELEMENT MODELLING

3.1 Introduction

In this section the method of developing the finite element models will be described. A nonlinear elastic-plastic finite element model of built-up lipped channels was developed using ABAQUS 6.13-1 [9]. The numerical model of built up lipped channel was verified against the experimental test results found by Ting [3]. Two types of finite element analysis were performed for buckling of built-up sections. Firstly, Eigenvalue analysis, which is a linear elastic analysis was used to determine the contours of the initial imperfections using the linear perturbation-buckle procedure available in the ABAQUS library. Then a load displacement nonlinear analysis is carried out using static, Riks algorithm which is a general step procedure available in the ABAQUS library. In total, 80 increments were used. The initial arc length increment was 0.001, whereas the minimum and maximum arc length increments were 1×10^{-10} and 0.01 respectively, with an estimated total arc length of 1. The geometric imperfections (local and global) and material nonlinearity are included in the finite element model. The Riks method includes the post buckling behavior of back-to-back steel lipped channels. From the analysis, the failure loads, buckling modes, displacement are determined. Specific modelling techniques are elaborated in the following sections.

3.2 Geometry and material properties

The full geometry of the built-up steel lipped channels has been modelled in this study. ABAQUS requires input of material strength provided as true stress and log plastic strain in its property module. Two different material models have been used in this modelling. Firstly, a simplified elastic perfect plastic stress-strain curve obeying Von mises yield criterion used. Yield strength of 560 MPa, ultimate strength of 690 MPa, along with Young's modulus of 207 GPa was used in modelling [42]. In plastic zone, the value of ultimate strain at ultimate stress was used as 0.113, which is determined from the equation given by Gardner and Yun [43] for cold formed steel.

Poisson's ratio of steel used as 0.3. Another type of material model used as well which includes full range stress-strain curve given by Gardner and Yun [43] specially for cold-formed steel. They mentioned that cold-formed steels are generally characterized by a rounded stress-strain response with no sharply defined yield point as presented in Figure 3-1. For materials and process routes that result in significant strength enhancement because of cold work in the corner areas, allowance should be made for the consequential increase in cross-section strength in the design method [44]. Suitable material strength was incorporated in this numerical models i.e. flat material data for elements in the flat regions and greater corner strength data for elements in the corner regions. Corner strength enhancement was extended to a length equal to section thickness 't' into the flat portion as reported in [45] for cold-formed steel. However, for stainless steel corner strength enhancement should be extended up to '2t' into the flat portion [46-48]. Following equations were developed by Gardner and Yun [43] for flat and corner region respectively:

the stress (f) – strain (ϵ) relationship is given by [11]

$$\epsilon = \begin{cases} \frac{f}{E} + 0.002\left(\frac{f}{f_y}\right)^n & \text{for } f \leq f_y \\ \left(\frac{f-f_y}{E_{0.2}} + \left(\epsilon_u - \epsilon_{0.2} - \frac{f_u-f_y}{E_{0.2}}\right)\left(\frac{f-f_y}{f_u-f_y}\right)^m + \epsilon_{0.2} \right) & \text{for } f_y < f \leq f_u \end{cases} \text{-----(3.1)}$$

Where f_y = yield strength

$\epsilon_{0.2}$ is the total strain at the yield strength f_y (0.2% proof stress), it is calculated from first equation by putting $f = f_y$.

$E_{0.2}$ is the tangent modulus of the stress-strain curve at the yield strength (0.2% proof stress) and given by

$$E_{0.2} = \frac{E}{1+0.002n\frac{E}{f_y}} \text{-----(3.2)}$$

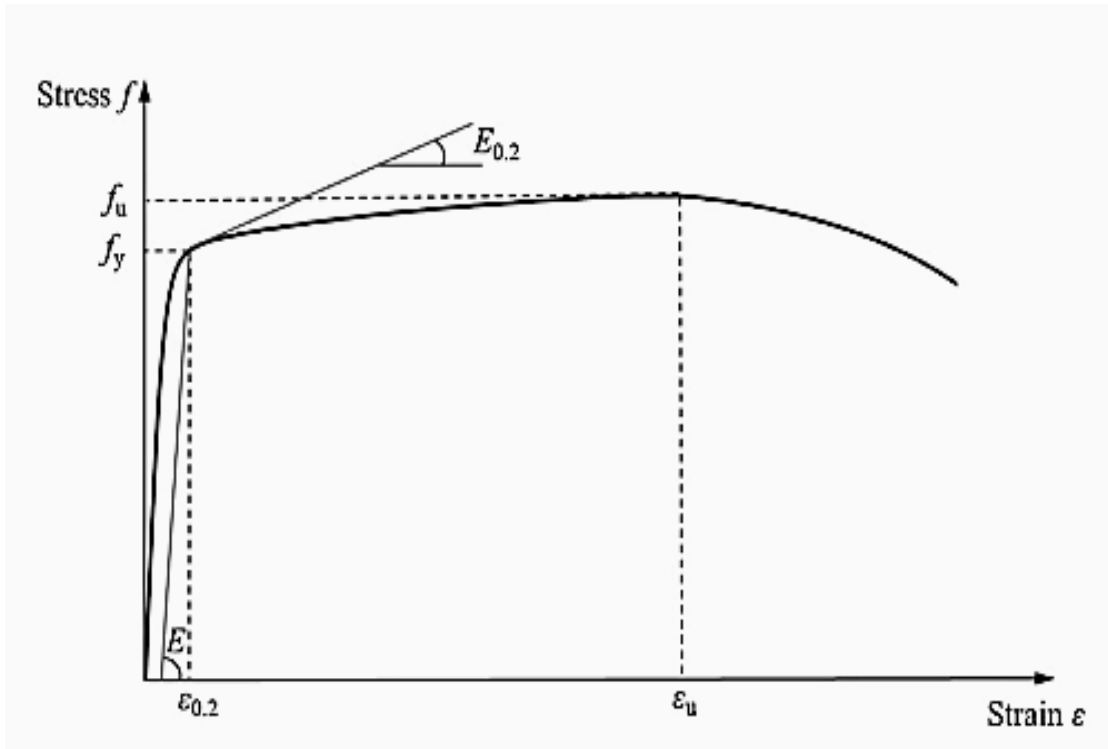


Figure 3-1. Typical cold-formed steel stress-strain curve with definitions of key material parameters [43]

The strain ϵ_u corresponding to the ultimate tensile strength f_u is obtained from

$$\epsilon_{0.2} = 0.6 \left(1 - \frac{f_y}{f_u} \right) \text{-----(3.3)}$$

Table 3-1. Recommended representative values for strain hardening exponents n and m [43]

	n	m
Flat coupons	7.6	3.8
Corner coupons	7.0	4.2

At corner zone increased yield strength $f_{y,c}$ is calculated from the following equation

$$f_{y,c} = \frac{B_C}{\left(\frac{r_i}{t}\right)^\alpha} f_y \text{-----(3.4)}$$

In which

$$B_C = 3.69 \left(\frac{f_u}{f_y} \right) - 0.819 \left(\frac{f_u}{f_y} \right)^2 - 1.79 \text{-----(3.5)}$$

And

$$\alpha = 0.192 \left(\frac{f_u}{f_y} \right) - 0.068 \text{ -----(3.6)}$$

This model assumes that the strength enhancement in the corner regions of cold-formed steel sections is dependent on (a) the ratio of the ultimate tensile strength (f_u) to the yield strength (f_y) of the unformed (virgin) material, which is indicative of the potential for cold-working, and (b) the ratio of the inner corner radius (r_i) to the thickness of the steel sheet (t), which is indicative of the induced level of plastic strain.

After calculating $f_{y,c}$ ultimate stress for corner region $f_{u,c}$ is obtained from the relationship

$$\frac{f_u}{f_y} = 1 + \left(\frac{130}{f_y} \right)^{1.4} \text{ -----(3.7)}$$

After calculating all the required values following tables have been derived for use in ABAQUS as nonlinear material property which is represented in Figure 3-2.

Table 3-2. Nonlinear material property for flat zone and corner zone

Flat zone		Corner zone	
Yield Stress (MPa)	Plastic Strain	Yield Stress (MPa)	Plastic Strain
560	0.00	771.12	0.00
573	0.005	777.50	0.0058
586	0.0057	783.87	0.0061
599	0.007	790.25	0.0064
612	0.0096	796.63	0.0071
625	0.014	803.01	0.0086
638	0.022	809.39	0.011
651	0.034	815.76	0.015
664	0.0527	822.14	0.022
677	0.0782	828.52	0.032
690	0.113	834.90	0.046

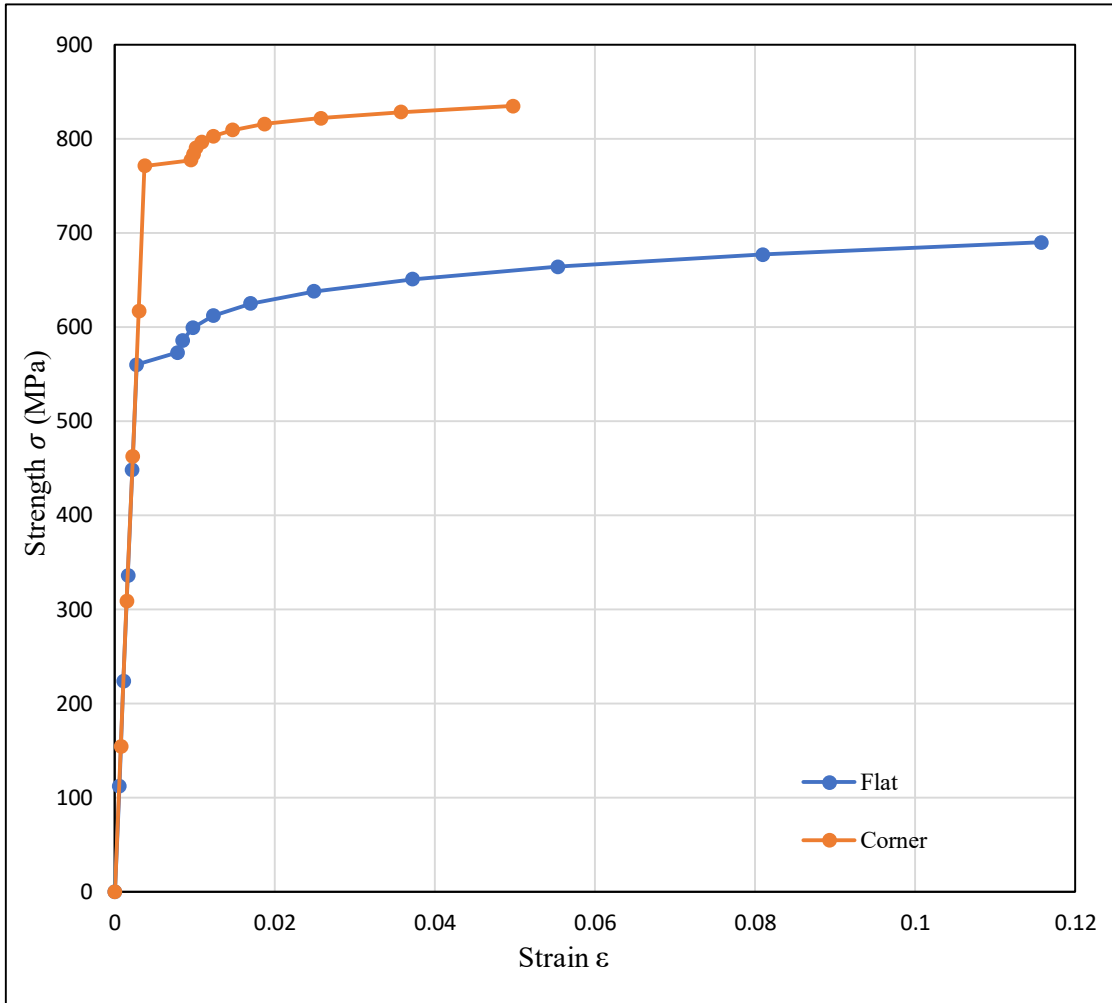


Figure 3-2. Full range stress-strain curve for flat and corner zone

3.3 Element type and mesh optimization

A linear 4-noded quadrilateral thick shell element with reduced integration (S4R5), available in ABAQUS mesh library was used to model the section which is reported in [38] also as perfect for thin walled metallic cross sections. A uniform square mesh size of 5 mm \times 5 mm (length \times width) was used for the convergence of the model. Table 3-3 and Figure 3-3 represents the appropriateness of this mesh size. Along the length of the sections, the number of elements was chosen so that aspect ratio of the elements was as close to one as possible. At corner, number of elements was two which was found to be appropriate for uniform meshing. Figure 3-4 shows a typical finite element mesh.

Table 3-3. Mesh Convergence Study

Section Considered	Mesh Name	Flat element size (mmXmm)	No of element in corner	No of elements	No of nodes
BU75-S50-L300-2	Fine	5x5	2	2016	2109
BU75-S50-L300-2	Medium	6x6	2	1513	1530
BU75-S50-L300-2	Course	8x8	2	1000	1023

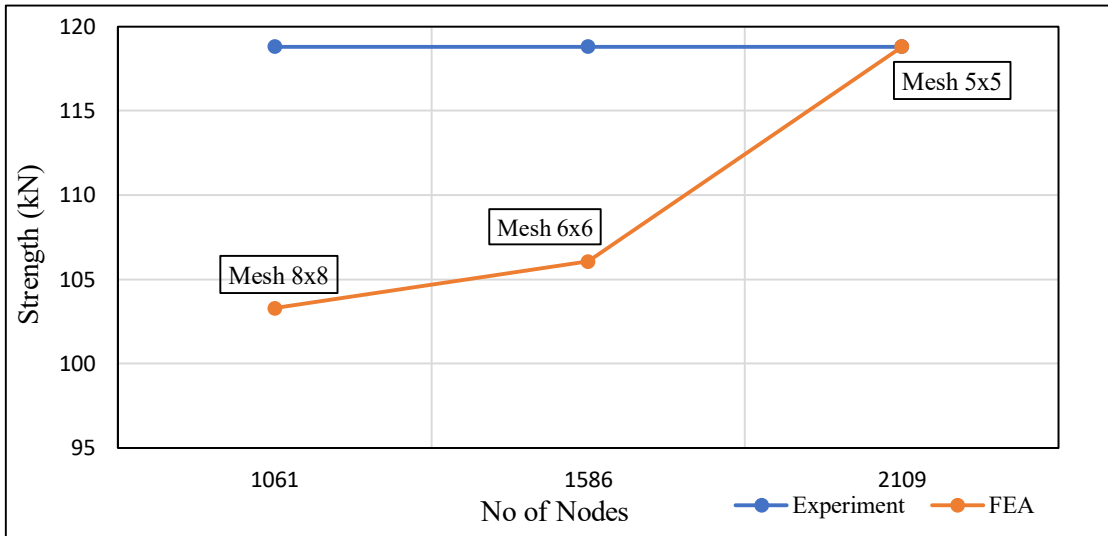


Figure 3-3. Comparison of FEA strength with experimental strength for different mesh sizes

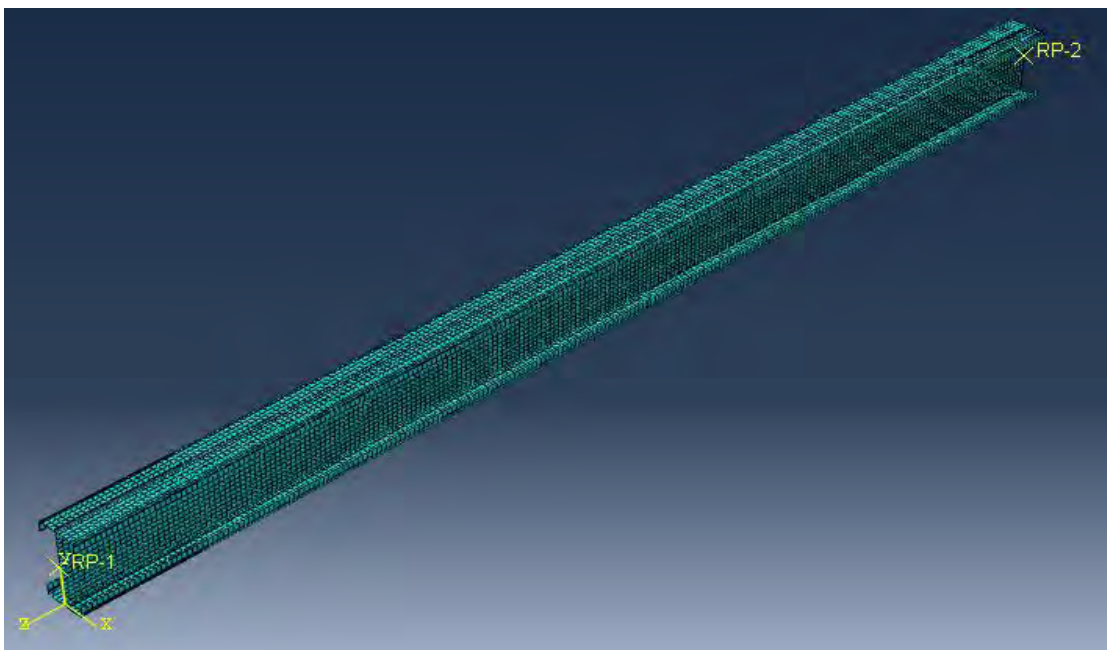


Figure 3-4. Finite element mesh used for verification of the model

3.4 Boundary conditions, constraints and load application

For stubs, ends were restrained against any movement except for the loaded end to be free against translation along the load direction. For other columns except stubs pin-ended boundary conditions were applied. In order to put on pin-ended boundary conditions, rotation was allowed at both upper and lower ends of the back-to-back cold-formed steel lipped channels through reference points. The reference point was considered as the center of gravity (CG) of the cross section of built up channels, hence no eccentricity was considered. The load was applied to the reference points of the upper end of the channels as shown in Figure 3-5.

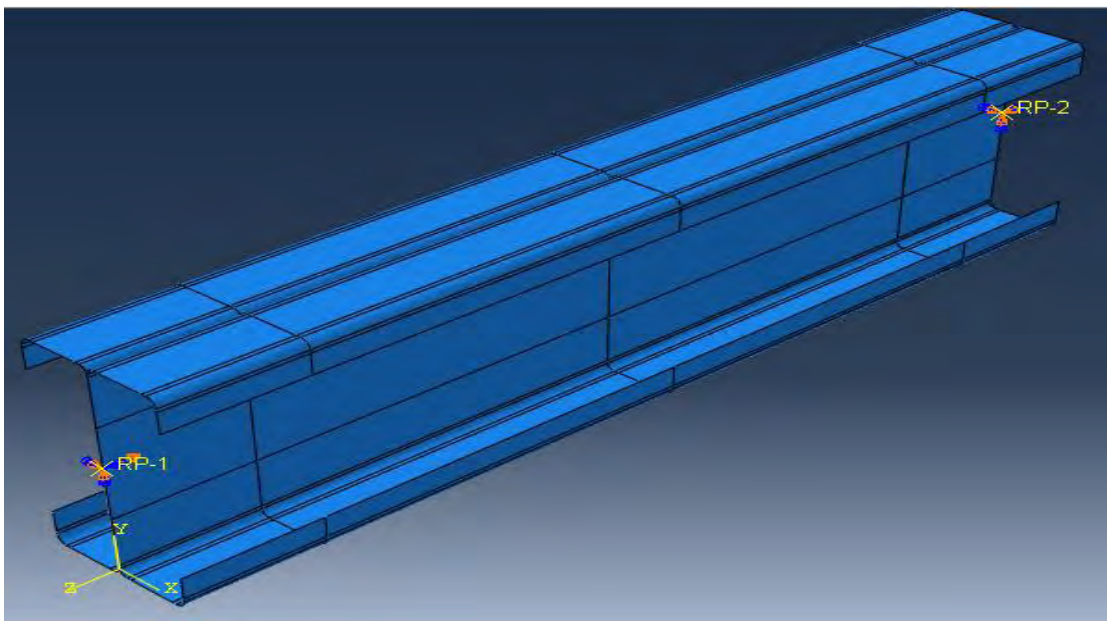


Figure 3-5. Pin ended boundary condition applied in FE model

The channels were bolted together to form a I-section, to mimic the bolts in modeling, a simpler technique was attained. A proper inclusion of the bolts within the model would incur greater number of surfaces, nodes and constraints, which eventually will make the model computationally more expensive. As the key aim of this study was to investigate the compression behavior of I-section, thus modeling of bolts was omitted. In the locations where bolts would have been inserted, simple node-to-node tied joint (physical representation of a screw) was used. These nodes connected using tie constraint option available in ABAQUS constraint library, ensured the webs of two back-to-back channels were attached together to form the I-section without any relative displacement. Tied joint was placed at a level of $h/4$ from top and bottom (h = height of web). The end nodes were tied with respect to reference point at top and bottom by

using rigid body constraint option available in ABAQUS constraint library to restrict any kind of movement at ends as shown in Figure 3-6.

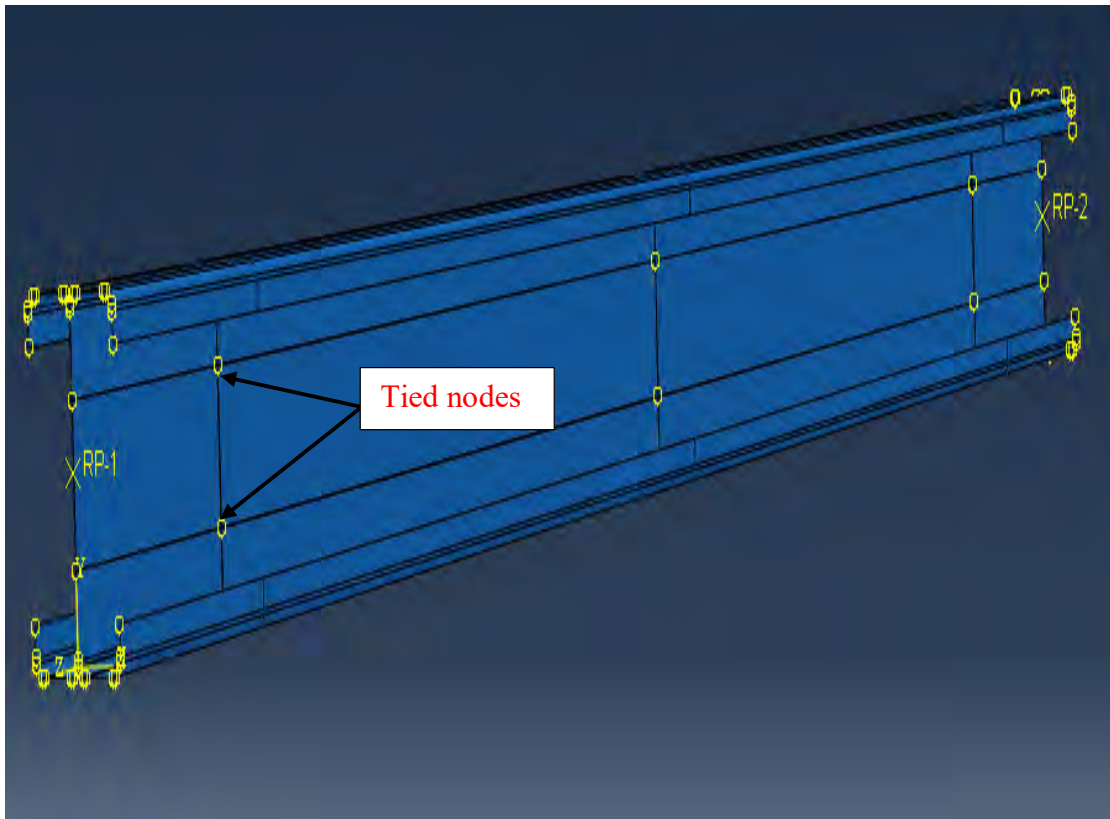


Figure 3-6. Tied joint and rigid body constraint used in FE model

3.5 Contact modeling

‘Surface to surface’ contact interactions define contact between two deformable surfaces. ‘Surface to surface’ contact using the finite-sliding tracking method was used for modelling the interaction between the webs of back-to-back lipped channels. The web of one lipped channel was modeled as slave surface, while the web of other lipped channel section was considered as master surface. The penalty friction method was used to approximate the hard-pressure-over-closure behavior with coefficient of friction as 0.19 for steel to steel [49]. There was no penetration between the two contact surfaces.

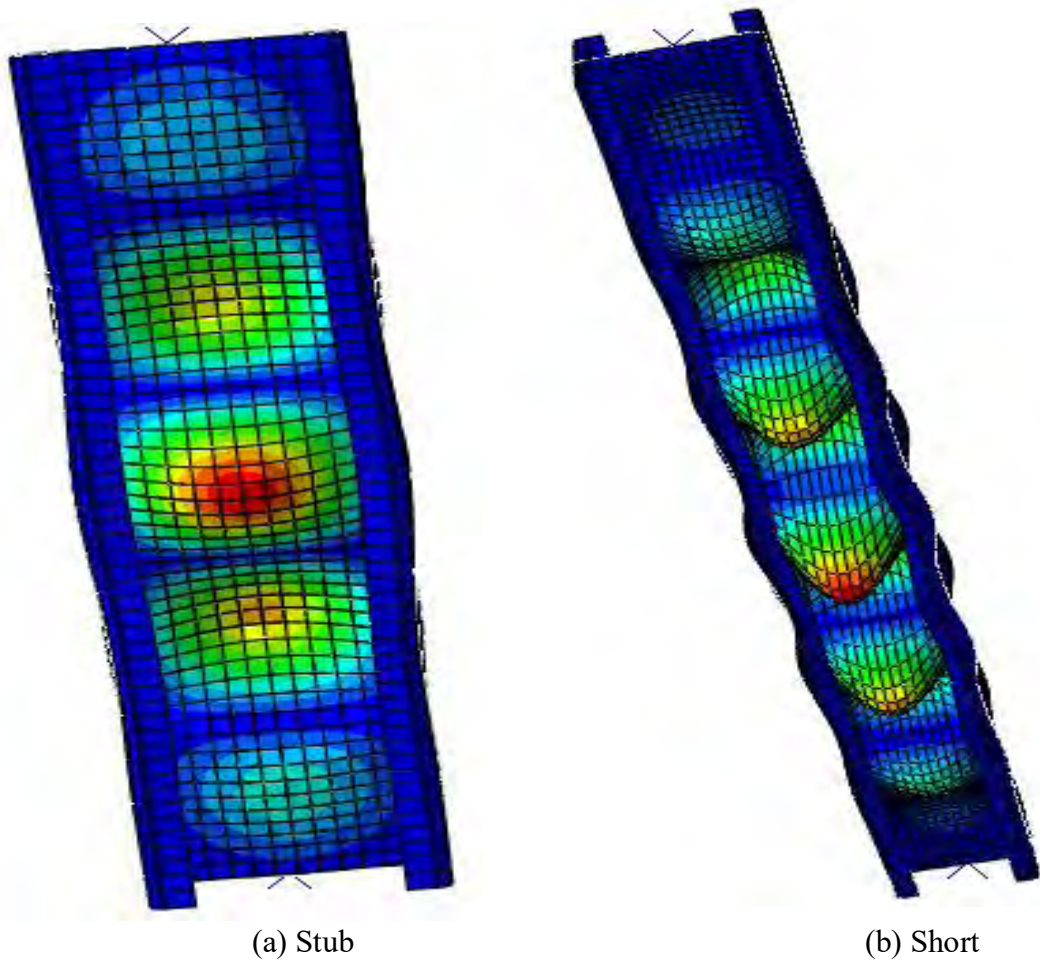
3.6 Modelling of local and global geometric imperfections

Local and global buckling behavior of back-to-back built up cold-formed steel lipped channel sections depends on numerous factors such as: Depth to thickness ratio (D/t), width to thickness ratio (b/t), slenderness around both x and y axis and spacing of tied joint [42].

Distribution of initial imperfections was simulated using the deformed shapes obtained from elastic buckling analysis [8]. Figure 3-7 shows the imperfection contours for stub, short, intermediate and slender column respectively. The lowest eigen mode was used as the imperfection shape. Four different amplitudes, Dawson-Walker model for cold formed steel [45], $t/100$, $t/10$ and 0.5% of t where t is the section thickness, were used to observe the effect of initial imperfections on compressive behavior.

Four different amplitudes, $L/1000$, $L/100$, $L/200$ and $L/300$ where L is the length were used to observe the effect of global imperfections on compressive behavior.

For stub and short column only local imperfections, for slender column only global imperfections and for intermediate columns both local and global imperfections were considered.



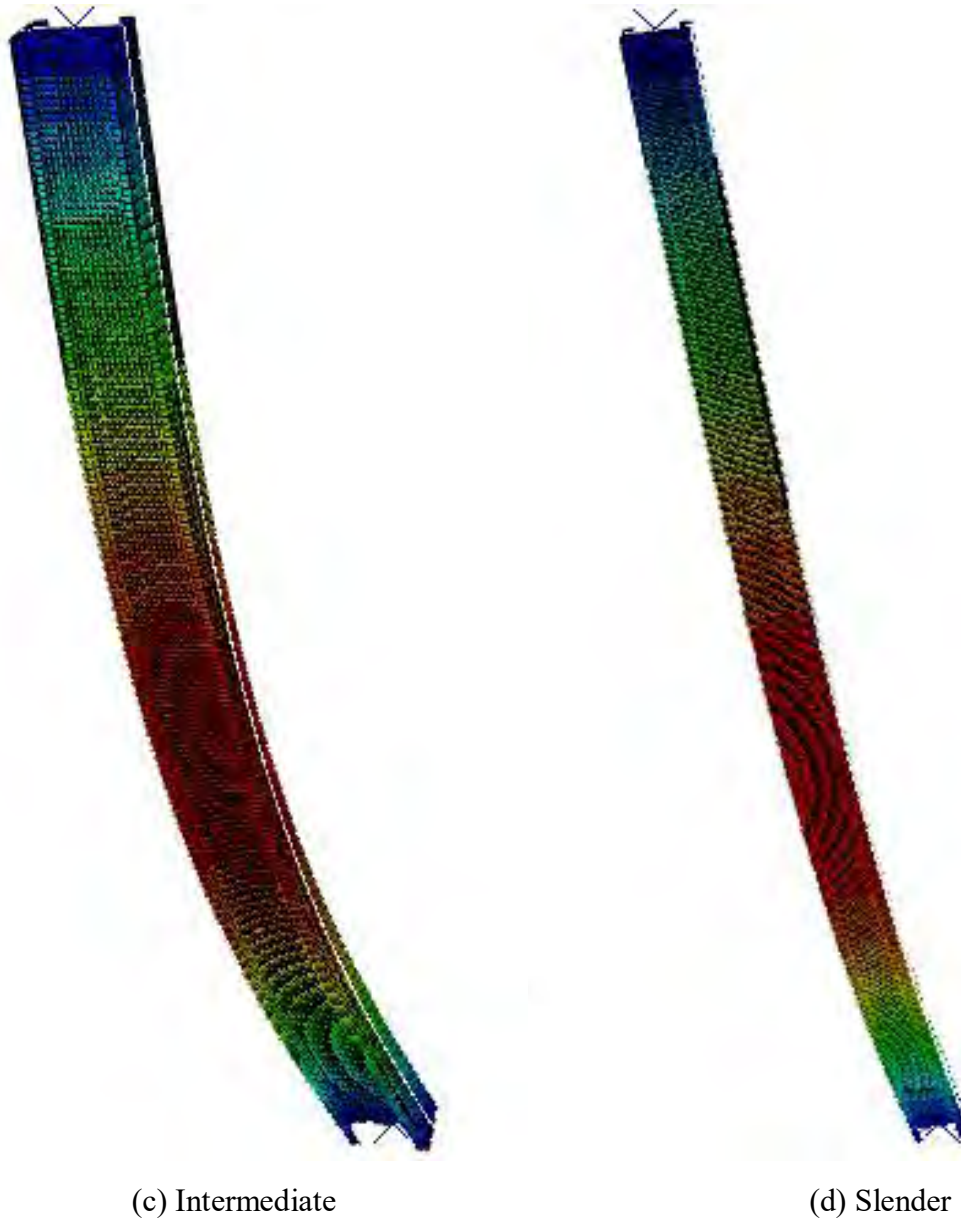


Figure 3-7. Initial imperfection contours for different columns

3.7 Verification of finite element model with experimental results

The finite element models developed in this research for back-to-back cold-formed steel lipped channels by following above mentioned techniques are verified against the test results reported by Ting [3]. The built up lipped channels were tested under compression for different column lengths beginning from stub (length of 300 mm) to slender (length of 2000 mm) columns. Figure 2-2 shows details of the section used in the experiment to be referred to as BU75. The measured specimen dimensions are available in [3]. In total 30 specimens were tested in four different categories based on length as:300 mm, 500 mm, 1000 mm and 2000 mm. Specimens were labeled in a way

so that type of section, longitudinal spacing between the tied joint, nominal length of specimen and specimen number were represented by the label. Figure 3-8 shows a representation of the labelling used in this research.

Tensile coupon tests were conducted to determine the material properties of the steel used in the experimental program. The measured average yield and ultimate stresses were 560 MPa and 690 MPa respectively, while the Young's modulus was 207000 MPa. Axial load was applied to the specimens by a 600 kN capacity GOTECH, GT-7001-LC60 Universal Testing Machine (UTM). The loading rate was kept below 25 kg/cm²/s for all specimens. The columns were centered and aligned to ensure that load would be applied through the centroid of the sections. An LVDT having 0.11 mm accuracy was used to measure initial geometric imperfections exist in the sections. Other details related with experimental program can be found in Ting's study [3].

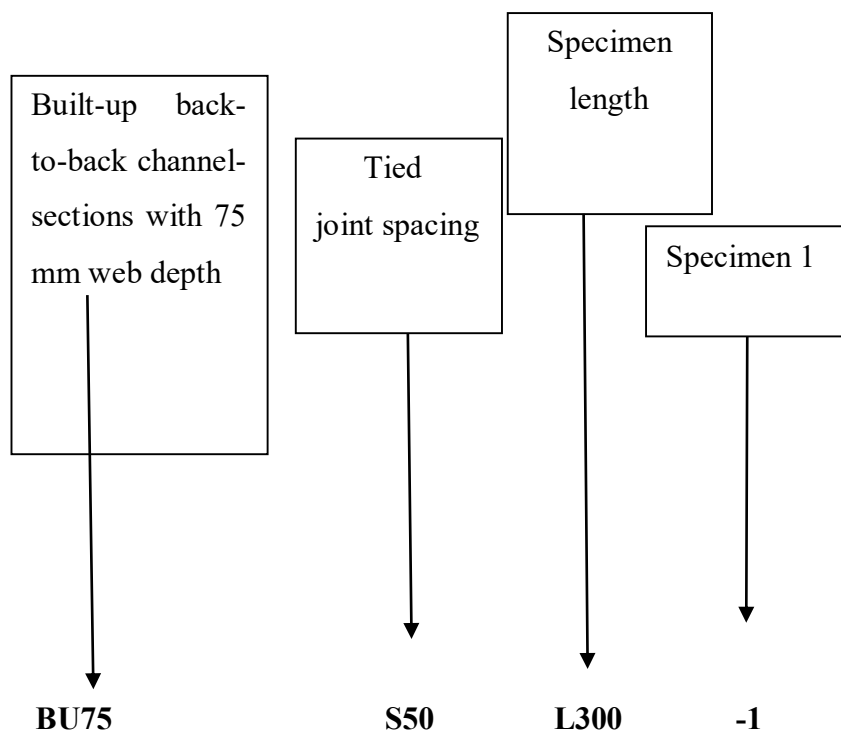


Figure 3-8. Specimen labeling [3]

Table 3-4. Comparison of capacity predicted by present model and experimental results [3]

Specimen ID	Experiment Results		FEA Results		
	P_{EXP}	$P_{FEA} (min)$	$P_{FEA} (max)$	$P_{EXP}/P_{FEA} (max)$	$P_{EXP}/P_{FEA} (min)$
	kN	kN	kN	-	-
Stub					
BU75-S50-L300-1	120.7	110.73	123.16	1.09	0.98
BU75-S50-L300-2	118.8	106.07	118.8	1.12	1.00
BU75-S50-L300-3	118.7	105.98	118.7	1.12	1.00
BU75-S100-L300-2	117.5	102.17	117.5	1.15	1.00
BU75-S100-L300-3	122.7	101.4	116.9	1.21	1.05
BU75-S100-L300-4	115.4	106.85	118.97	1.08	0.97
BU75-S200-L300-1	122.5	103.81	112.38	1.18	1.09
BU75-S200-L300-2	119.1	100.9	108.27	1.18	1.10
BU75-S200-L300-3	113.1	102.81	113	1.10	1.00
Short					
BU75-S100-L500-1	83.0	96.51	102.45	0.86	0.81
BU75-S100-L500-3	74.1	93.8	98.8	0.79	0.75
BU75-S200-L500-1	86.2	95.78	99.08	0.90	0.87
BU75-S200-L500-2	88.9	83.08	91.65	1.07	0.97
BU75-S200-L500-3	93.6	93.5	96.5	1.00	0.97
BU75-S400-L500-1	74.8	78.74	83.1	0.95	0.90
BU75-S400-L500-2	80.6	80.6	84.84	1.00	0.95

Table 3-4. (Continued)

Specimen ID	Experiment Results		FEA Results		
	P_{EXP}	$P_{FEA} (min)$	$P_{FEA} (max)$	$P_{EXP}/P_{FEA} (max)$	$P_{EXP}/P_{FEA} (min)$
	kN	kN	kN	-	-
Intermediate					
BU75-S225-L1000-1	47	33.1	43.93	1.42	1.07
BU75-S225-L1000-2	46.3	33.07	43.27	1.40	1.07
BU75-S450-L1000-1	50.4	34.76	42.35	1.45	1.19
BU75-S450-L1000-2	45	24.86	35.71	1.81	1.26
BU75-S450-L1000-3	41.8	32.15	36.99	1.30	1.13
BU75-S900-L1000-1	39.9	34.1	39.5	1.17	1.01
BU75-S900-L1000-2	33.7	32.09	37.03	1.05	0.91
BU75-S900-L1000-3	31.5	31.82	37.5	0.99	0.84
Slender					
BU75-S475-L2000-2	10.9	9.82	12.53	1.11	0.87
BU75-S475-L2000-3	10.8	9.82	12.41	1.10	0.87
BU75-S950-L2000-2	8.8	9.36	11.89	0.94	0.74
BU75-S950-L2000-3	8.6	10	11.32	0.86	0.76
BU75-S1900-L2000-2	7.6	8.35	11.34	0.91	0.67
BU75-S1900-L2000-3	7.5	9.15	11.72	0.82	0.64

Table 3-5. Representation of P_{EXP}/P_{FE} for all types of imperfections

	Full nonlinear stress strain Curve				Simplified elastic plastic stress strain curve			
Model Name	Imp 1	Imp 2	Imp 3	Imp 4	Imp 1	Imp 2	Imp 3	Imp 4
Stub								
BU75-S50-L300-1	0.99	0.98	1.01	1.00	1.09	1.08	1.08	1.09
BU75-S50-L300-2	1.00	1.00	1.00	1.00	1.12	1.12	1.12	1.11
BU75-S50-L300-2	1.00	1.00	1.00	1.00	1.12	1.12	1.12	1.11
BU75-S100-L300-2	1.00	1.00	1.00	1.02	1.14	1.15	1.15	1.15
BU75-S100-L300-3	1.05	1.05	1.05	1.05	1.19	1.20	1.21	1.19
BU75-S100-L300-4	0.97	0.97	0.97	0.97	1.08	1.08	1.08	1.08
BU75-S200-L300-1	1.10	1.09	1.10	1.09	1.17	1.18	1.18	1.17
BU75-S200-L300-2	1.12	1.11	1.11	1.10	1.18	1.18	1.17	1.16
BU75-S200-L300-3	1.00	1.00	1.00	1.00	1.10	1.08	1.08	1.09
Average	1.03	1.02	1.03	1.03	1.13	1.13	1.13	1.13
COV	0.05	0.05	0.05	0.04	0.04	0.04	0.04	0.04
Short								
BU75-S100-L500-1	0.82	0.83	0.83	0.81	0.86	0.86	0.86	0.85
BU75-S100-L500-3	0.75	0.76	0.76	0.75	0.78	0.78	0.79	0.79
BU75-S200-L500-1	0.88	0.89	0.89	0.87	0.88	0.90	0.90	0.87
BU75-S200-L500-2	0.98	1.02	0.99	0.97	1.00	1.07	1.00	0.98
BU75-S200-L500-3	0.97	0.99	0.99	0.99	0.98	1.00	1.00	0.99
BU75-S400-L500-1	0.91	0.91	0.91	0.90	0.95	0.95	0.95	0.94
BU75-S400-L500-2	0.96	0.95	0.96	0.96	1.00	0.99	0.99	0.99
Average	0.90	0.91	0.90	0.89	0.92	0.94	0.93	0.92
COV	0.10	0.10	0.10	0.10	0.09	0.10	0.09	0.09

Table 3-5. (Continued)

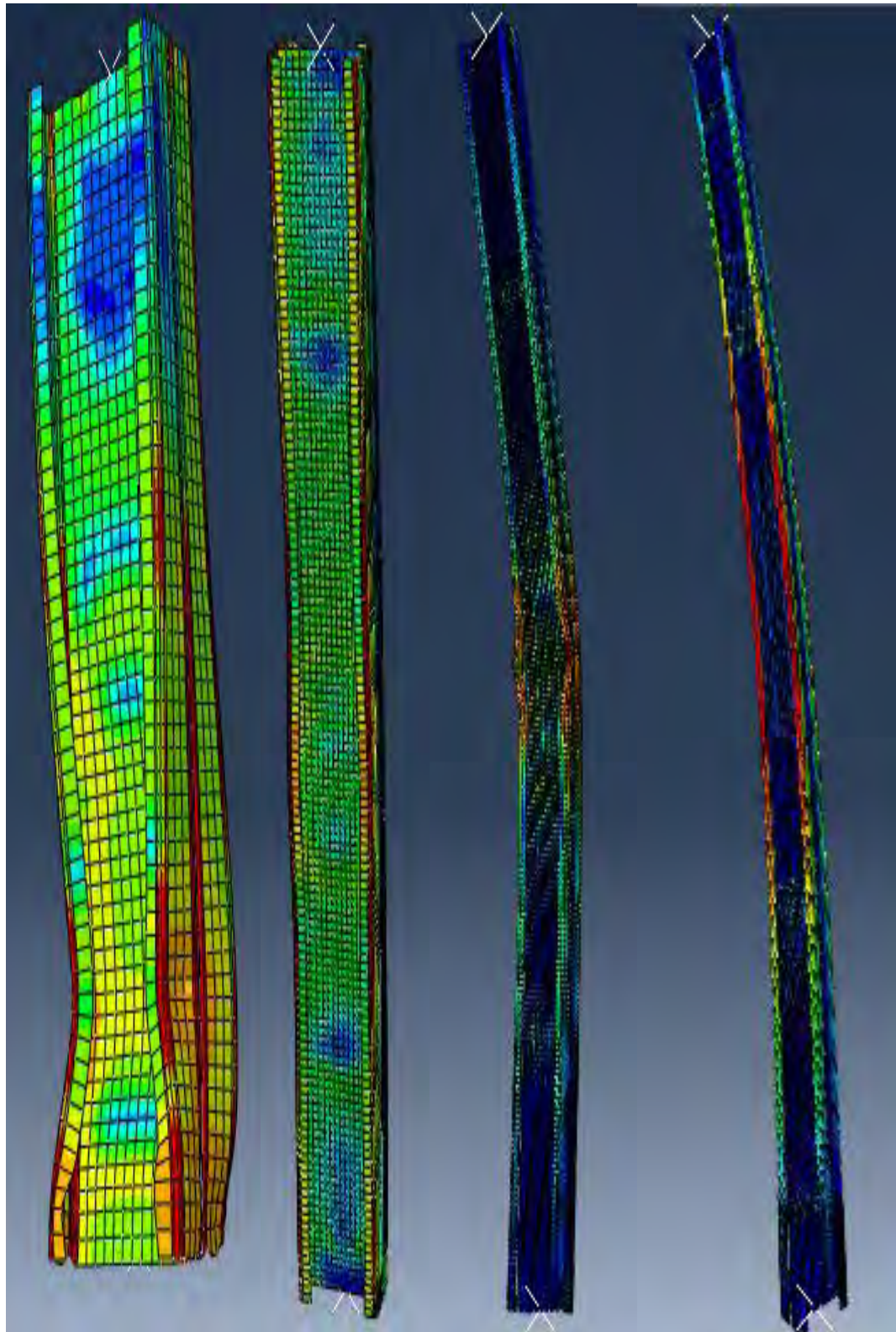
Model Name	Full nonlinear stress strain Curve				Simplified elastic plastic stress strain curve			
	Imp 1	Imp 2	Imp 3	Imp 4	Imp 1	Imp 2	Imp 3	Imp 4
Slender								
BU75-S475-L2000-2	0.87	1.10	0.97	0.93	0.89	1.11	0.97	0.93
BU75-S475-L2000-3	0.89	1.09	0.97	0.93	0.87	1.10	0.97	0.92
BU75-S950-L2000-2	0.74	0.93	0.86	0.78	0.76	0.94	0.84	0.78
BU75-S950-L2000-3	0.77	0.84	0.79	0.85	0.76	0.85	0.78	0.86
BU75-S1900-L2000-2	0.67	0.77	0.83	0.91	0.71	0.79	0.81	0.87
BU75-S1900-L2000-3	0.65	0.79	0.81	0.66	0.64	0.78	0.82	0.65
Average	0.77	0.92	0.87	0.84	0.77	0.93	0.87	0.84
COV	0.13	0.16	0.09	0.13	0.12	0.16	0.10	0.13

Intermediate	Full nonlinear Stress Strain Curve					
	Imp 1-L/1000	Imp 1-L/1000	Imp 1-L/1000	Imp 2-L/300	Imp 2-L/300	Imp 2-L/300
Local Imperfection	t/10	t/100	0.2t	t/10	t/100	0.2t
Specimen						
BU75-S225-L1000-1	1.07	1.09	1.08	1.25	1.25	1.42
BU75-S225-L1000-2	1.08	1.09	1.1	1.27	1.27	1.4
BU75-S450-L1000-1	1.19	1.20	1.25	1.43	1.42	1.44
BU75-S450-L1000-2	1.28	1.35	1.6	1.8	1.78	1.80
BU75-S450-L1000-3	1.19	1.17	1.13	1.29	1.28	1.29
BU75-S900-L1000-1	1.02	1.05	1.01	1.16	1.15	1.16
BU75-S900-L1000-2	0.94	0.91	0.92	1.04	1.03	1.04
BU75-S900-L1000-3	0.85	0.90	0.84	0.98	0.99	0.98
Average	1.07	1.09	1.11	1.27	1.27	1.31
COV	0.13	0.14	0.21	0.20	0.20	0.20

Table 3-5. (Continued)

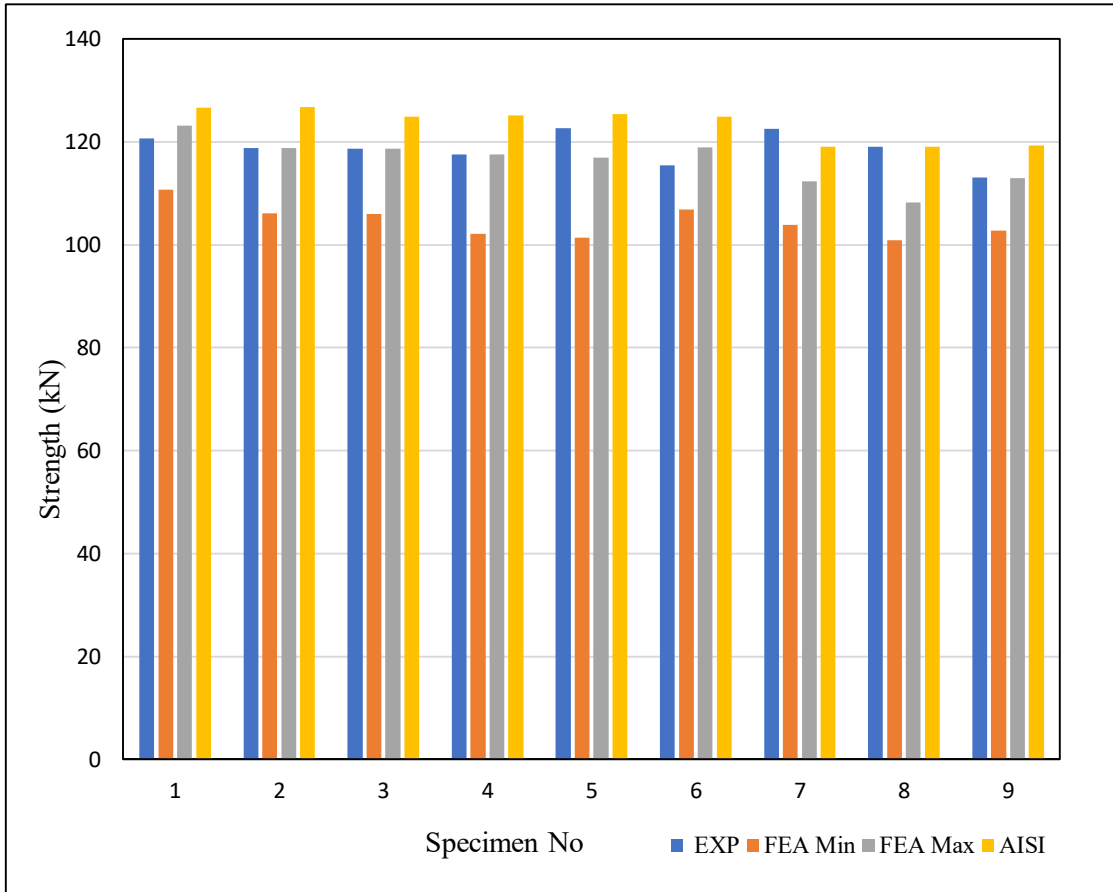
	Simplified elastic plastic stress strain curve					
BU75-S225-L1000-1	1.08	1.08	1.07	1.28	1.27	1.38
BU75-S225-L1000-2	1.07	1.08	1.11	1.29	1.29	1.36
BU75-S450-L1000-1	1.23	1.21	1.26	1.43	1.44	1.45
BU75-S450-L1000-2	1.26	1.4	1.5	1.81	1.75	1.80
BU75-S450-L1000-3	1.22	1.22	1.24	1.29	1.30	1.30
BU75-S900-L1000-1	1.02	1.02	1.03	1.17	1.16	1.17
BU75-S900-L1000-2	0.91	0.92	0.93	1.04	1.05	1.05
BU75-S900-L1000-3	0.86	0.87	0.88	0.99	0.98	0.98
Average	1.08	1.10	1.13	1.29	1.28	1.31
COV	0.14	0.16	0.18	0.20	0.19	0.20

The numerical modelling for verification with experiments includes 2 types of material properties [full nonlinear stress-strain curve, simplified elastic plastic stress strain curve] and 4 different local imperfection amplitudes for stub and short columns. Therefore, there are eight different numerical data of failure load for one single stub or short column. For intermediate column, two types of global imperfection with a combination of three types of local imperfection were applied for both type of material modelling. Thus there are twelve different numerical data of maximum force for one single intermediate column. For slender columns, four types of global imperfection were applied for both type of material modelling. Hence there are eight different numerical data of maximum force for one single slender column. Thus from experimental data of 30 specimens 272 numerical models were analyzed. Figure 3-9 shows the modes of failure for the stub, short, intermediate and slender columns whereas Table 3-4 and Figure 3-10 represents the comparison of capacity predicted by present model and experimental results. Figure 3-11 and Figure 3-12 represents the comparison of deformed shapes between experimental and FEA results and comparison of load-displacement curve between experimental and FEA results for one stub column (BU75-S50-L300-1) respectively. Figure 3-13 represents the comparison of capacity vs slenderness ratio curve between experimental and FEA results for all four types of columns.

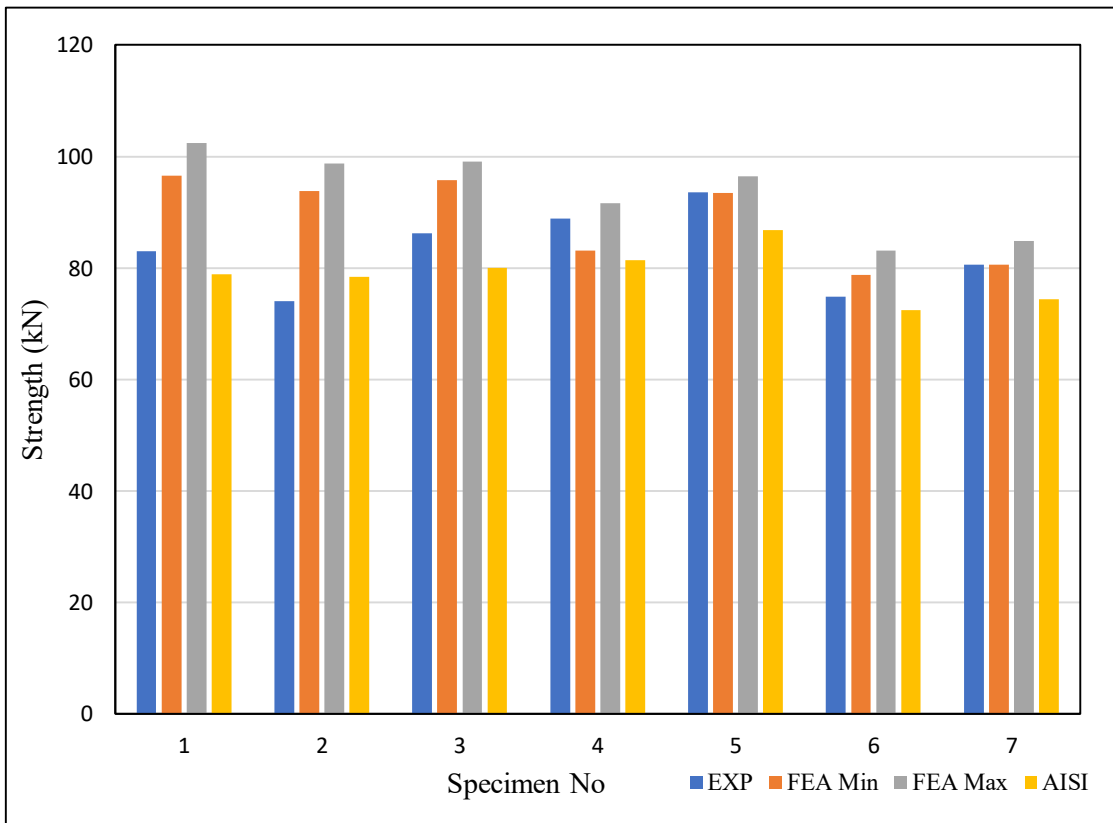


(a) Stub column (b) Short column (c) Intermediate column (d) Slender column

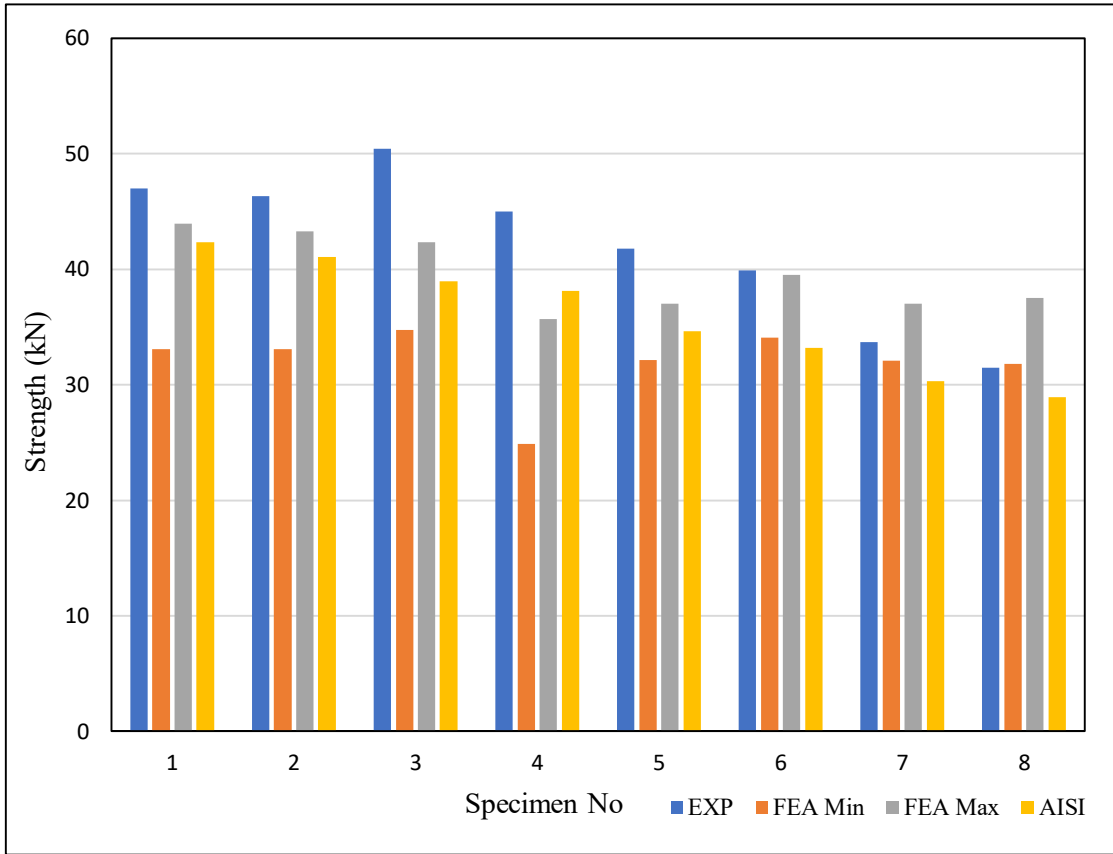
Figure 3-9. Failure pattern of back-to-back built-up lipped channels under axial load



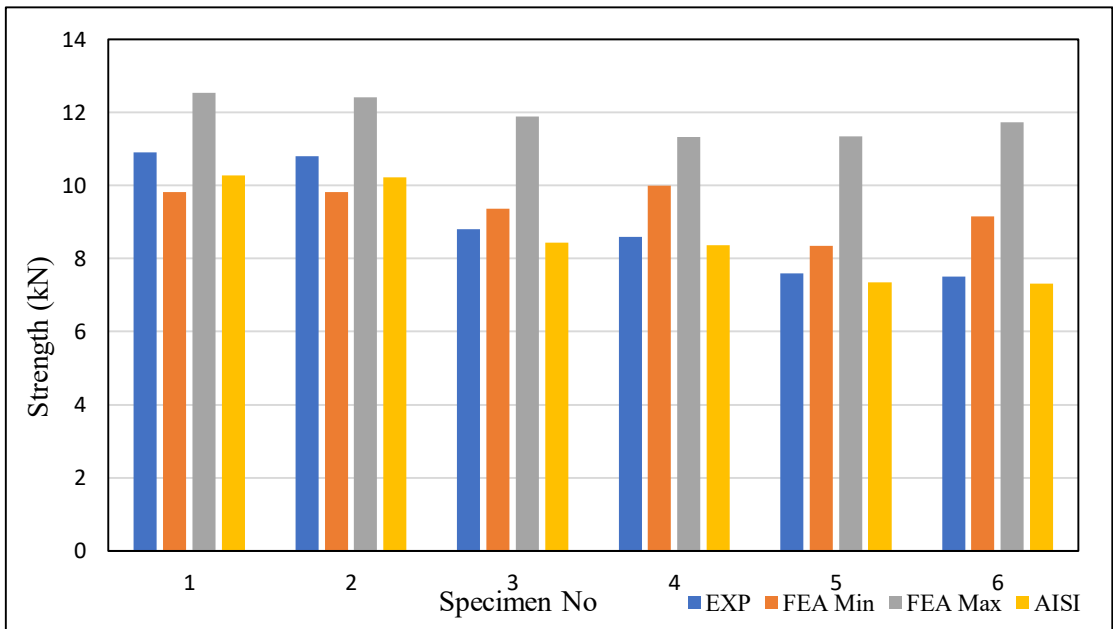
(a)



(b)



(c)

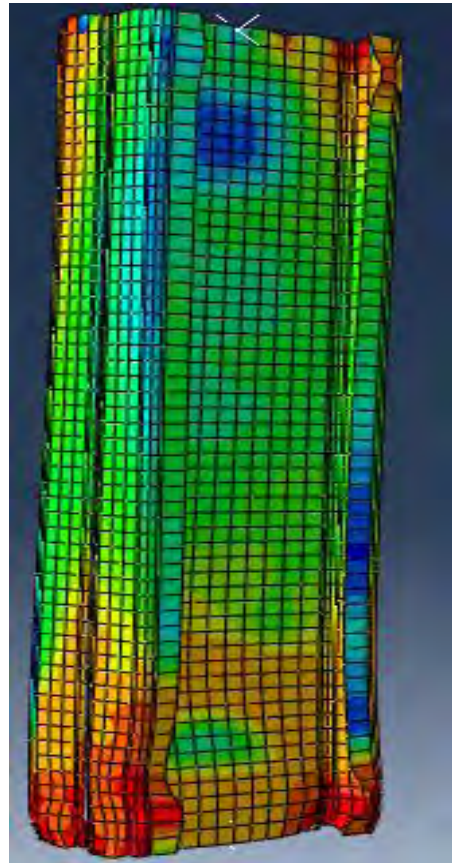


(d)

Figure 3-10. Comparison of capacity predicted by present model and experimental results for (a) stub column (b) short column (c) intermediate column and (d) slender column



(a) Experimental



(b) FEA

Figure 3-11. Comparison of deformed shapes between experimental and FEA

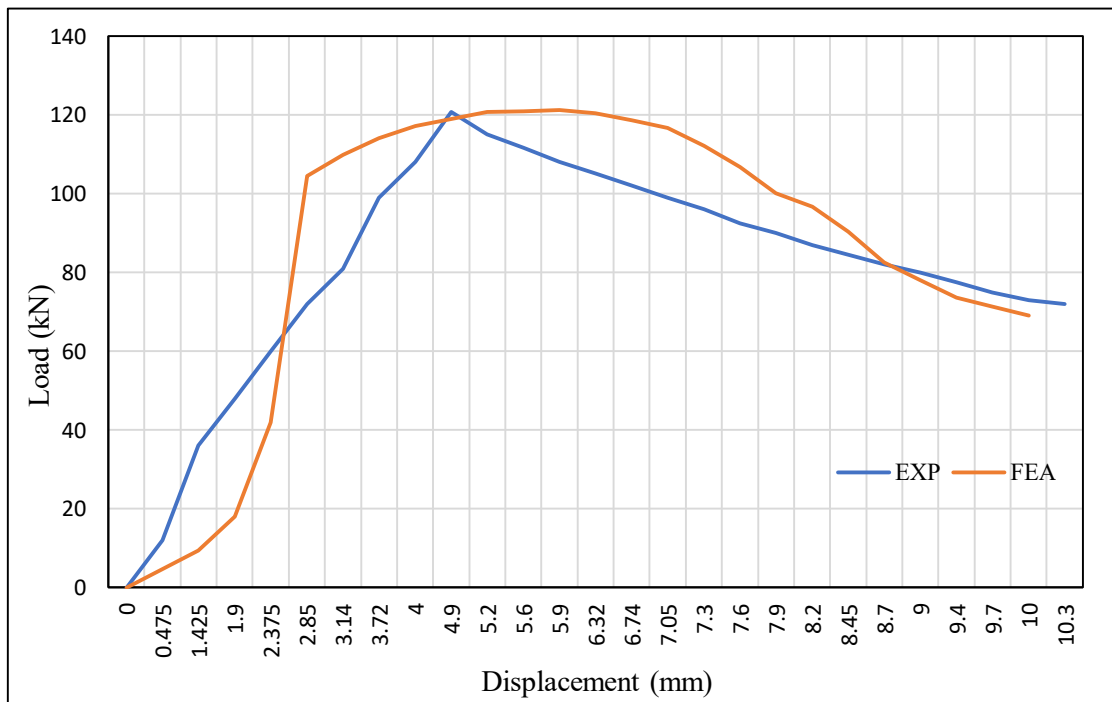
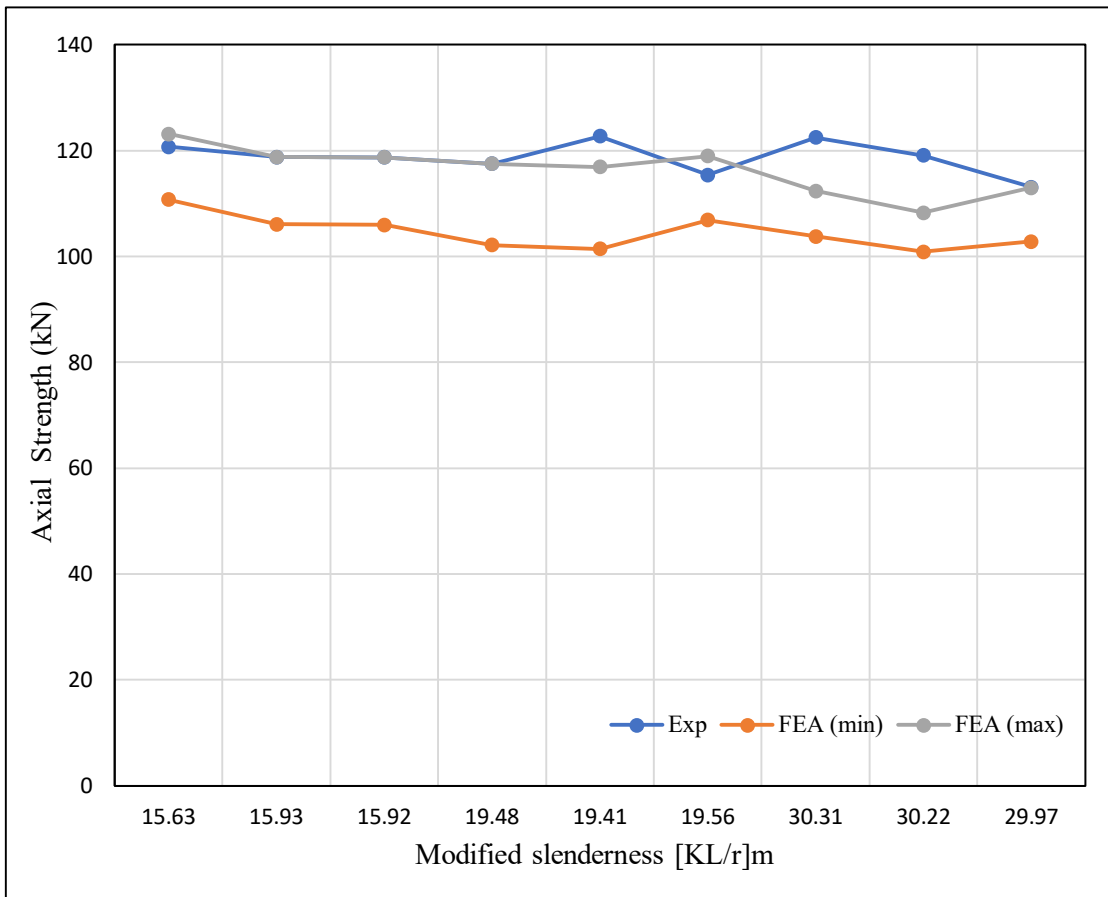
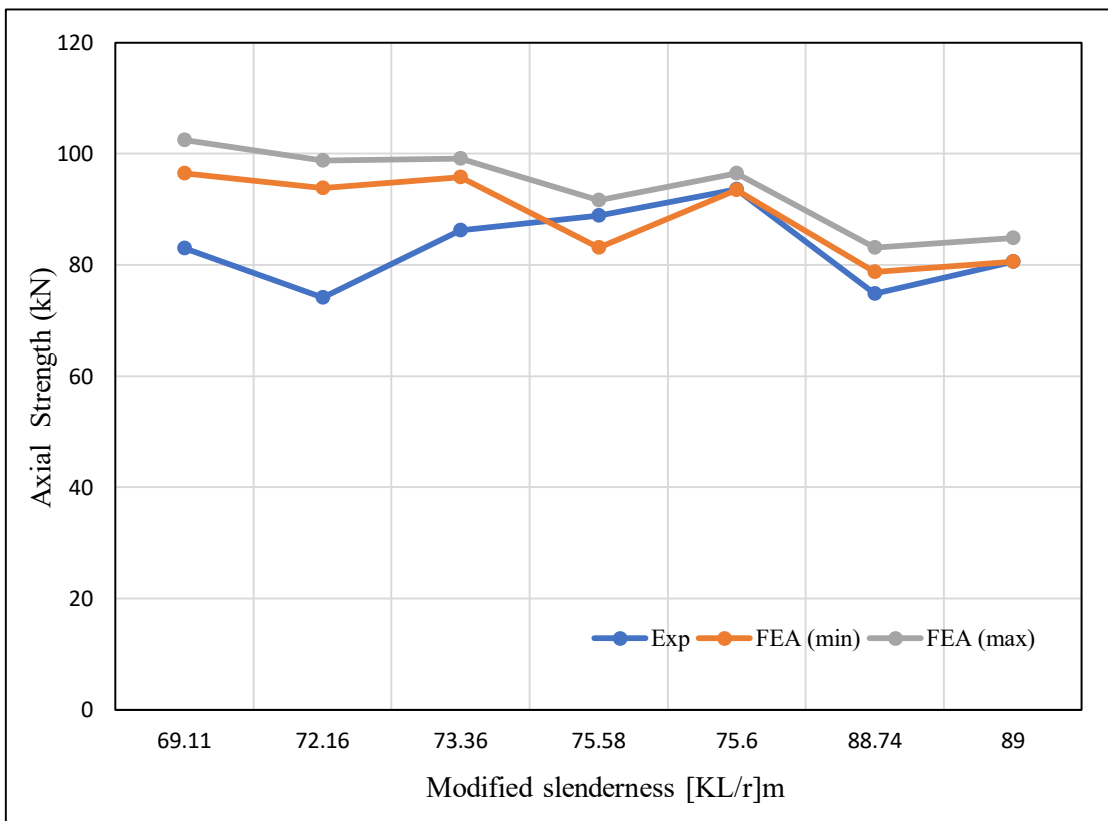


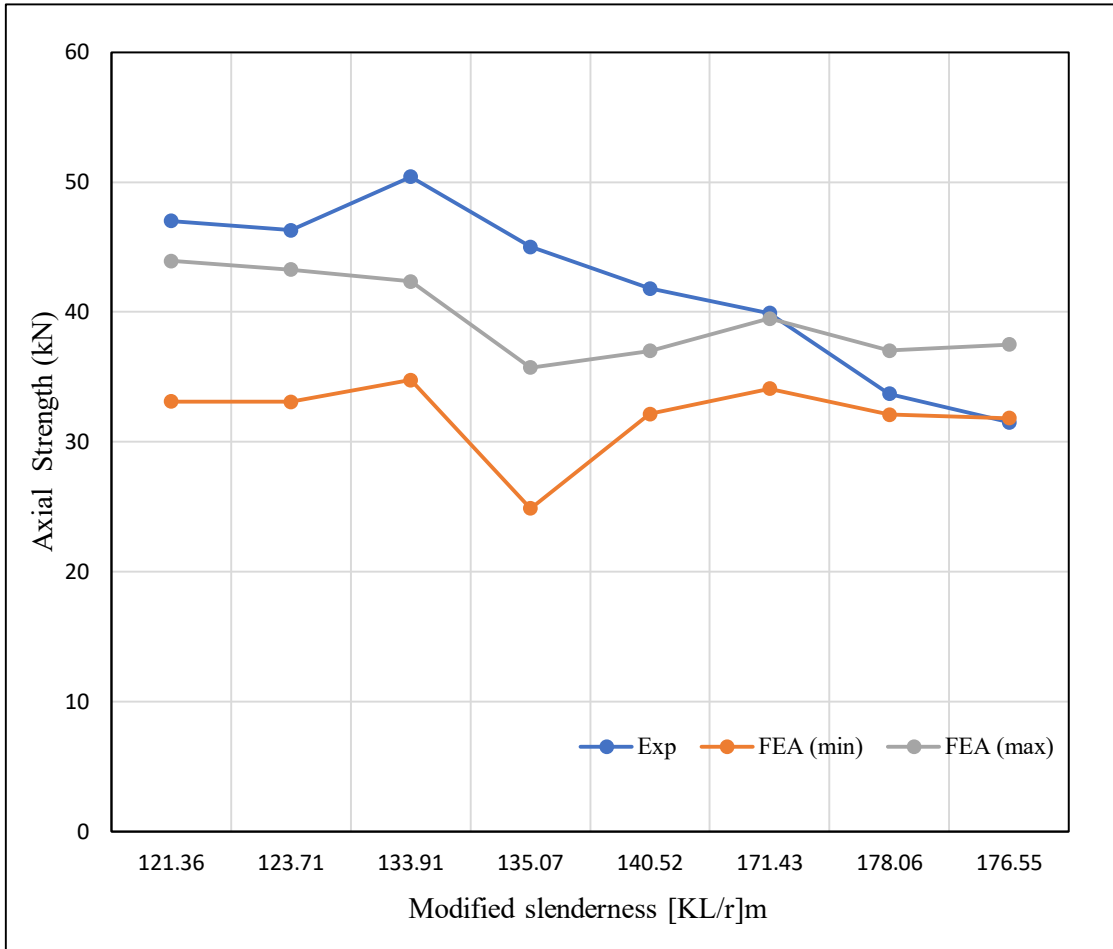
Figure 3-12. Comparison of load-displacement curve between experimental and FEA results (BU75-S50-L300-1)



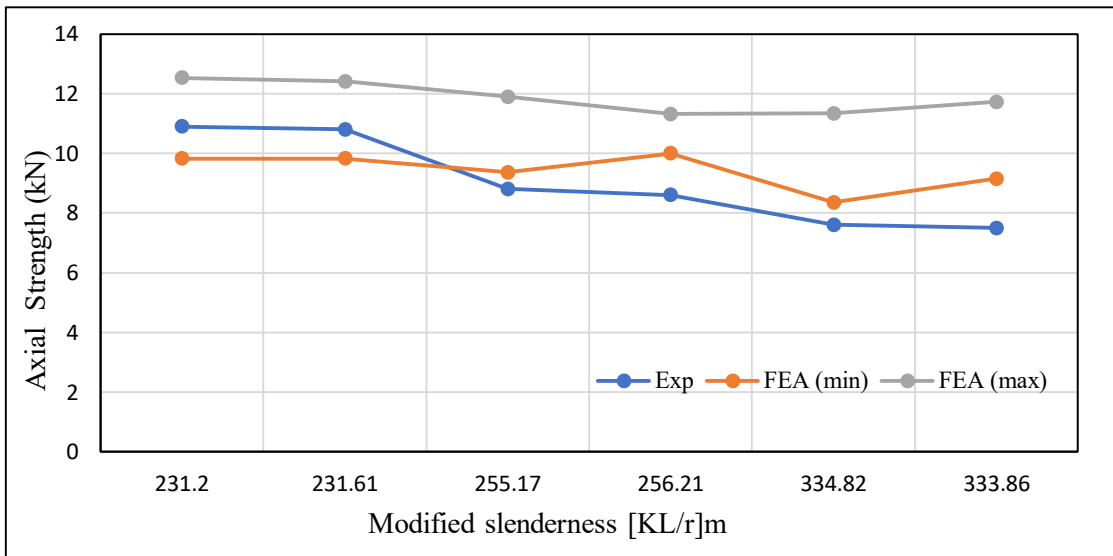
(a)



(b)



(c)



(d)

Figure 3-13. Comparison of capacity vs slenderness ratio curve between experimental and FEA results for (a) stub (b) short (c) intermediate and (d) short column

After investigating all these data, a conclusion was drawn on respective of accuracy regarding material modelling as well as imperfection amplitude. It is concluded that full nonlinear stress-strain curve gives better accuracy than simplified elastic-plastic model as presented in Table 3-5. By using local imperfection as $t/100$ numerical value matches better with experimental data for stub and short columns which is also reported in [38]. By using global imperfection as $L/100$ numerical value matches better with experimental data for slender columns whereas use of the combination of $L/1000$ as global imperfection and $t/10$ as local imperfection numerical value matches better with experimental data for intermediate columns.

Chapter 4

PARAMETRIC STUDY FOR BACK-TO-BACK CFS LIPPED CHANNELS

4.1 Introduction

A parametric study is carried out in this research by using a validated finite element model. Key parameter varied was the width-to-thickness ratio and lip height-to-thickness ratio for the lip channel covering a wide range of lengths named as stub, short, intermediate and slender respectively. Stub column is defined as the short compression member which do not have a foundation and directly rests on a slab or column to transfer the load on the primary beam. Short column is the one whose ratio of effective length to its least lateral dimension is less than or equal to 12. Steel columns with a slenderness ratio of $40 \leq Kl/r \leq 120$ are defined as intermediate columns. A column is said to be slender if its cross-sectional dimensions are small compared to its length. Two different material models are used. The results of parametric study were further used to evaluate the existing code provided guidelines to design back-to-back built-up CFS lipped channels for axial strength.

4.2 Parametric Study

With the purpose of examining the effect of width-to-thickness ratio (b/t) and lip height-to-thickness ratio (l/t) on axial strength of back-to-back built-up cold-formed steel lipped channel sections, a total of 88 different finite element models with various section dimensions, different lengths (stub, short, intermediate and slender) were considered. The number of tied joints was kept constant as three for all types of columns. In total four types of columns were considered as presented in Table 4-1.

Table 4-1. Types of columns considered in parametric study

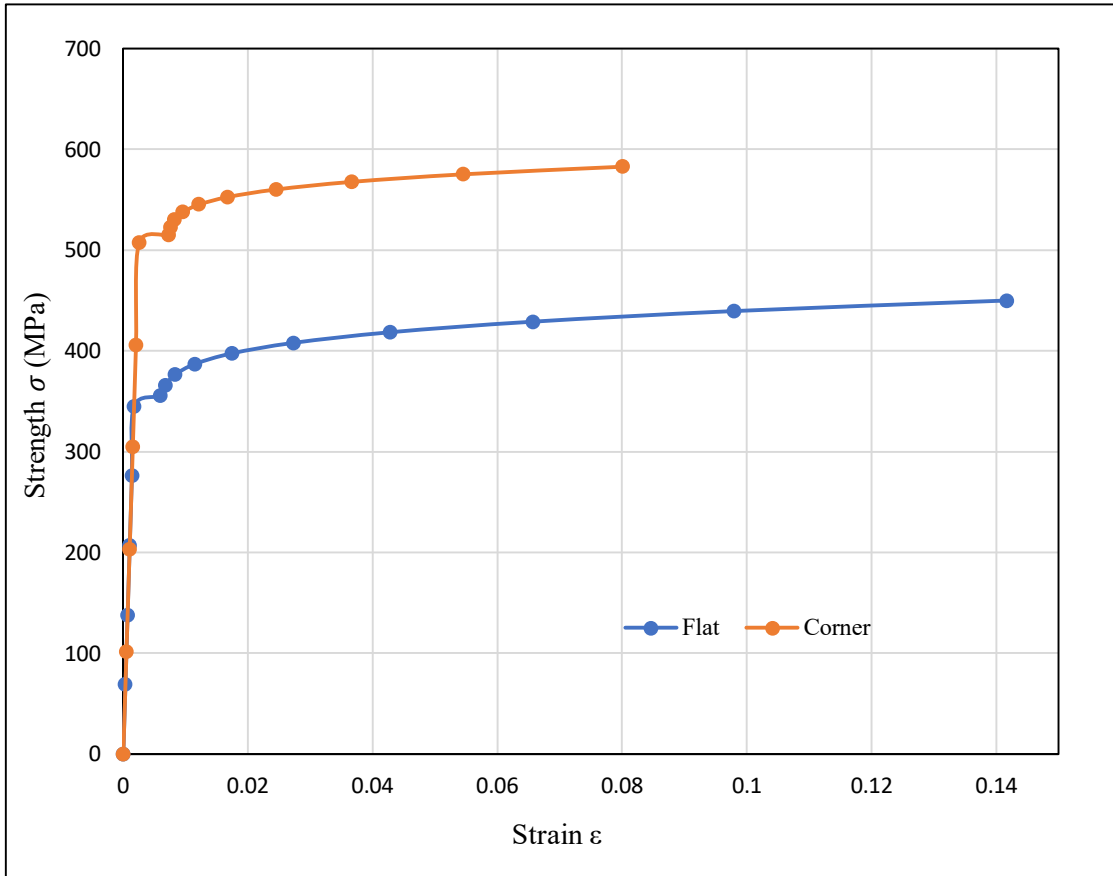
Type of column	Length (mm)	Modified slenderness ratio $(Kl/r)_m$
Stub	300	2.73 - 9.19
Short	700	12.38 - 40.12
Intermediate	1200	21.22 - 68.78
Slender	2200	38.9 - 126.09

Two different material models are used. Full range stress strain curve has been developed for both types of material according to the equations given by Gardner and Yun [43] as represented in Figure 4-1. Yield strength and ultimate tensile strength data have been collected from a renowned local steel fabricator, Bangladesh for two mostly used steel grade because of unavailability of full tensile coupon test data. Material specification is presented in Table 4-2.

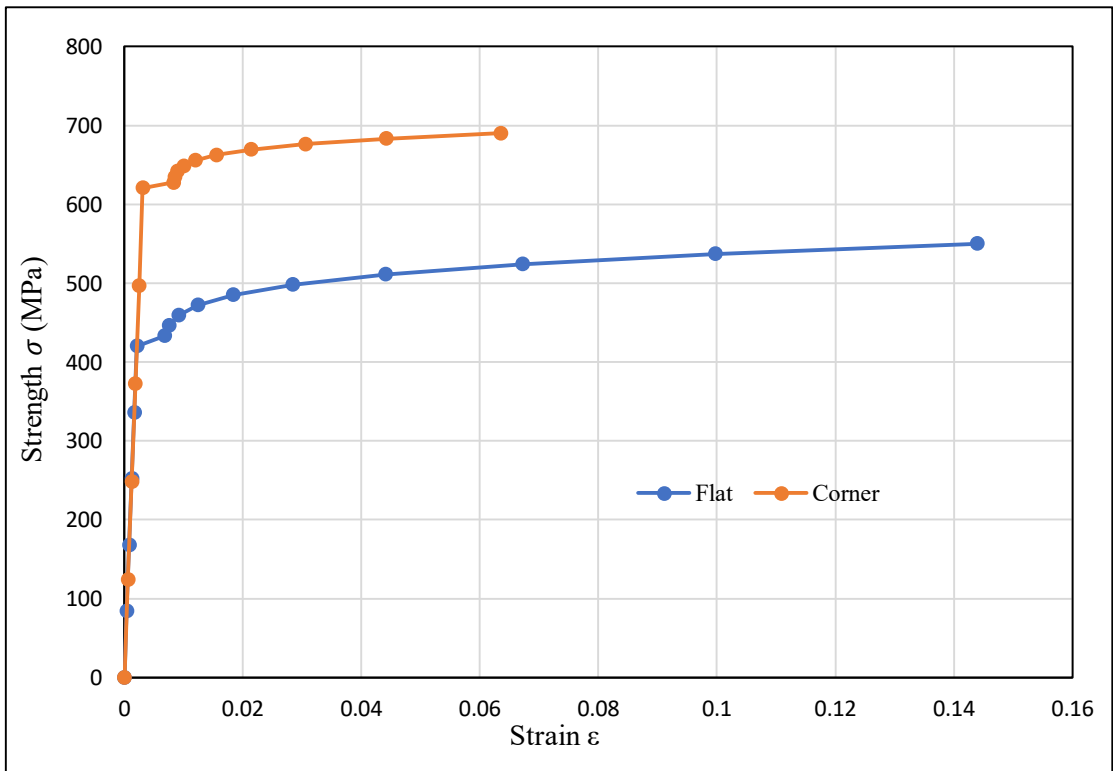
Table 4-2. Specification of materials used in parametric study

Name of material	Yield strength (MPa)	Ultimate tensile strength (MPa)	Modulus of elasticity (MPa)	Poisson's ratio
Material 1	345	450	200000	0.3
Material 2	420	550	200000	0.3

Corner strength enhancement have been applied according to the equations given by Gardner and Yun [43]. In total 22 specimens were modelled under every material modelling for all four types (stub, short, intermediate and slender) of columns. So in total 88 models were analyzed.



(a)



(b)

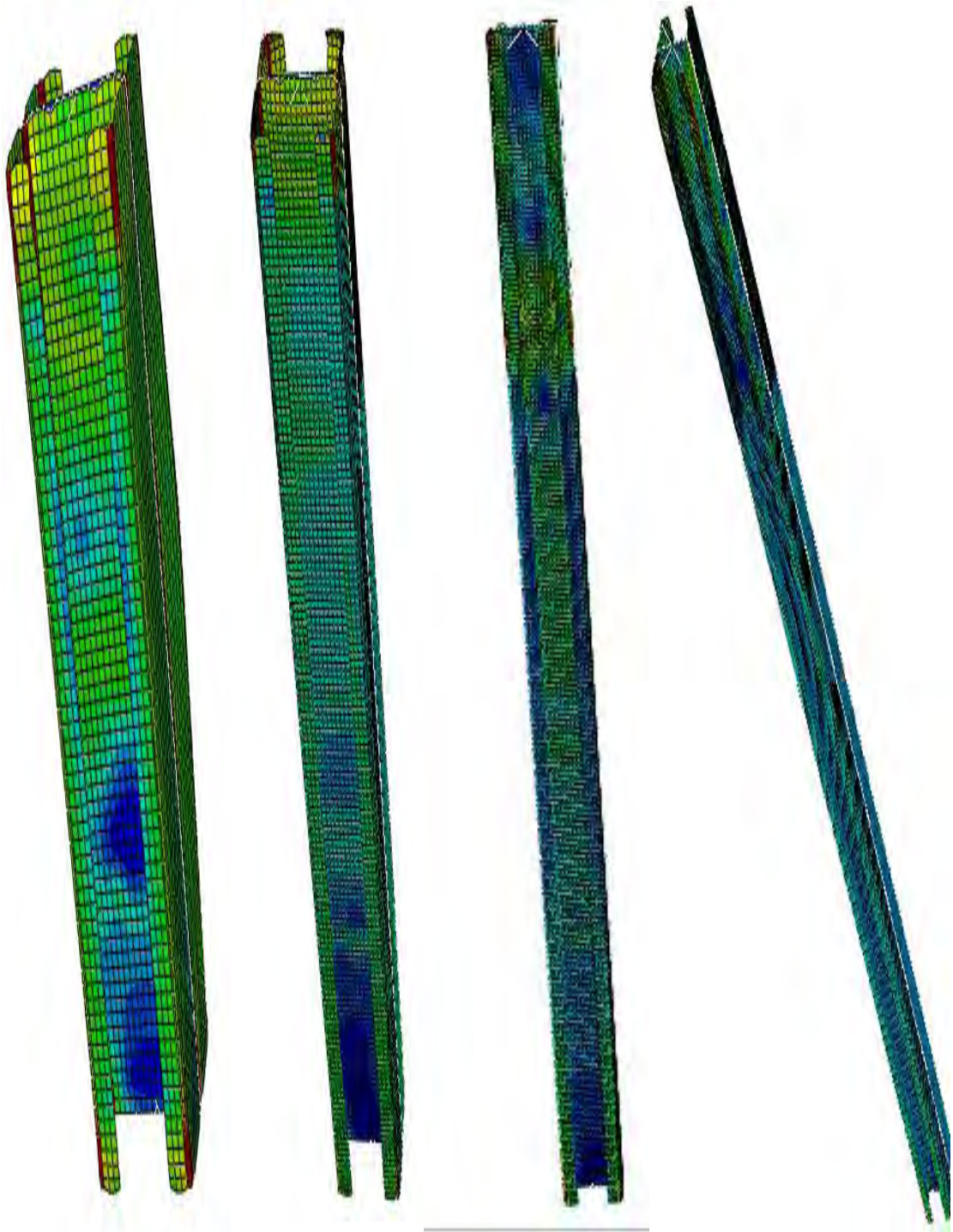
Figure 4-1. Full range stress-strain curve using (a) material 1 (b) material 2

Figure 4-2 shows the failure mode of stub, short, intermediate and slender column respectively. Eleven specimens were divided into two categories. For first six specimens web dimension of 80 mm, thickness of 1.20 mm and lip height of 18 mm is used. It makes constant lip height-to-thickness ratio (l/t) as 15 which is in accordance with Eurocode as well as AISI. Various flange dimension is used as 36mm, 48 mm, 60 mm, 72 mm, 84 mm and 108 mm respectively to use various flange-to-thickness ratio (b/t) as 30, 40, 50, 60, 70 and 90. According to Eurocode-1993 and AISI-2013 b/t ratio should be less than or equal to 60. So here four ratios have been taken within the limit and two ratios have been taken outside the limit to investigate the effect of not maintaining the ratio within the limits. For last five specimens web dimension of 100 mm, thickness of 1 mm and flange dimension of 40 mm is used. It makes constant flange-to-thickness ratio (b/t) as 40 which is in accordance with Eurocode as well as AISI. Various lip height is used as 15 mm, 20 mm, 25 mm, 30 mm and 40 mm respectively to use various lip height-to-thickness ratio (l/t) as 15, 20, 25, 30 and 40. According to Eurocode-1993 [40] and AISI-2013 l/t ratio should be less than or equal to 50. So here all the ratio has been taken within the limit as any l/t ratio beyond the limit will require a considerable increase in web dimension which may affect overall structural stability.

It was assumed that back-to-back CFS lipped channel sections were subjected to pure compression only. Bi-axial, uniaxial or even pure bending was not considered in this research. It was also assumed that stub column is totally restrained including rotation. For short, intermediate and slender column only flexural buckling was considered. Other types of buckling like distortional or any combination of two types of buckling was not considered in this study. Regarding axis, buckling only about minor axis was assumed to be contributor whereas buckling about major axis was ignored in this investigation.

4.1.1 Comparison of the FE results with Design Standards

Axial strengths calculated from finite element analyses are compared with strength calculated in accordance with AISI/AS-NZ code.



(a) Stub column (b) Short column (c) Intermediate column (d) Slender column

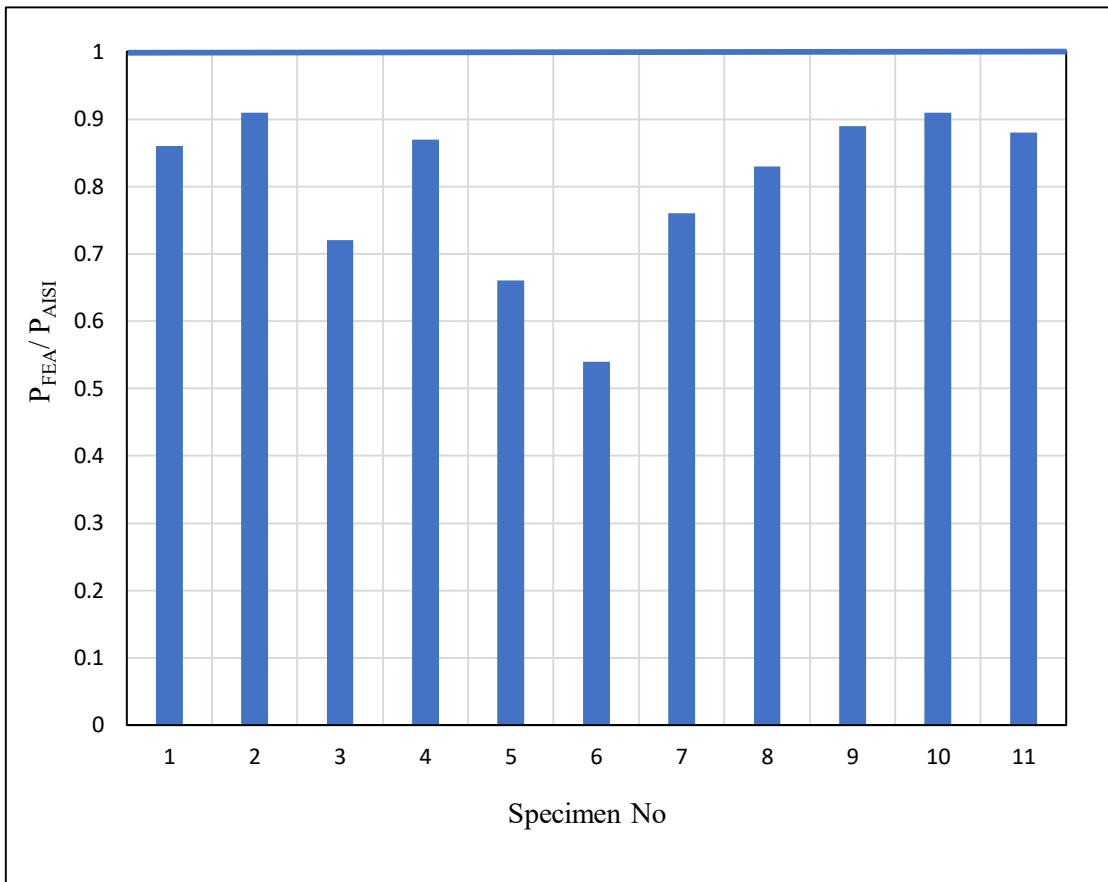
Figure 4-2. Von-Mises stress contour at ultimate load for different columns

Table 4-3. Comparison of Axial Capacity obtained from FE Analysis with AISI Design Guidelines (stub - material 1)

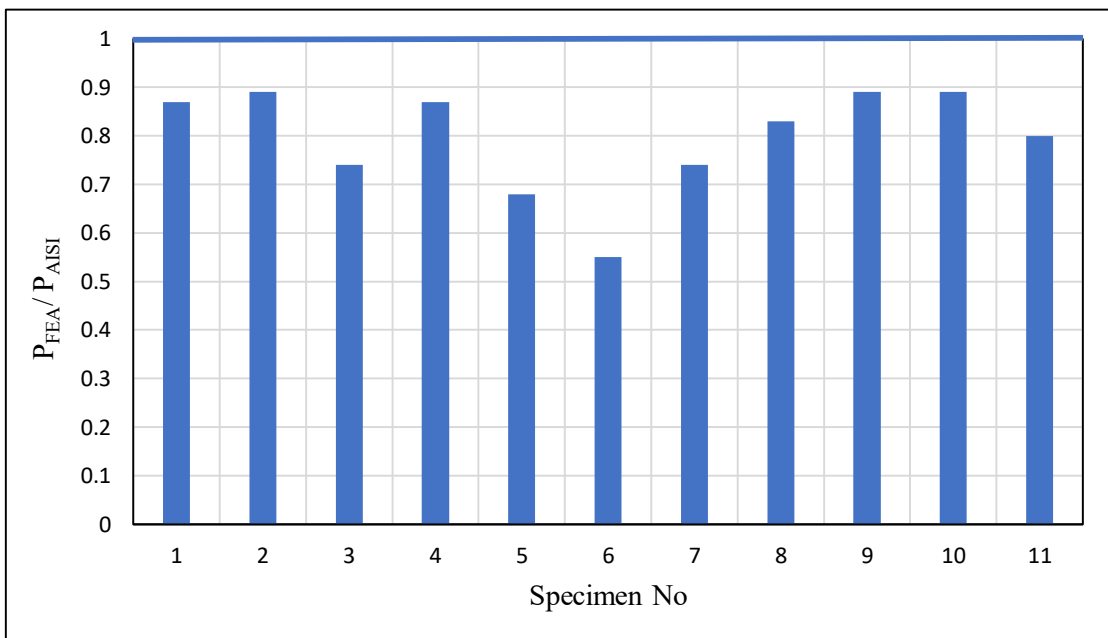
Specimen	Web A	Flange B	Lip C	Thickness t	b/t	c/t	Spacing S	P _{FEA}	P _{AISI}	P _{FEA} /P _{AISI}
	mm	mm	mm	mm	-	-	mm	kN	kN	-
BU80-L300	80	36	18	1.20	30	15	75	102.15	119	0.86
BU80-L300	80	48	18	1.20	40	15	75	103.59	113.71	0.91
BU80-L300	80	60	18	1.20	50	15	75	99.3	138.84	0.72
BU80-L300	80	72	18	1.20	60	15	75	97.08	111.76	0.87
BU80-L300	80	84	18	1.20	70	15	75	96.74	146.21	0.66
BU80-L300	80	108	18	1.20	90	15	75	93.29	173.36	0.54
BU100-L300	100	40	15	1.00	40	15	75	70.8	93.32	0.76
BU100-L300	100	40	20	1.00	40	20	75	75.57	91.38	0.83
BU100-L300	100	40	25	1.00	40	25	75	77.56	87.60	0.89
BU100-L300	100	40	30	1.00	40	30	75	76.59	84.53	0.91
BU100-L300	100	40	40	1.00	40	40	75	74.6	85.22	0.88
Avg.										0.80
COV										0.17

**Table 4-4. Comparison of Axial Capacity obtained from FE Analysis with
AISI Design Guidelines (stub - material 2)**

Specimen	Web A	Flange B	Lip C	Thickness t	b/t	c/t	Spacing S	P _{FEA}	P _{AISI}	P _{FEA} /P _{AISI}
	mm	mm	mm	mm	-	-	mm	kN	kN	-
BU80-L300	80	36	18	1.20	30	15	75	118.1	136.2	0.87
BU80-L300	80	48	18	1.20	40	15	75	119.65	134.84	0.89
BU80-L300	80	60	18	1.20	50	15	75	114.9	154.7	0.74
BU80-L300	80	72	18	1.20	60	15	75	112.21	128.78	0.87
BU80-L300	80	84	18	1.20	70	15	75	111.36	162.95	0.68
BU80-L300	80	108	18	1.20	90	15	75	106.40	193.38	0.55
BU100-L300	100	40	15	1.00	40	15	75	79.1	106.22	0.74
BU100-L300	100	40	20	1.00	40	20	75	86.38	103.6	0.83
BU100-L300	100	40	25	1.00	40	25	75	87.8	99.02	0.89
BU100-L300	100	40	30	1.00	40	30	75	85.1	95.38	0.89
BU100-L300	100	40	40	1.00	40	40	75	76.88	96.08	0.80
Avg.										0.80
COV										0.15



(a)



(b)

Figure 4-3. Comparison of FEA strength with AISI strength for stub column using (a) material 1 (b) material 2

From the results shown in Table 4-3, Table 4-4 and Figure 4-3 it is clearly visible that AISI code is un-conservative with respect to finite element analysis while predicting the strengths of stub column for all eleven specimens and for both materials which is also reported in [3]. The mean value of P_{FEA}/P_{AISI} is 0.80 for both materials. While coefficient of variation is 0.17 and 0.15 respectively. For first six specimens under material 1 when four specimens have been taken in line with EC and AISI, strength prediction variation is 14%, 9%, 28% and 13% and for other two specimens when b/t ratio is beyond the limit, strength according to FEA is 34% and 46% less than AISI strength. This happens because when b/t ratio is beyond 60 keeping thickness t constant it results in huge flange dimension which is eventually increasing effective area of the section. Effective area is a vital parameter while calculating strength in AISI code but not so important in FEA. Entire scenario is quite similar for material 2. However, for second material with $f_y = 420$ MPa strengths are higher than first material with $f_y = 345$ MPa which is clarified by maximum strength value of 103.59 kN and 119.65 kN for FEA whereas 173.36 kN and 193.38 kN for AISI respectively for material 1 and 2.

For last five specimens where all specimens have been taken in line with EC and AISI, strength according to FEA is 24%, 17%, 11%, 9% and 12% less than AISI strength. Scenario is same for both the materials, nevertheless for second material with $f_y = 420$ MPa strengths are higher than first material having $f_y = 345$ MPa which is clarified by maximum strength value of 77.56 kN and 87.8 kN for FEA while 91.38 kN and 103.6 kN for AISI respectively for material 1 and 2.

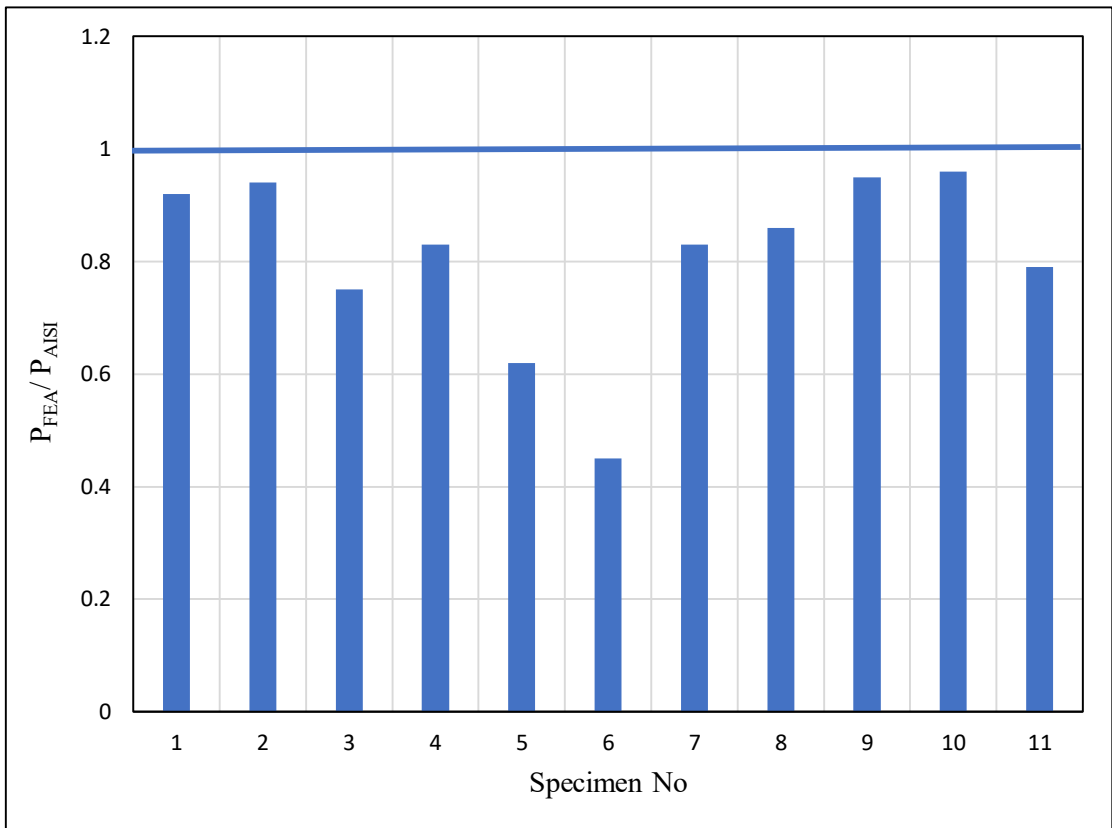
**Table 4-5. Comparison of Axial Capacity obtained from FE Analysis with
AISI Design Guidelines (short - material 1)**

Specimen	Web A	Flange B	Lip C	Thickness t	b/t	c/t	Spacing S	P _{FEA}	P _{AISI}	P _{FEA} /P _{AISI}
	mm	mm	mm	mm	-	-	mm	kN	kN	-
BU80-L700	80	36	18	1.20	30	15	175	102.35	111	0.92
BU80-L700	80	48	18	1.20	40	15	175	103.57	109.69	0.94
BU80-L700	80	60	18	1.20	50	15	175	101.2	135.98	0.75
BU80-L700	80	72	18	1.20	60	15	175	92.07	110.33	0.83
BU80-L700	80	84	18	1.20	70	15	175	83.9	135.7	0.62
BU80-L700	80	108	18	1.20	90	15	175	77.2	172.4	0.45
BU100-L700	100	40	15	1.00	40	15	175	72.06	86.57	0.83
BU100-L700	100	40	20	1.00	40	20	175	74.03	85.69	0.86
BU100-L700	100	40	25	1.00	40	25	175	78.54	82.79	0.95
BU100-L700	100	40	30	1.00	40	30	175	76.80	80.3	0.96
BU100-L700	100	40	40	1.00	40	40	175	64.1	81.49	0.79
Avg.										0.81
COV										0.22

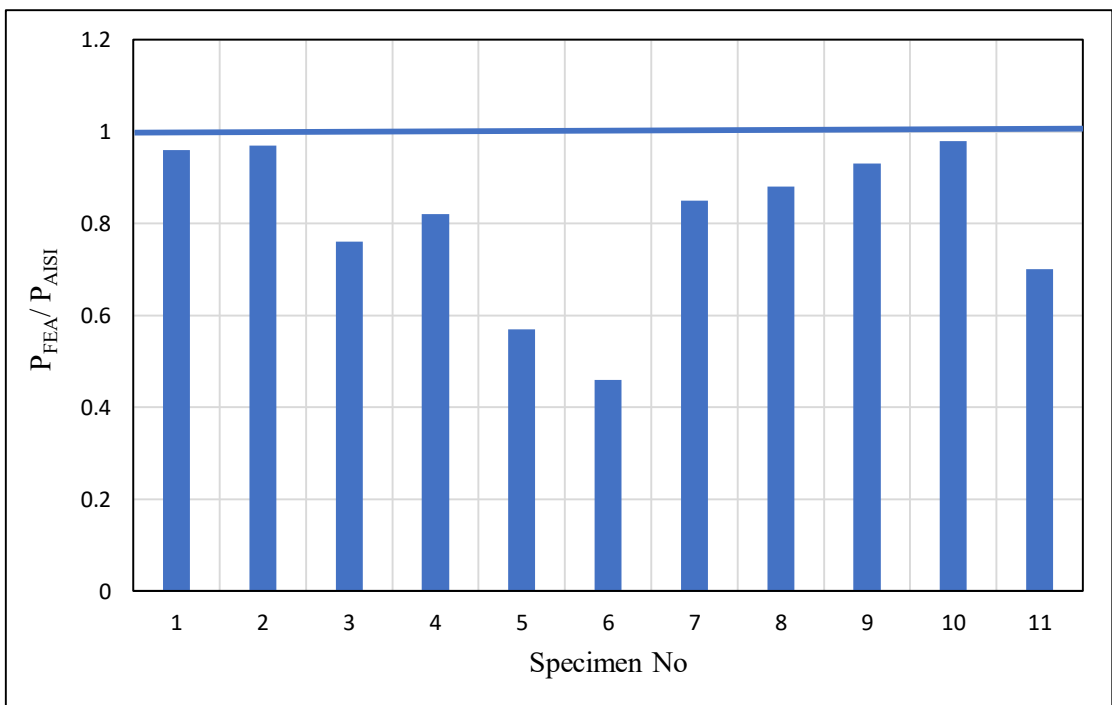
Table 4-6. Comparison of Axial Capacity obtained from FE Analysis with AISI

Design Guidelines (short - material 2)

Specimen	Web A	Flange B	Lip C	Thickness t	b/t	c/t	Spacing S	P _{FEA}	P _{AISI}	P _{FEA} /P _{AISI}
	mm	mm	mm	mm	-	-	mm	kN	kN	-
BU80-L700	80	36	18	1.20	30	15	175	120.1	125.3	0.96
BU80-L700	80	48	18	1.20	40	15	175	119.38	123.58	0.97
BU80-L700	80	60	18	1.20	50	15	175	114.73	151.15	0.76
BU80-L700	80	72	18	1.20	60	15	175	100.78	122.19	0.82
BU80-L700	80	84	18	1.20	70	15	175	92.84	160.86	0.57
BU80-L700	80	108	18	1.20	90	15	175	87.5	191.9	0.46
BU100-L700	100	40	15	1.00	40	15	175	82.65	97.11	0.85
BU100-L700	100	40	20	1.00	40	20	175	84.15	95.92	0.88
BU100-L700	100	40	25	1.00	40	25	175	85.68	92.49	0.93
BU100-L700	100	40	30	1.00	40	30	175	88.1	89.65	0.98
BU100-L700	100	40	40	1.00	40	40	175	70.5	91.01	0.70
Avg.										0.81
COV										0.24



(a)



(b)

Figure 4-4. Comparison of FEA strength with AISI strength for short column using (a) material 1 (b) material 2

Results presented in Table 4-5, Table 4-6 and Figure 4-4 indicates that AISI code is un-conservative with respect to finite element analysis while predicting the strengths of short column for all eleven specimens and all materials which is contradictory with Ting's investigation [3]. The mean value of P_{FEA}/P_{AISI} for short columns is 0.81 for both the materials. While coefficient of variation is 0.22 and 0.24 respectively. For first six specimens where four specimens have been taken in line with Eurocode and AISI and other two are not within the limit, strength prediction variation is 8%, 6%, 25% and 17% for material 1 whereas 4%, 3%, 24% and 18% for material 2 when b/t ratio is within the limit. Column strength according to finite element analysis is 38% and 55% less than strength calculated in accordance with AISI for material 1 whereas 43% and 54% less than for material 2 when b/t ratio is beyond the limit as 70 and 90. The reason of these types of results is explained earlier. Moreover, for second material with $f_y = 420$ MPa strengths are higher than first material with $f_y = 345$ MPa which is clarified by maximum strength value of 103.57 kN and 120.1 kN for FEA whereas 172.4 kN and 191.9 kN for AISI respectively for material 1 and 2.

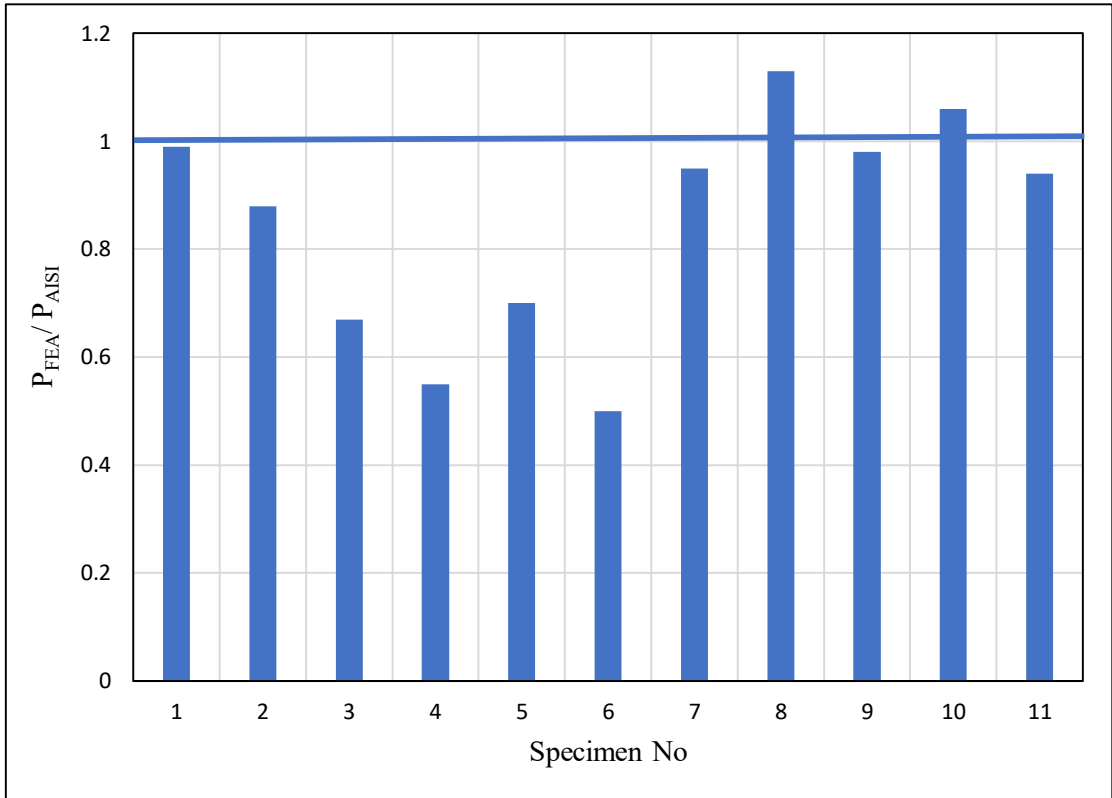
For last five specimens where all specimens have been taken in line with Eurocode and AISI, Column strength according to finite element analysis is 17%, 14%, 5%, 4% and 21% less than strength calculated in accordance with AISI for material 1 whereas strength is 15%, 12%, 7%, 2% and 30% less than for material 2 given l/t ratio is within the limit. Furthermore, for second material with $f_y = 420$ MPa strengths are higher than first material with $f_y = 345$ MPa which is clarified by maximum strength value of 78.54 kN and 88.1 kN for FEA whereas 86.57 kN and 97.11 kN for AISI respectively for material 1 and 2.

**Table 4-7. Comparison of Axial Capacity obtained from FE Analysis with
AISI Design Guidelines (intermediate - material 1)**

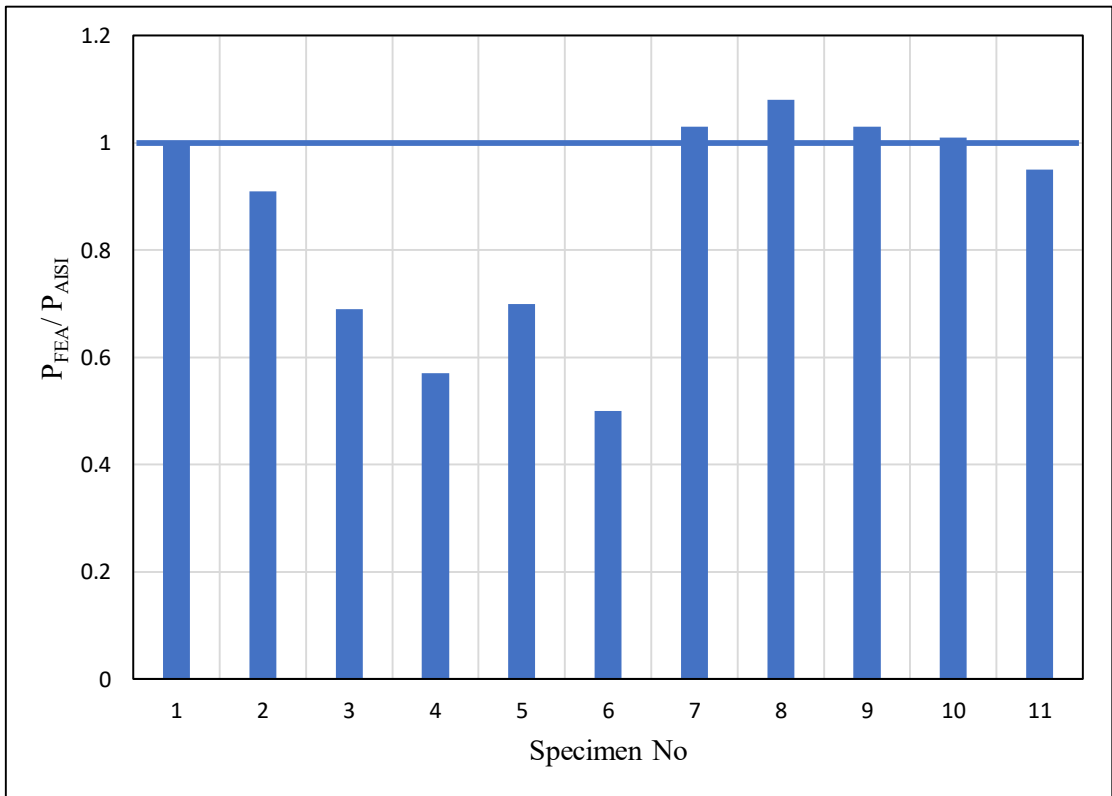
Specimen	Web A	Flange B	Lip C	Thickness t	b/t	c/t	Spacing S	P _{FEA}	P _{AISI}	P _{FEA} /P _{AISI}
	mm	mm	mm	mm	-	-	mm	kN	kN	-
BU80-L1200	80	36	18	1.20	30	15	300	93.23	94.57	0.99
BU80-L1200	80	48	18	1.20	40	15	300	89.84	101.86	0.88
BU80-L1200	80	60	18	1.20	50	15	300	86.34	129.47	0.67
BU80-L1200	80	72	18	1.20	60	15	300	59.20	107.45	0.55
BU80-L1200	80	84	18	1.20	70	15	300	98.9	142.13	0.70
BU80-L1200	80	108	18	1.20	90	15	300	85.32	170.2	0.50
BU100-L1200	100	40	15	1.00	40	15	300	70.47	74.0	0.95
BU100-L1200	100	40	20	1.00	40	20	300	84.46	75.03	1.13
BU100-L1200	100	40	25	1.00	40	25	300	72.17	73.67	0.98
BU100-L1200	100	40	30	1.00	40	30	300	76.47	72.27	1.06
BU100-L1200	100	40	40	1.00	40	40	300	70.1	74.33	0.94
Avg.										0.85
COV										0.28

**Table 4-8. Comparison of Axial Capacity obtained from FE Analysis with
AISI Design Guidelines (intermediate - material 2)**

Specimen	Web A	Flange B	Lip C	Thickness t	b/t	c/t	Spacing S	P _{FEA}	P _{AISI}	P _{FEA} /P _{AISI}
	mm	mm	mm	mm	-	-	mm	kN	kN	-
BU80-L1200	80	36	18	1.20	30	15	300	105.1	105.12	1.00
BU80-L1200	80	48	18	1.20	40	15	300	102.5	113.07	0.91
BU80-L1200	80	60	18	1.20	50	15	300	98.99	143.8	0.69
BU80-L1200	80	72	18	1.20	60	15	300	67.25	118.34	0.57
BU80-L1200	80	84	18	1.20	70	15	300	110.2	157.2	0.70
BU80-L1200	80	108	18	1.20	90	15	300	93.8	189.15	0.50
BU100-L1200	100	40	15	1.00	40	15	300	83.27	80.5	1.03
BU100-L1200	100	40	20	1.00	40	20	300	88.1	81.75	1.08
BU100-L1200	100	40	25	1.00	40	25	300	82.82	80.36	1.03
BU100-L1200	100	40	30	1.00	40	30	300	79.76	78.91	1.01
BU100-L1200	100	40	40	1.00	40	40	300	77.1	81.43	0.95
Avg.										0.86
COV										0.27



(a)



(b)

Figure 4-5. Comparison of FEA strength with AISI strength for intermediate column using (a) material 1 (b) material 2

Results shown in Table 4-7, Table 4-8 and Figure 4-5 specifies that AISI code is un-conservative with respect to finite element analysis while predicting the strengths of intermediate column for all specimens except specimen-8 and specimen-10 under material 1. At material 2 scenario is different as AISI code is conservative with respect to finite element analysis while predicting the strengths for specimen-7, specimen-8 and specimen-9 whereas AISI code is un-conservative for specimen-2, specimen-3, specimen-4, specimen-5, specimen-6 and specimen-11. Strengths are same from AISI and finite element analysis for specimen-1 and specimen-10. The mean value of P_{FEA}/P_{AISI} for intermediate columns is 0.85 and 0.86 respectively for material 1 and 2 with coefficient of variation as 0.28 and 0.27. For first six specimens where four specimens have been taken in line with Eurocode and AISI and other two are not within the limit, strength prediction variation is only 1%, 12%, 33% and 45% for material 1 whereas 0% that means same, 9%, 31% and 43% for material 2 when b/t ratio is within the limit. Column strength according to finite element analysis is 30% and 50% less than strength calculated in accordance with AISI for both the materials when b/t ratio is beyond the limit as 70 and 90. Moreover, for second material with $f_y = 420$ MPa strengths are higher than first material model with $f_y = 345$ MPa which is clarified by maximum strength value of 98.9 kN and 110.2 kN for FEA whereas 170.2 kN and 189.15 kN for AISI respectively for material 1 and 2.

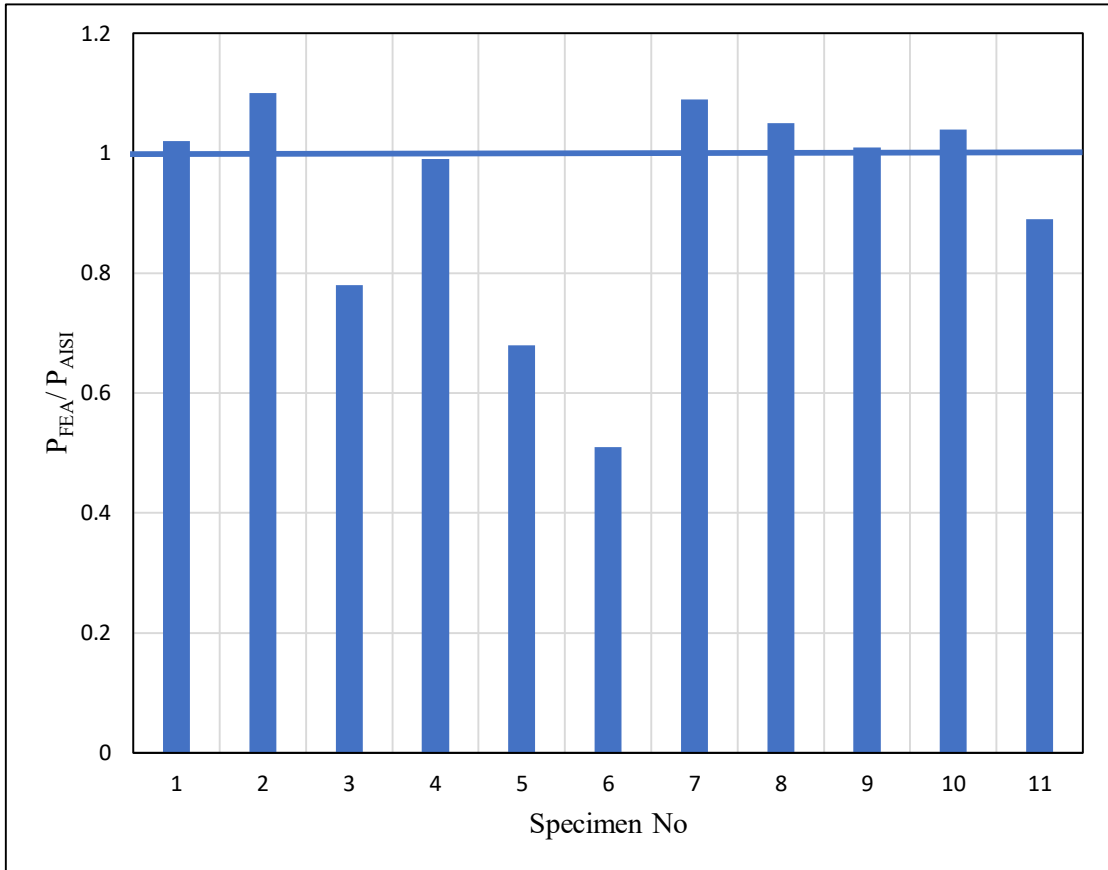
For last five specimens where all specimens have been taken in line with Eurocode and AISI, Column strength according to finite element analysis shows strong agreement with strength calculated in accordance with AISI as variation is 5%, 13%, 2%, 6% and 6% for material 1 which is 3%, 8%, 3%, 1% and 5% for material 2 given l/t ratio is within the limit, Furthermore for second material with $f_y = 420$ MPa strengths are higher than first material with $f_y = 345$ MPa which is clarified by maximum strength value of 84.46 kN and 88.1 kN for FEA while 75.03 kN and 81.75 kN for AISI respectively for material 1 and 2.

**Table 4-9. Comparison of Axial Capacity obtained from FE Analysis with
AISI Design Guidelines (slender - material 1)**

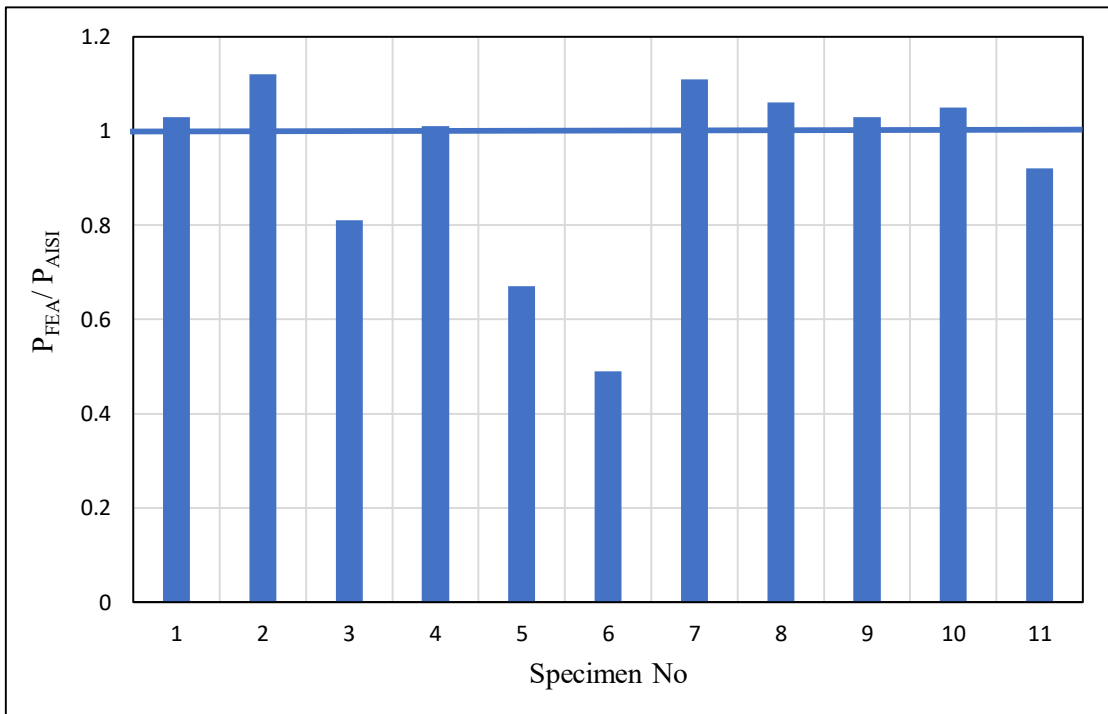
Specimen	Web A	Flange B	Lip C	Thickness t	b/t	c/t	Spacing S	P _{FEA}	P _{AISI}	P _{FEA} /P _{AISI}
	mm	mm	mm	mm	-	-	mm	kN	kN	-
BU80-L2200	80	36	18	1.20	30	15	550	51.1	50.24	1.02
BU80-L2200	80	48	18	1.20	40	15	550	85.47	77.21	1.10
BU80-L2200	80	60	18	1.20	50	15	550	84.8	109.0	0.78
BU80-L2200	80	72	18	1.20	60	15	550	96.28	97.72	0.99
BU80-L2200	80	84	18	1.20	70	15	550	90.18	132.3	0.68
BU80-L2200	80	108	18	1.20	90	15	550	82.25	162.65	0.51
BU100-L2200	100	40	15	1.00	40	15	550	41.2	37.82	1.09
BU100-L2200	100	40	20	1.00	40	20	550	46.3	44.25	1.05
BU100-L2200	100	40	25	1.00	40	25	550	48.3	47.82	1.01
BU100-L2200	100	40	30	1.00	40	30	550	51.1	49.1	1.04
BU100-L2200	100	40	40	1.00	40	40	550	47.42	53.17	0.89
Avg.										0.92
COV										0.23

**Table 4-10. Comparison of Axial Capacity obtained from FE Analysis with
AISI Design Guidelines (slender - material 2)**

Specimen	Web A	Flange B	Lip C	Thickness t	b/t	c/t	Spacing S	P _{FEA}	P _{AISI}	P _{FEA} /P _{AISI}
	mm	mm	mm	mm	-	-	mm	kN	kN	-
BU80-L2200	80	36	18	1.20	30	15	550	51.9	50.24	1.03
BU80-L2200	80	48	18	1.20	40	15	550	91.2	81.36	1.12
BU80-L2200	80	60	18	1.20	50	15	550	95.35	118.18	0.81
BU80-L2200	80	72	18	1.20	60	15	550	107	105.48	1.01
BU80-L2200	80	84	18	1.20	70	15	550	96.76	144.15	0.67
BU80-L2200	80	108	18	1.20	90	15	550	87.62	179.79	0.49
BU100-L2200	100	40	15	1.00	40	15	550	41.9	37.82	1.11
BU100-L2200	100	40	20	1.00	40	20	550	46.9	44.25	1.06
BU100-L2200	100	40	25	1.00	40	25	550	49.05	47.82	1.03
BU100-L2200	100	40	30	1.00	40	30	550	51.79	49.37	1.05
BU100-L2200	100	40	40	1.00	40	40	550	49.98	54.27	0.92
Avg.										0.94
COV										0.24



(a)



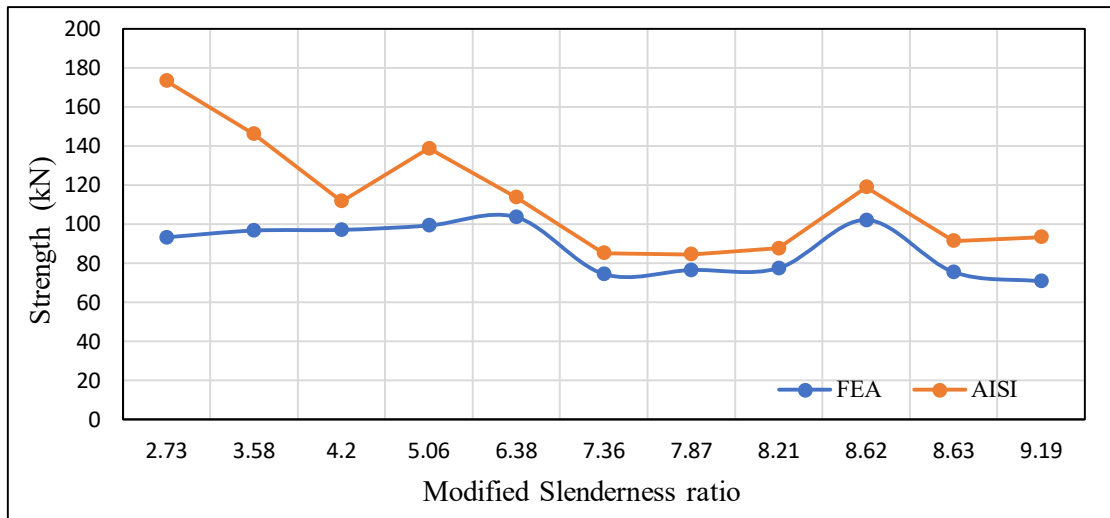
(b)

Figure 4-6. Comparison of FEA strength with AISI strength for slender column using (a) material 1 (b) material 2

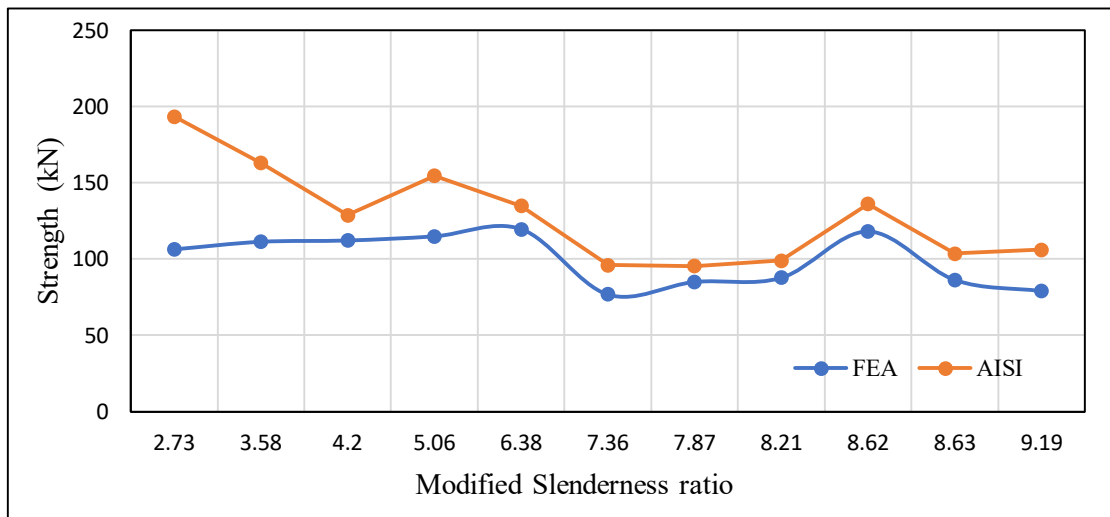
Results represented in Table 4-9, Table 4-10 and Figure 4-6 notifies that AISI code is un-conservative with respect to finite element analysis while predicting the strengths of slender column for specimen-3, specimen-5, specimen-6 and specimen-11 whereas AISI code is conservative or same for other specimens under both the materials. The mean value of P_{FEA}/P_{AISI} for slender columns is 0.92 and 0.94 respectively for material 1 and 2 with coefficient of variation as 0.23 and 0.24. For first six specimens where four specimens have been taken in line with Eurocode and AISI and other two are not within the limit, strength prediction variation is only 2%, 10%, 22% and 1% for material 1 whereas 3%, 12%, 19% and 1% for material 2 when b/t ratio is within the limit. Column strength according to finite element analysis is 32% and 49% less than strength calculated in accordance with AISI for material 1 whereas 33% and 51% for material 2 when b/t ratio is beyond the limit as 70 and 90. Moreover, for second material model with $f_y = 420$ MPa strengths are higher than first material model with $f_y = 345$ MPa which is clarified by maximum strength value of 96.28 kN and 107 kN for FEA whereas 162.65 kN and 179.79 kN for AISI respectively for material 1 and 2.

For last five specimens where all specimens have been taken in line with Eurocode and AISI, Column strength according to finite element analysis shows strong agreement with strength calculated in accordance with AISI as variation is 9%, 5%, 1%, 4% and 11% for material 1 which is 11%, 6%, 3%, 5% and 8% for material 2 given l/t ratio is within the limit, Furthermore ranges of strength values are quite similar for both the materials which is clarified by maximum strength value of 51.1 kN and 51.79 kN for FEA whereas 53.17 kN and 54.27 kN for AISI respectively.

4.1.2 Formulation of Design Guideline and Derivation of Design Curves



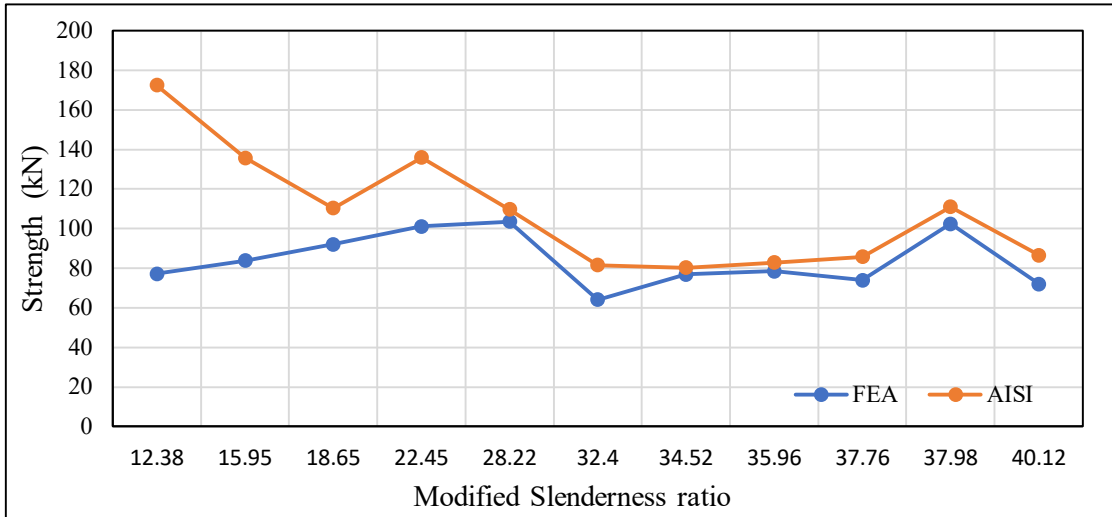
(a)



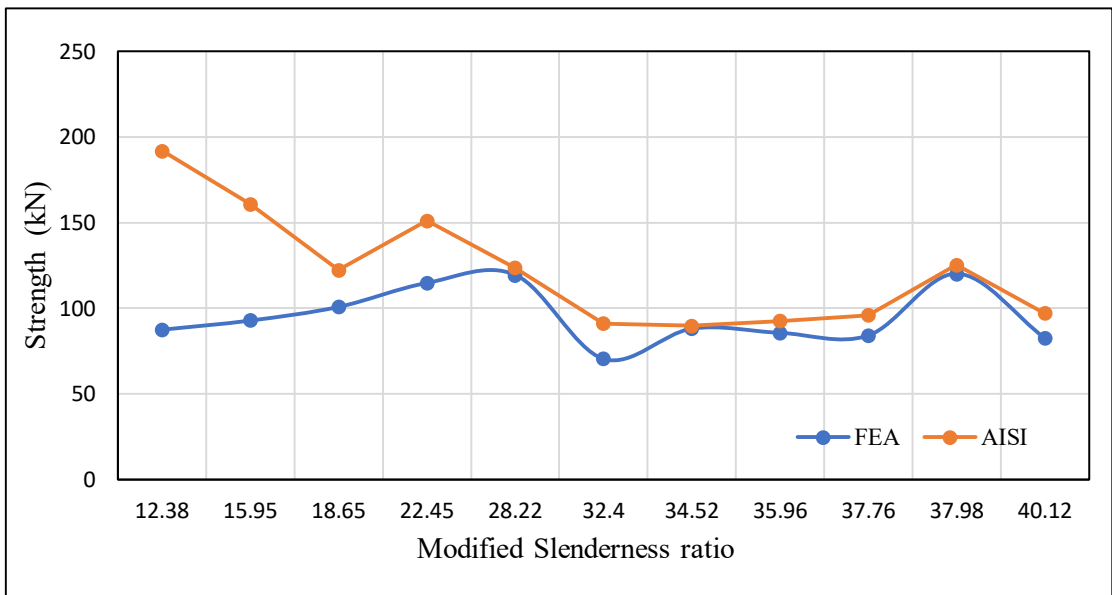
(b)

Figure 4-7. Strength vs Slenderness ratio curve for stub column using (a) material 1 (b) material 2

Figure 4-7 shows the variation of strength calculated from FEA and predicted by AISI and AS/NZ standards against modified slenderness ratio $(Kl/r)_m$ for all eleven specimens of stub column under material 1 and material 2. From the graph it is seen that strengths calculated in accordance with AISI shows strong agreement with finite element model for all specimen except specimen-3, specimen-5 and specimen-6. Scenario is same for both the materials. For these three specimens AISI standard is unconservative with respect to FEM analysis by 28%, 34% and 46% under material 1 and by 26%, 32% and 45% under material 2 having modified slenderness ratio $(Kl/r)_m$ as 5.06, 3.58 and 2.73 respectively.



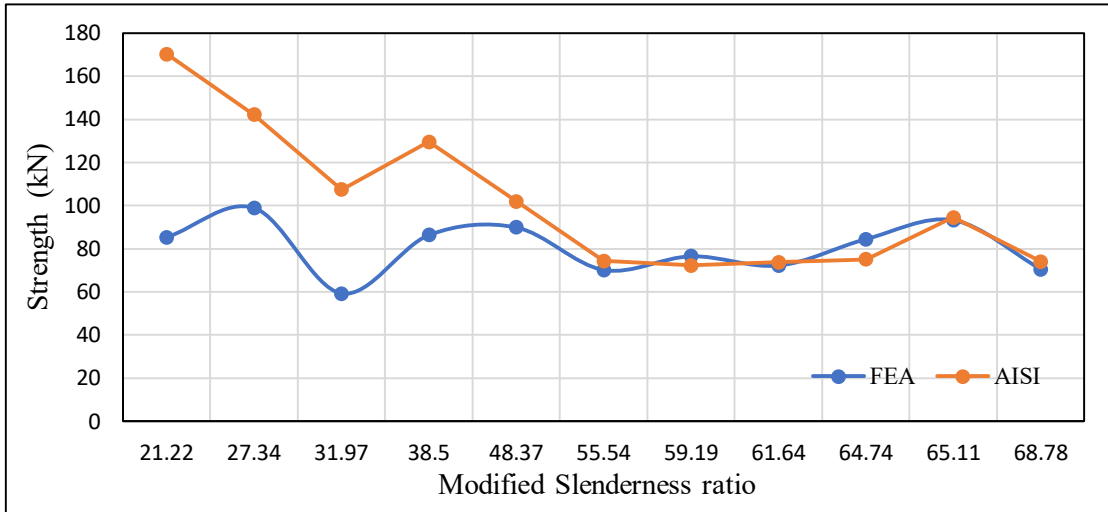
(a)



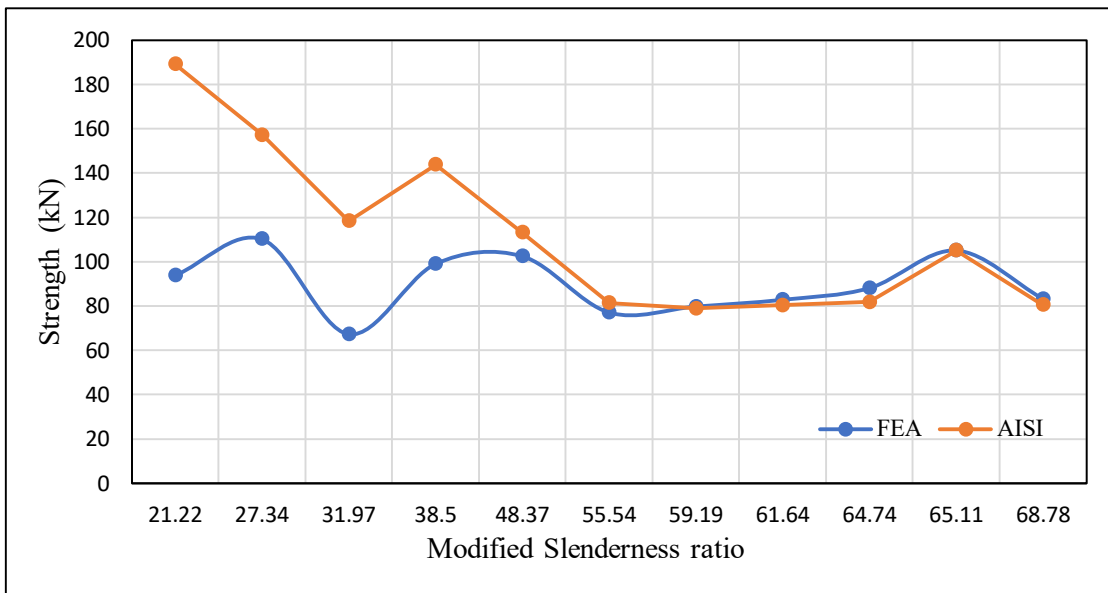
(b)

Figure 4-8. Strength vs Slenderness ratio curve for short column using (a) material 1 (b) material 2

Figure 4-8 shows the variation of strength calculated from FEA and predicted by AISI and AS/NZ standards against modified slenderness ratio $(Kl/r)_m$ for all eleven specimens of short column under material -1 and material -2. From the graph it is seen that strengths calculated in accordance with AISI shows strong agreement with FEA for all specimen except specimen-3, specimen-5 and specimen-6. Scenario is same for both the materials. For these three specimens AISI standard is un-conservative with respect to FEM analysis by 25%, 38% and 55% under material 1 and by 24%, 43% and 54% under material 2 having modified slenderness ratio $(Kl/r)_m$ as 22.45, 15.95 and 12.38 respectively.



(a)

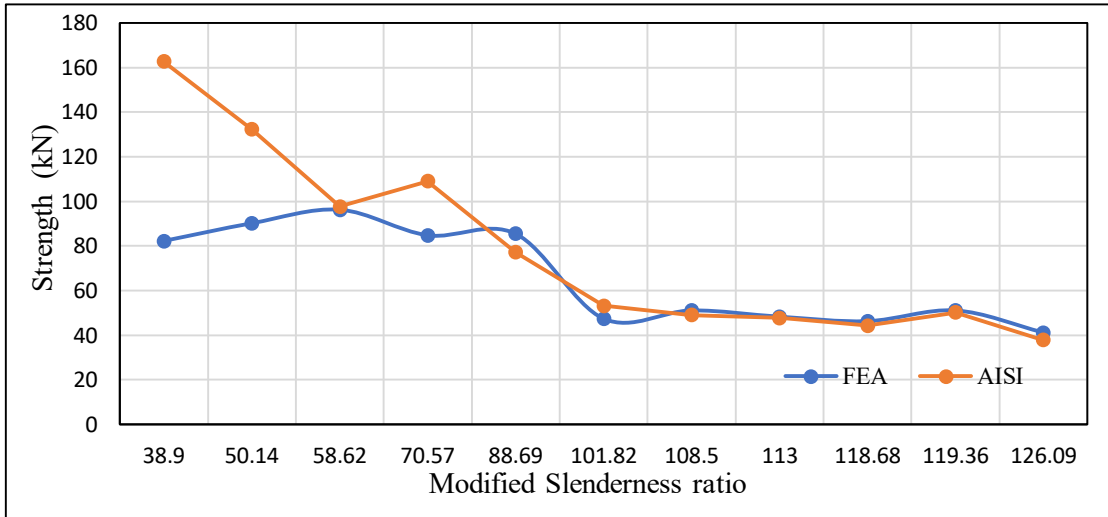


(b)

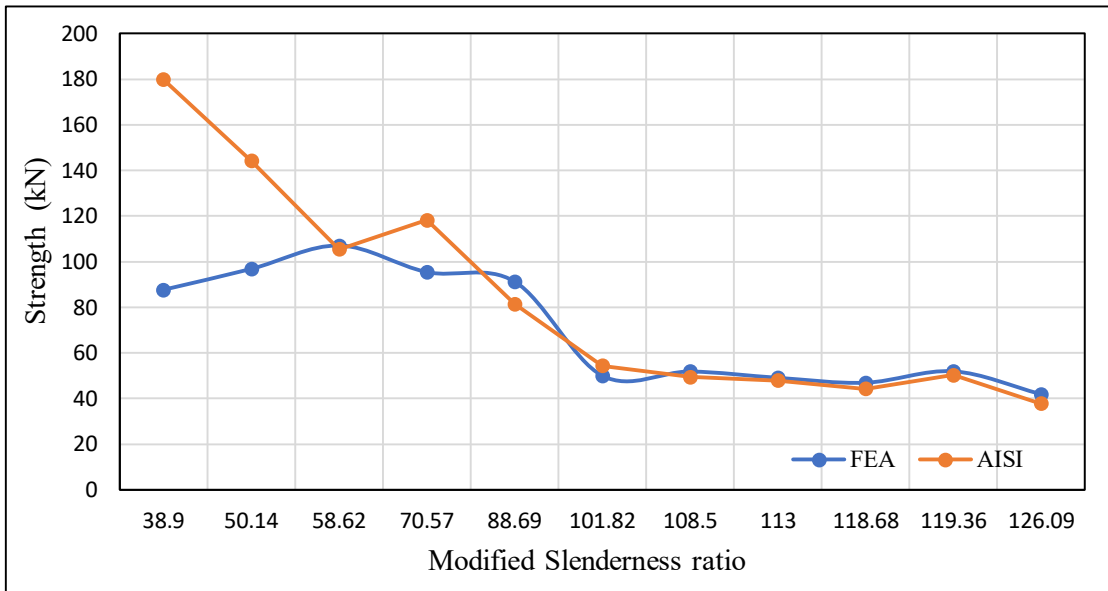
Figure 4-9. Strength vs Slenderness ratio curve for intermediate column using

(a) material 1 (b) material 2

Figure 4-9 shows the variation of strength calculated from FEA and predicted by AISI and AS/NZ standards against modified slenderness ratio $(Kl/r)_m$ for all eleven specimens of intermediate column under material 1 and material 2. From the graph it is seen that strengths calculated in accordance with AISI shows strong agreement with FEA for all specimen except specimen-3, specimen-4, specimen-5 and specimen-6. Scenario is same for both the materials. For these four specimens AISI standard is unconservative with respect to FEM analysis by 33%, 45%, 30% and 50% under material 1 and by 31%, 43%, 30% and 50% under material 2 having modified slenderness ratio $(Kl/r)_m$ as 38.5, 31.97, 27.34 and 21.22 respectively.



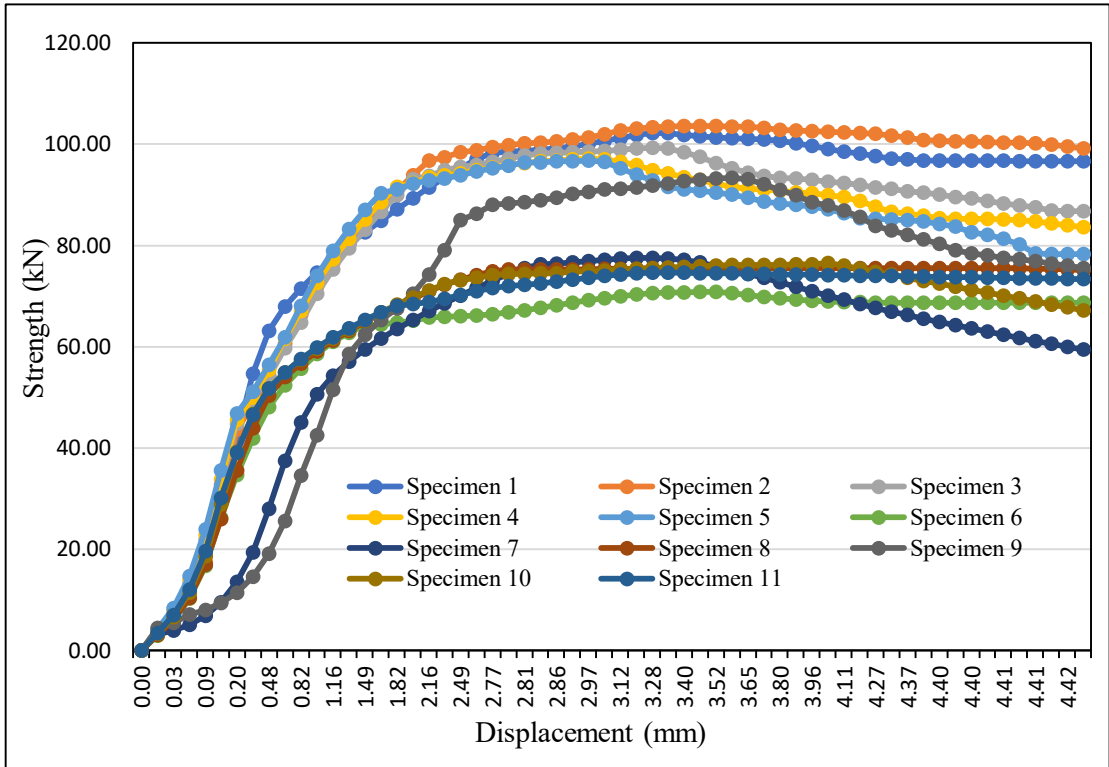
(a)



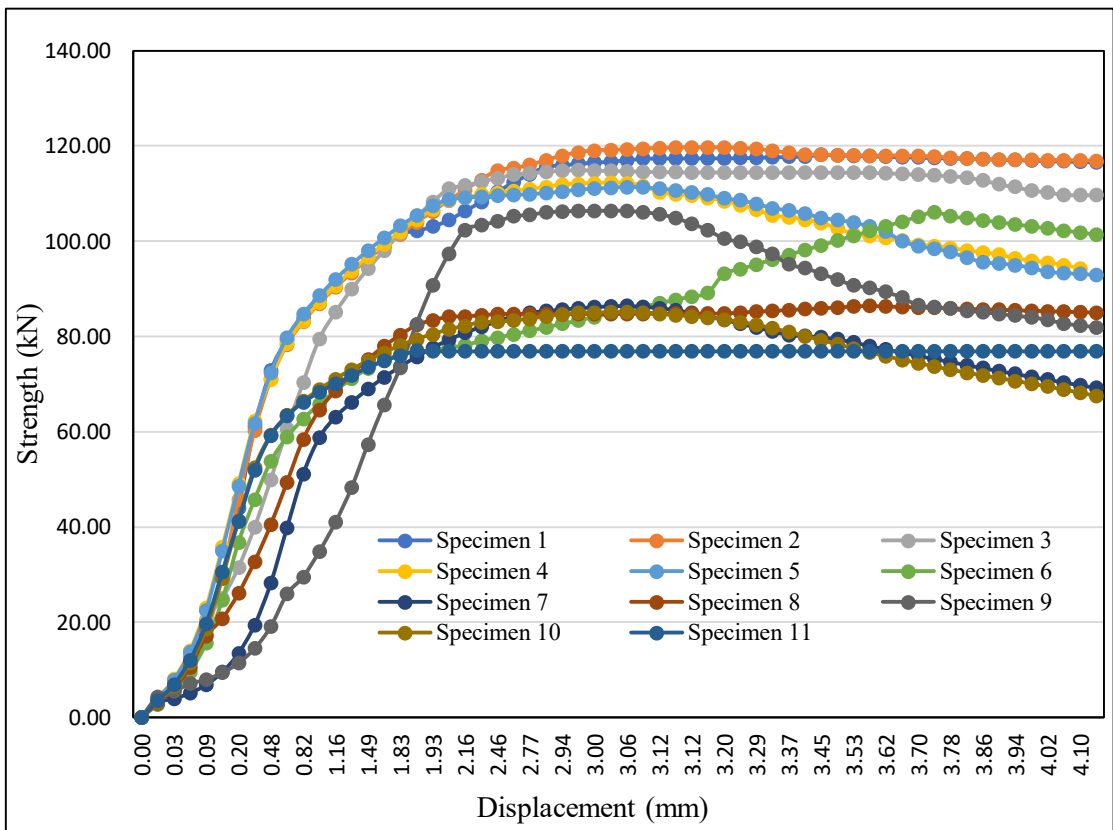
(b)

Figure 4-10. Strength vs Slenderness ratio curve for slender column using (a) material 1 (b) material 2

Figure 4-10 shows the variation of strength calculated from FEA and predicted by AISI and AS/NZ standards against modified slenderness ratio $(Kl/r)_m$ for all eleven specimens of slender column under material 1 and material -2. From the graph it is seen that strengths calculated in accordance with AISI shows strong agreement with FEA for all specimen except specimen-3, specimen-5 and specimen-6. Scenario is same for both the materials. For these three specimens AISI standard is un-conservative with respect to FEM analysis by 22%, 32% and 49% under material 1 and by 19%, 33% and 51% under material 2 having modified slenderness ratio $(Kl/r)_m$ as 70.57, 50.14 and 38.9 respectively.

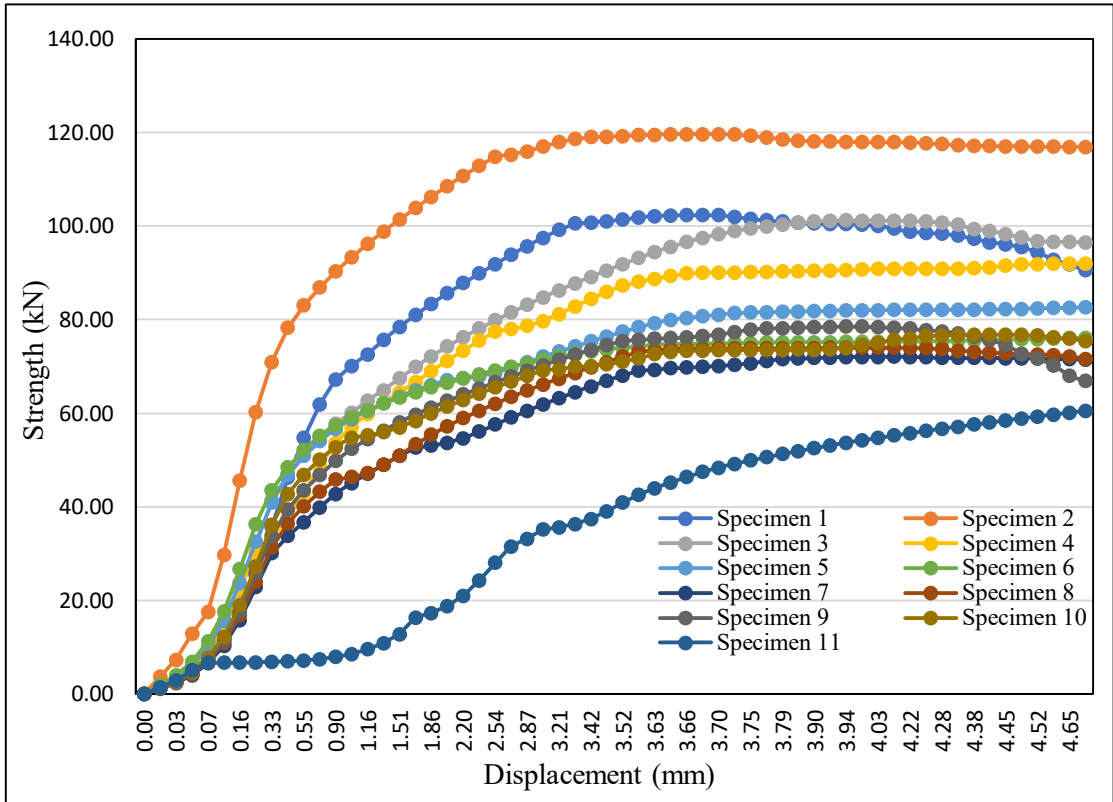


(a)

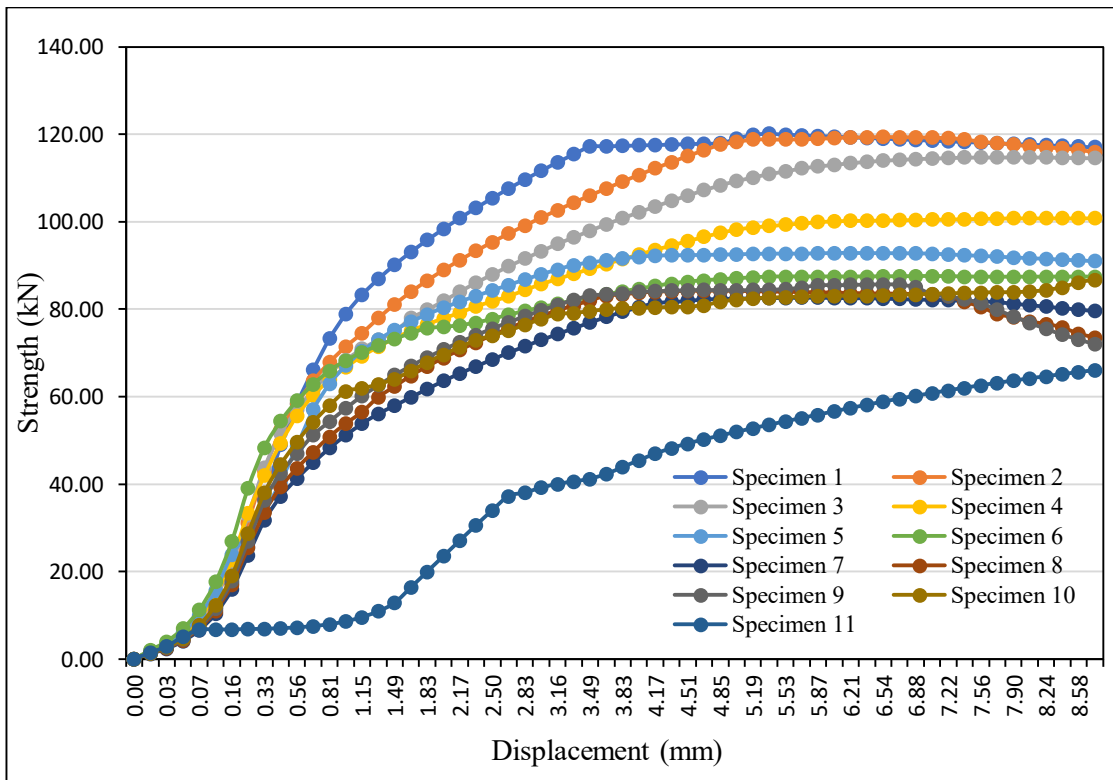


(b)

**Figure 4-11. Strength vs Displacement curve for stub column using (a) material 1
(b) material 2**

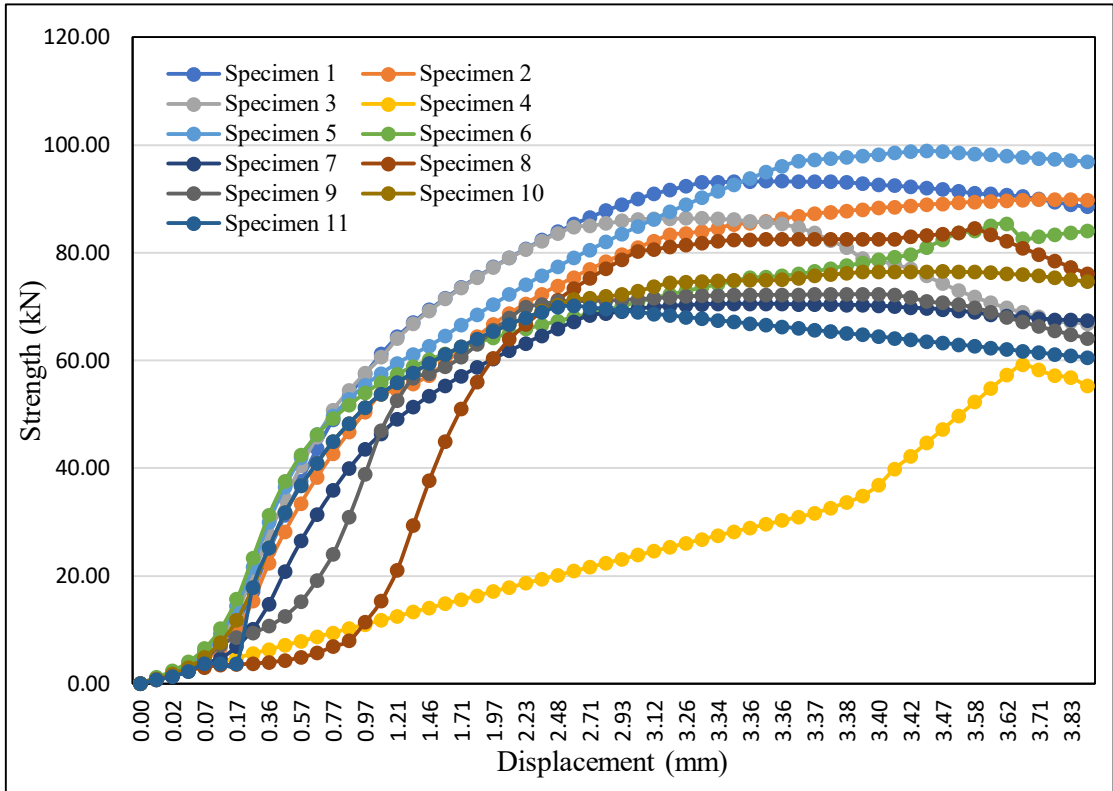


(a)

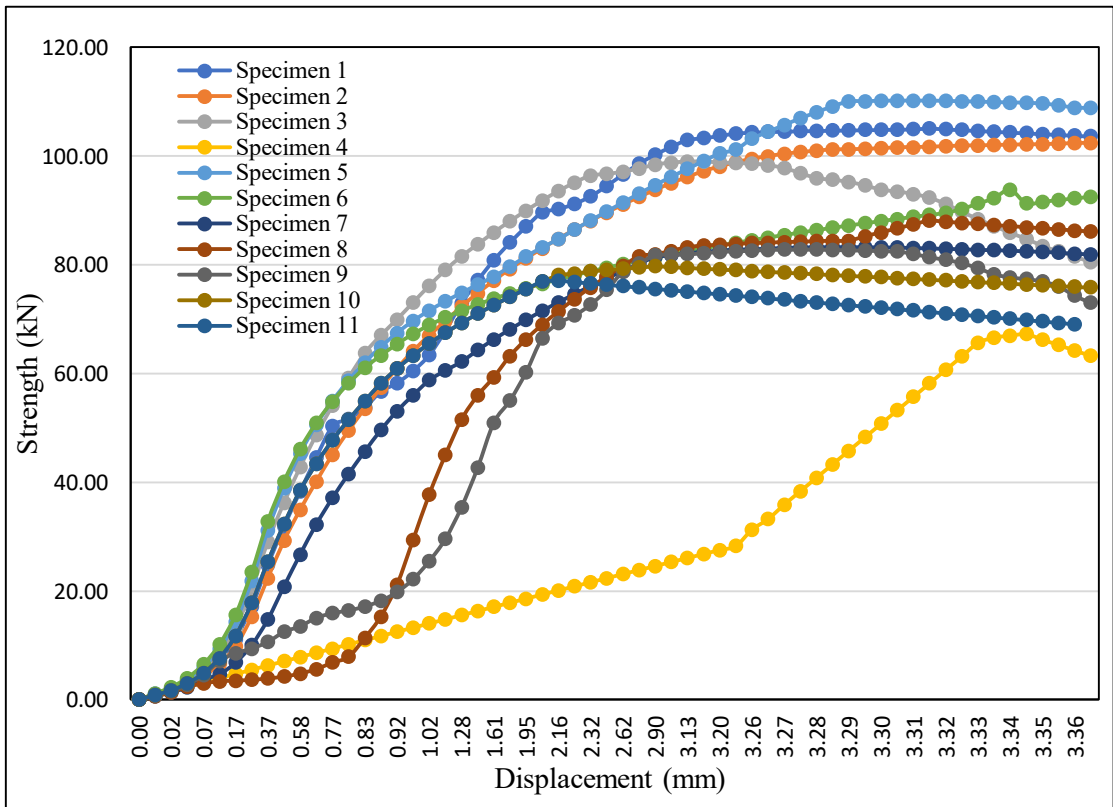


(b)

Figure 4-12. Strength vs Displacement curve for short column using (a) material 1 (b) material 2

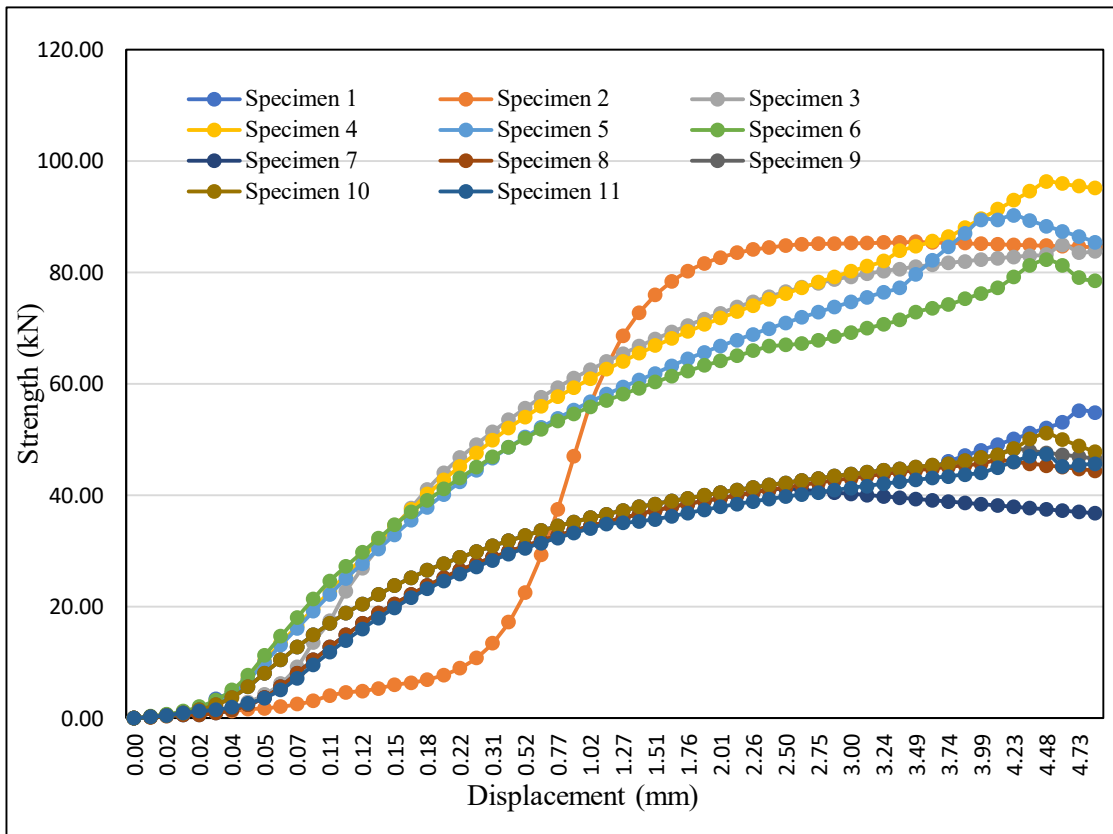


(a)

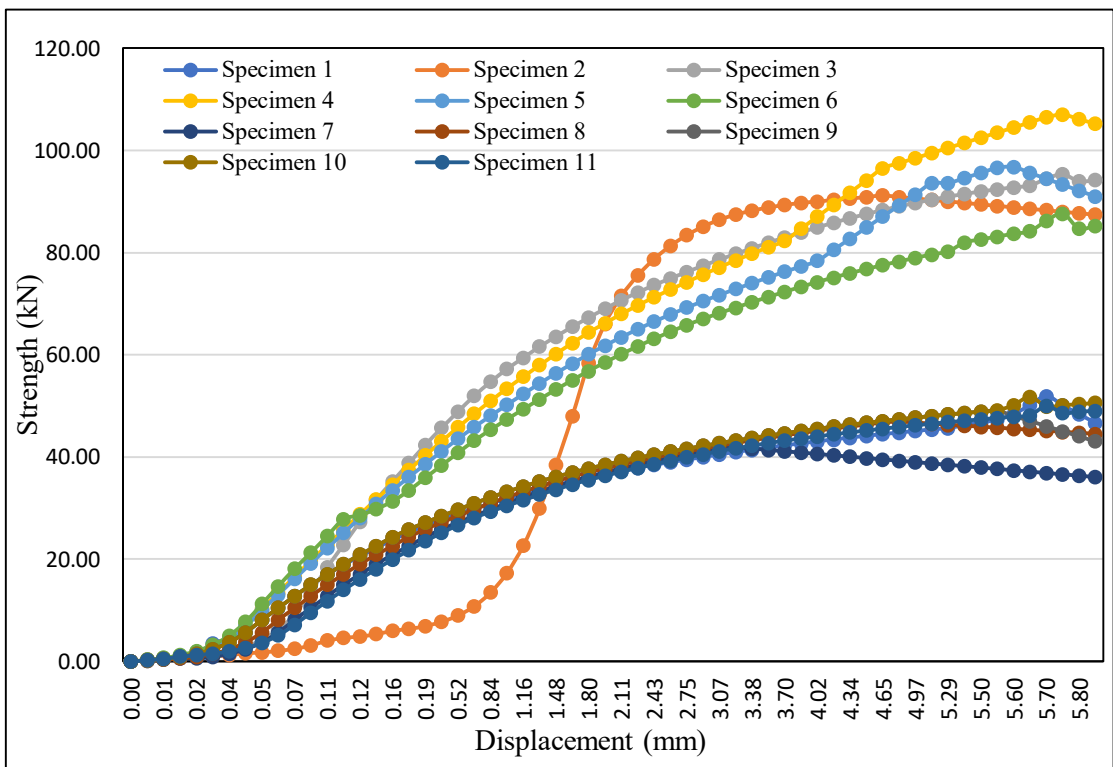


(b)

Figure 4-13. Strength vs Displacement curve for intermediate column using (a) material 1 (b) material 2



(a)



(b)

Figure 4-14. Strength vs Displacement curve for slender column using (a) material 1 (b) material

Figure 4-11 shows the variation of strength against displacement for all eleven specimens of stub column under material 1 and material 2. It can be noted from the graph that under material 1 maximum displacement is 8.03 mm for specimen-11 at strength 73.35 kN and minimum displacement is 2.84 mm for specimen-8 having strength as 81.17 kN whereas under material 2 maximum displacement is 6.36 mm for specimen-9 at strength 81.93 kN and minimum displacement is 1.53 mm for specimen-11 having strength as 76.87 kN.

Figure 4-12 shows the variation of strength against displacement for all eleven specimens of short column under material 1 and material 2. It can be noted from the graph that under material 1 maximum displacement is 5.29 mm for specimen-9 at strength 66.9 kN and minimum displacement is 1.28 mm for specimen-11 having strength as 60.54 kN whereas under material 2 maximum displacement is 8.74 mm for specimen-1 at strength 117.04 kN and minimum displacement is 1.01 mm for specimen-11 having strength as 65.99 kN.

Figure 4-13 shows the variation of strength against displacement for all eleven specimens of intermediate column under material 1 and material 2. It can be noted from the graph that under material 1 maximum displacement is 4.35 mm for specimen-3 at strength 66.8 kN and minimum displacement is 1.45 mm for specimen-4 having strength as 55.2 kN whereas under material 2 maximum displacement is 4.3 mm for specimen-9 at strength 73.03 kN and minimum displacement is 1.29 mm for specimen-4 having strength as 63.25 kN.

Figure 4-14 shows the variation of strength against displacement for all eleven specimens of slender column under material 1 and material 2. It can be noted from the graph that under material 1 maximum displacement is 4.85 mm for specimen-1 at strength 55.16 kN and minimum displacement is 1.29 mm for specimen-11 having strength as 45.64 kN whereas under material 2 maximum displacement is 5.85 mm for specimen-1 at strength 46.64 kN and minimum displacement is 1.34 mm for specimen-11 having strength as 49.05 kN.

A relation between AISI strength and FEA strength using two materials for all four types of columns has been derived by performing linear regression analysis which is represented in Figure 4-15 to Figure 4-18. For stub, short and slender column regression analysis has not been performed for specimen-5 and specimen 6 where b/t ratio was outside the limit stated by AISI as 70 and 90 respectively. For intermediate column analysis has not been performed for specimen-3, specimen-4, specimen-5 and specimen 6 where b/t ratio was 50, 60, 70 and 90 respectively. After analyzing the relationship, a multiplier of AISI design equation for obtaining better strength result is suggested for all types of columns which is presented in Table 4-11.

For stub column the relationship between AISI strength and FEA strength for material 1 is

$$y = 1.1986x - 0.6973 \text{-----(4.1)}$$

here y = AISI strength (kN)

x = FEA strength (kN)

For example, if the design strength of a stub column using material 1 according to AISI guideline is 130 kN then according to the relationship presented above finite element strength will be

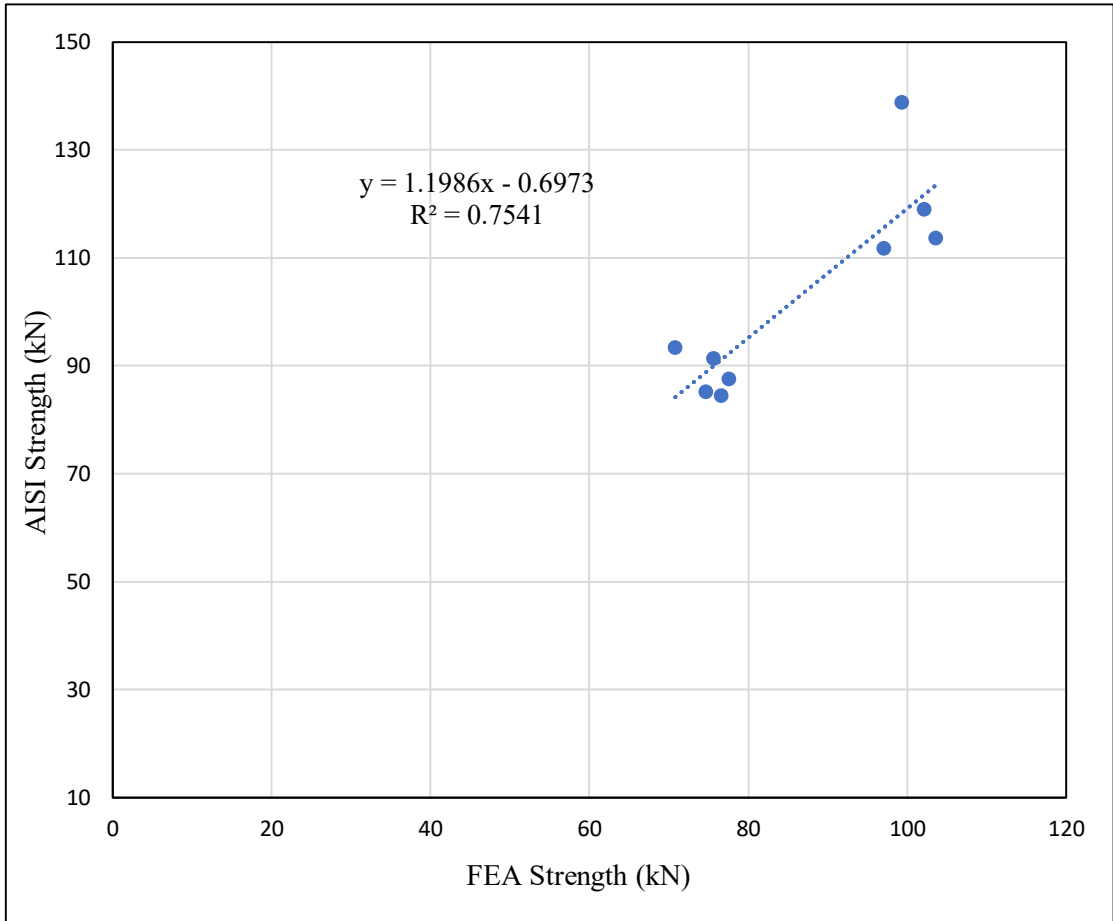
$$130 = 1.1986x - 0.6973$$

$$x = (130 + 0.6973) / 1.1986$$

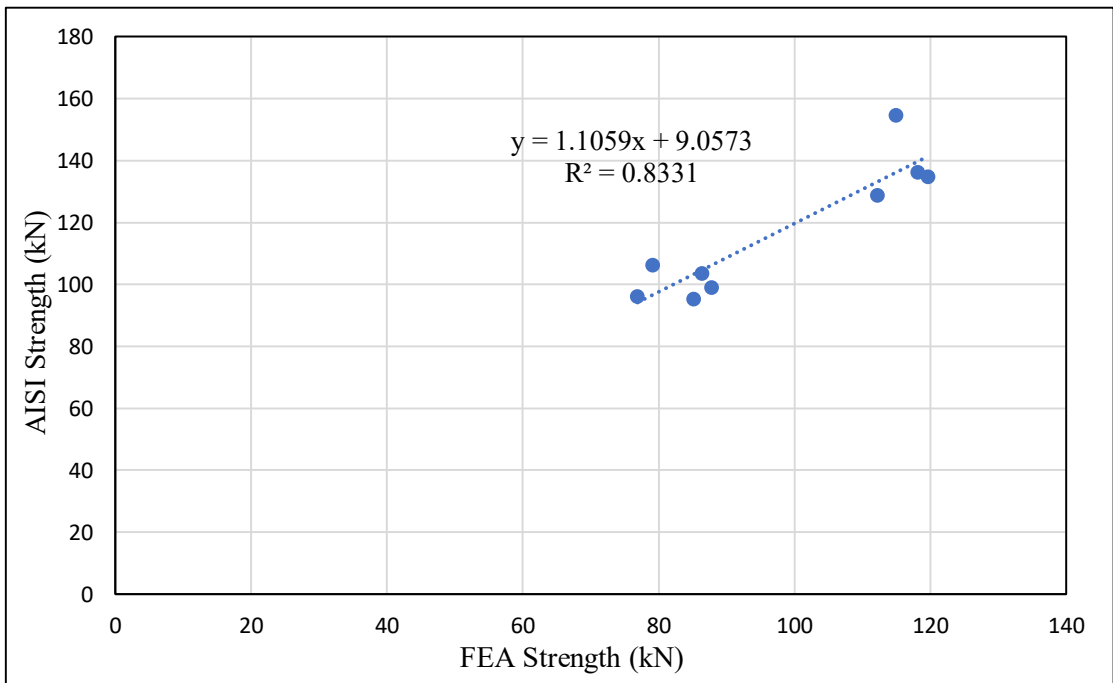
therefore, x = 109.04 kN

Table 4-11. Suggested multiplier of AISI design equation

Type of Column	Material 1	Material 2
Stub	0.84	0.91
Short	0.89	0.99
Intermediate	0.96	0.84
Slender	0.88	0.91

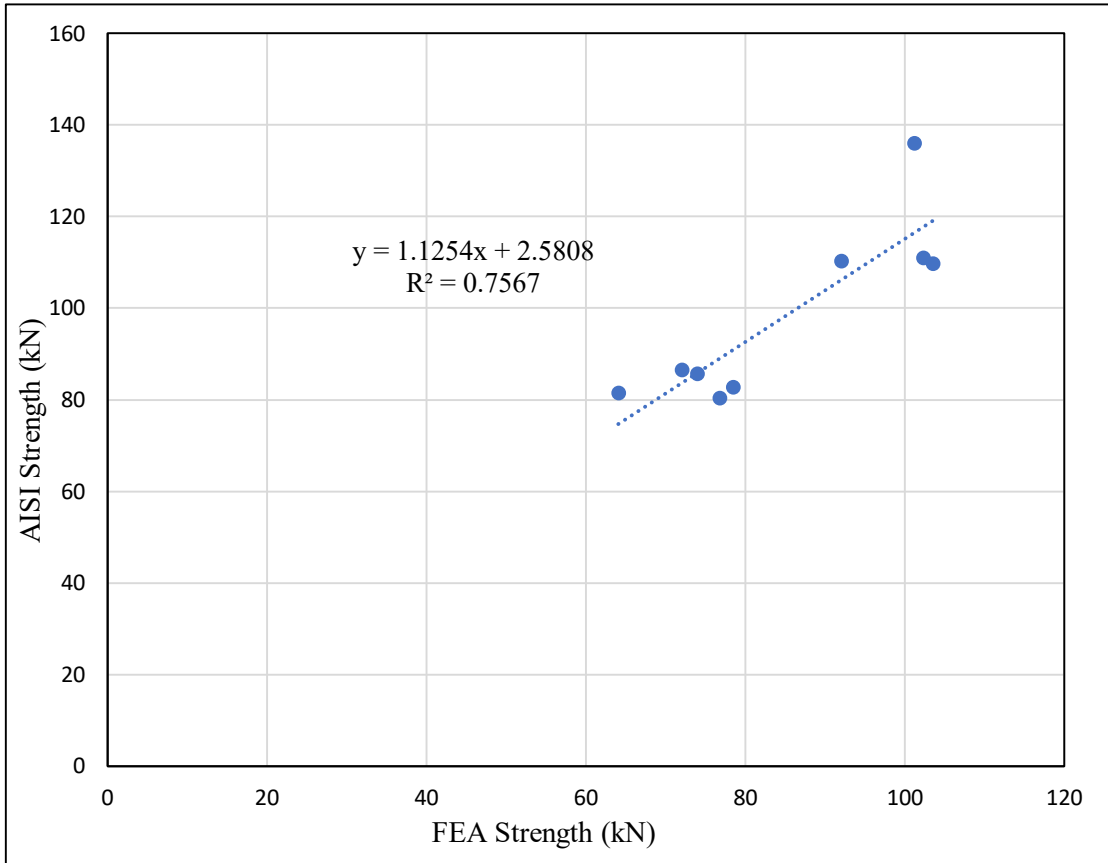


(a)

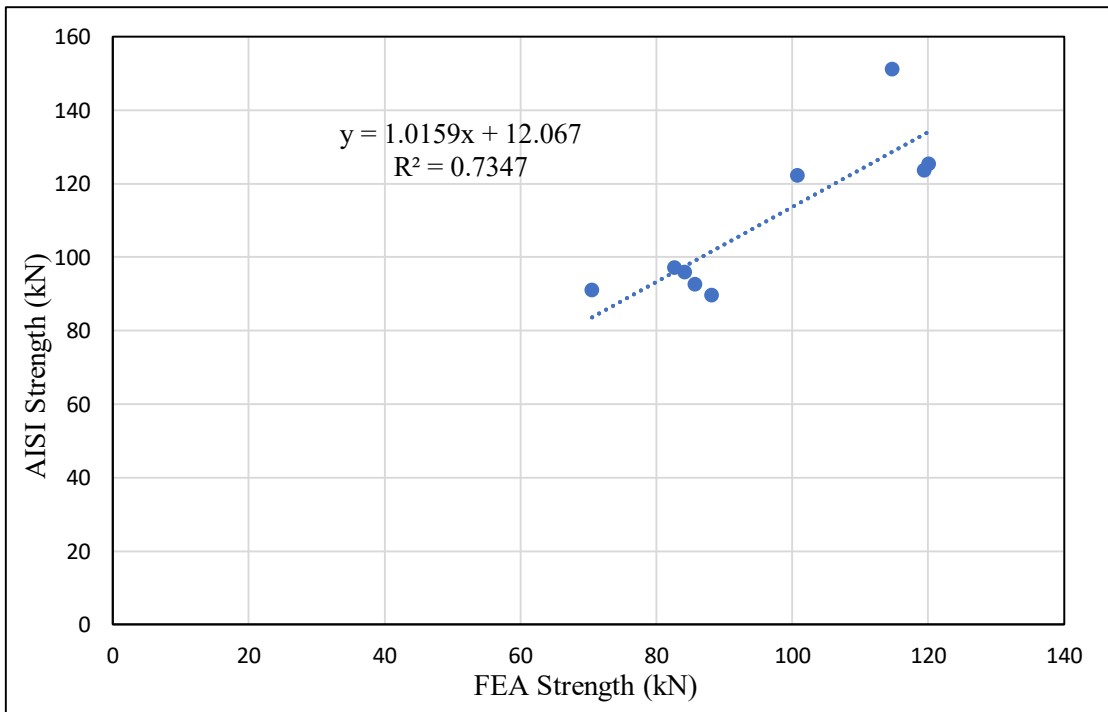


(b)

Figure 4-15. Relation between FEA and AISI strength for stub column using (a) material 1 (b) material 2



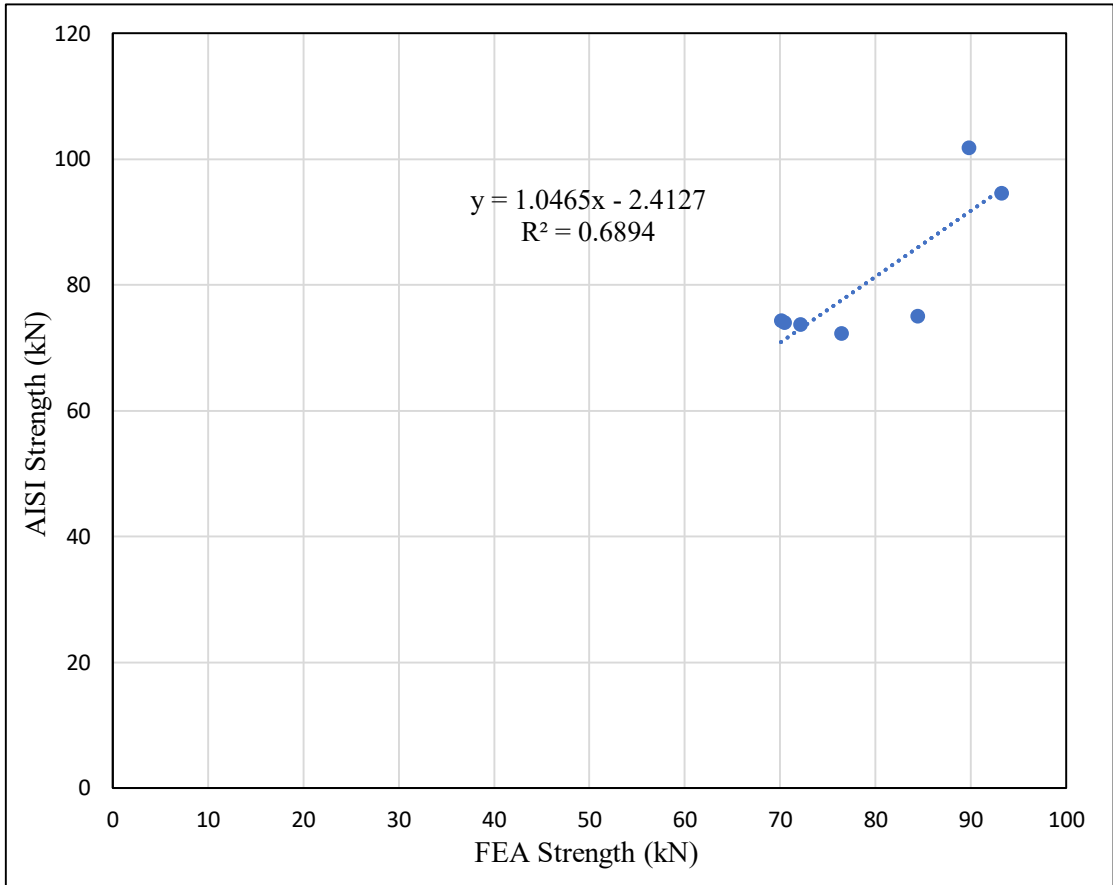
(a)



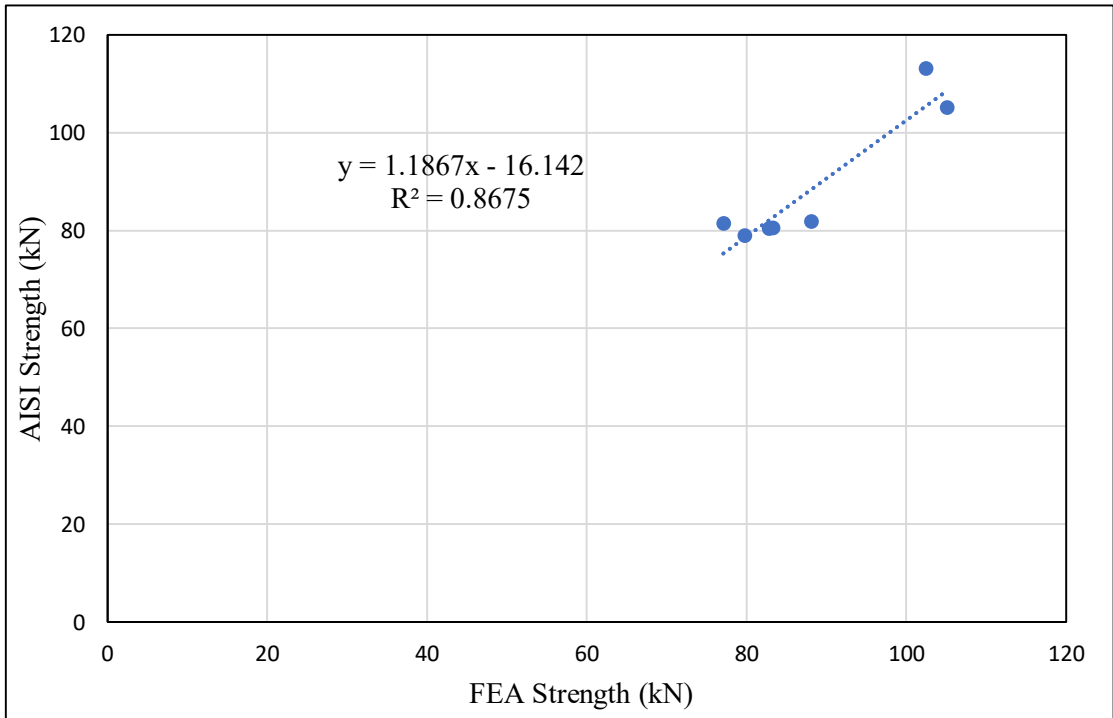
(b)

Figure 4-16. Relation between FEA and AISI strength for short column using

(a) material 1 (b) material 2

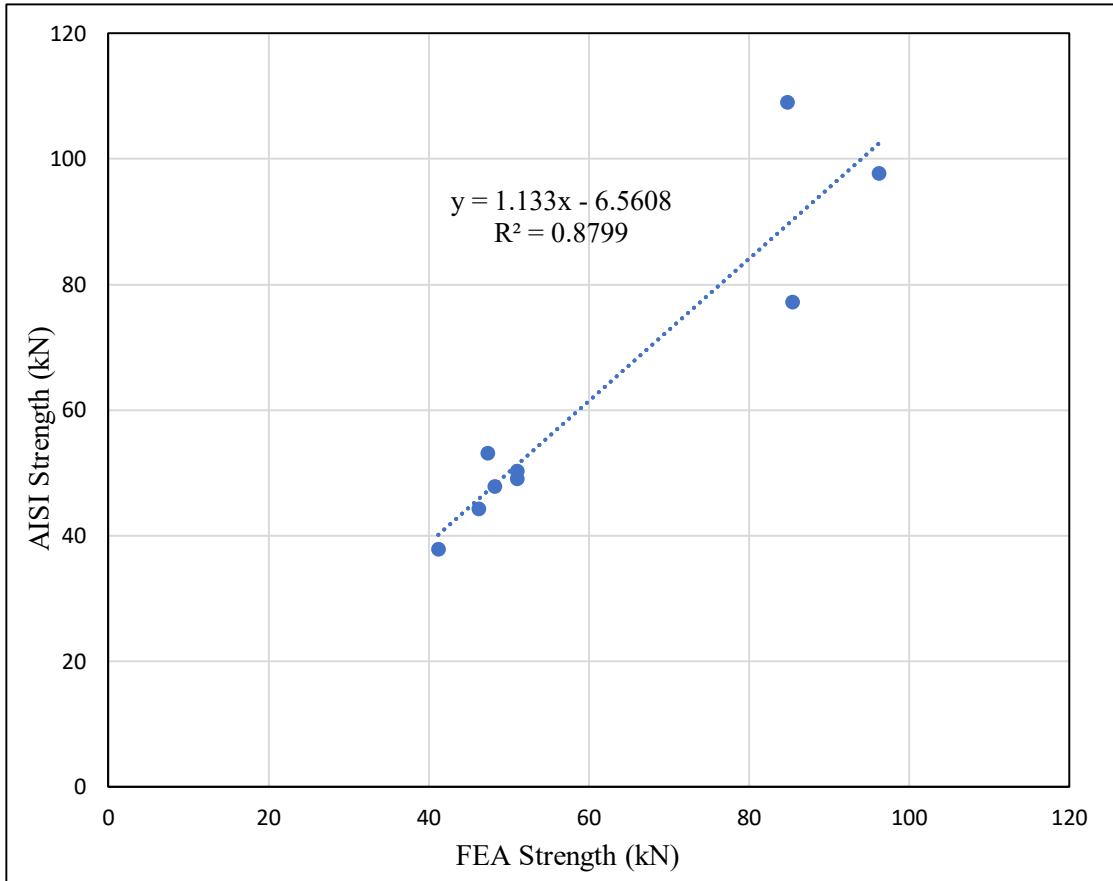


(a)

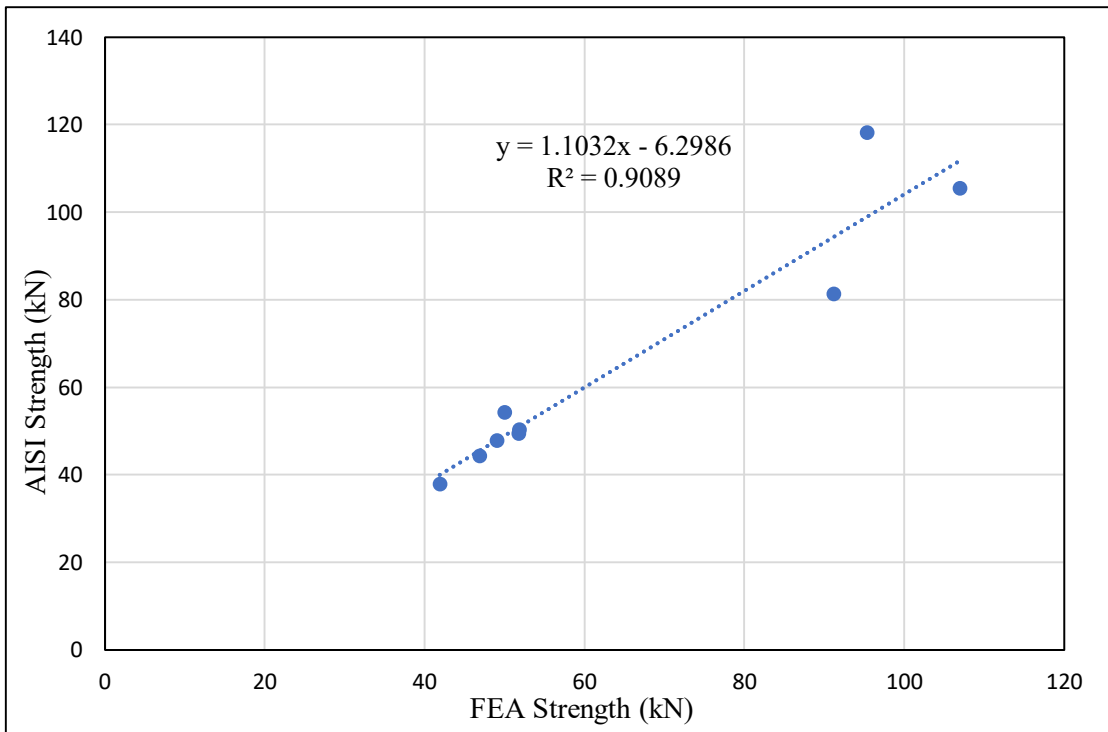


(b)

Figure 4-17. Relation between FEA and AISI strength for intermediate column using (a) material 1 (b) material 2



(a)



(b)

Figure 4-18. Relation between FEA and AISI strength for slender column using (a) material 1 (b) material 2

Chapter 5

CONCLUSIONS AND FUTURE WORKS

5.1 Conclusions

This research presents a finite element investigation on the behavior of back-to-back CFS lipped channels subjected to pure compression.

The major findings of this research are listed below:

i. A nonlinear numerical analysis was conducted while validating the model with test results considering two stress-strain curve. It was concluded that use of full stress-strain curve shows stronger agreement with test results than simplified elastic-plastic model. By using local imperfection as $t/100$ numerical value matches better with test data for stub and short columns. By using global imperfection as $L/100$ numerical value matches better with test data for slender columns whereas the combination of $L/1000$ as global imperfection and $t/10$ as local imperfection works better for intermediate columns.

ii. The axial column strengths calculated from parametric study were compared against the AISI code. Strong agreement is shown between the strength values from FEA and AISI for all lip height-to-thickness ratio (c/t) given it was taken in line with EC and AISI in all cases.

iii. It was concluded that the AISI standard are somewhat un-conservative with respect to experimental results found by previous researchers and finite element results in most of the cases for all four types of columns. Moreover, when width-to-thickness ratio is within the range given by EC and AISI, strength values are close whereas deviation of result is significant when b/t ratio is outside the limit.

iv. A design guideline was proposed by performing linear regression analysis between FEA strength and AISI strength for the data when b/t ratio and c/t ratio is within the limit stated by AISI and after analyzing the relationship, a multiplier of AISI design equation for obtaining better strength result is suggested.

5.2 Recommendations for Future Works

In this research it was assumed that back-to-back built-up CFS lipped channel sections were subjected to pure compression only and the stub column is totally restrained including rotation whereas for short, intermediate and slender column only flexural buckling was considered. Considering all these limitations, the following aspects should be given attention in future.

i. Pure bending, Bi-axial or uniaxial bending can be considered along with pure compression for back-to-back lipped channels.

ii. Not only flexural buckling but also other types of buckling like distortional or any combination of buckling can be considered for short, intermediate and slender column. Effect of buckling about major axis can be checked along with minor axis.

iii. In parametric study if full tensile coupon test data can be used for developing material model then more accurate result will be achieved.

iv. In this research width-to-thickness ratio is taken up to 90 which is limited to 60 in AISI and EC and all lip height-to-thickness ratio is taken within the limit stated by AISI and EC as 50. More finite element models can be analyzed considering width-to-thickness ratio further beyond the limit and lip height-to-thickness ratio can be taken beyond the limit to investigate the effects of these ratios on axial strength of back-to-back lipped channels more accurately.

v. The column strengths calculated from the finite element analyses were compared only against the design strengths calculated in compliance with the AISI which also covers BNBC and AS/NZ standard. Some other design guidelines like Eurocode, Direct Strength Method (DSM), Continuous Strength Method (CSM) can be used for comparing the results to obtain better knowledge about buckling behavior of such channels.

REFERENCES

- [1] Darcy, G., and Mahendran, M. (2008). Development of a new cold-formed steel building system. *Advances in Structural Engineering*, 11(6), 661-677.
- [2] Lawson, R. M., Ogden, R. G., Pedreschi, R., and Popo-Ola, S. O. (2008). Developments of cold-formed steel sections in composite applications for residential buildings. *Advances in structural engineering*, 11(6), 651-660.
- [3] Ting, T. C. H., Roy, K., Lau, H. H., and Lim, J. B. (2018). Effect of screw spacing on behavior of axially loaded back-to-back cold-formed steel built-up channel sections. *Advances in Structural Engineering*, 21(3), 474-487.
- [4] Kechidi, S., Fratamico, D. C., Schafer, B. W., Castro, J. M., and Bourahla, N. (2020). Simulation of screw connected built-up cold-formed steel back-to-back lipped channels under axial compression. *Engineering Structures*, 206, 110109.
- [5] American Iron Steel Institute (2016). North American specification for the design of cold formed steel structural members. Washington, D.C. (United States): AISI S100.
- [6] Standards Australia (2005), Cold-Formed Steel Structures; AS/NZS 4600:2005, Standards Australia / Standards New Zealand.
- [7] American Institute of Steel Construction (2010). Specification for structural steel buildings. Chicago (IL, United States): AISC 360.
- [8] Roy, K., Lau, H. H., and Lim, J. B. (2019). Finite element modelling of back-to-back built-up cold-formed stainless-steel lipped channels under axial compression. *Steel Compos. Struct*, 33(1), 37-66.
- [9] ABAQUS (2014), Version 6.13-1, SIMULIA, Providence, RI, USA.
- [10] Build Steel, <https://buildsteel.org/why-steel/cold-formed-steel-101/what-is-cold-formed-steel-framing>.
- [11] Cold formed steel, https://en.wikipedia.org/wiki/Cold-formed_steel.
- [12] Cold formed section, <https://www.exportersindia.com/ranflex-metals-company5491163/cold-formed-section-3611412.htm>.

- [13] Ye, Z. M., Kettle, R. J., Li, L. Y., and Schafer, B. W. (2002). Buckling behavior of cold-formed zed-purlins partially restrained by steel sheeting. *Thin-walled structures*, 40(10), 853-864.
- [14] Zhou, X. H., and Shi, Y. (2011). Flexural strength evaluation for cold-formed steel lip-reinforced built-up I-beams. *Advances in Structural Engineering*, 14(4), 597-611.
- [15] Silvestre, N., and Camotim, D. (2004). Distortional buckling formulae for cold-formed steel C and Z-section members: Part I—derivation. *Thin-walled structures*, 42(11), 1567-1597.
- [16] Young, B., and Ellobody, E. (2005). Buckling analysis of cold-formed steel lipped angle columns. *Journal of structural engineering*, 131(10), 1570-1579.
- [17] Zhou, W., and Jiang, L. (2017). Distortional buckling of cold-formed lipped channel columns subjected to axial compression. *Steel and Composite Structures*, 23(3), 331-338.
- [18] Roy, K., Ting, T. C. H., Lau, H. H., and Lim, J. B. (2018, November). Effect of thickness on the behaviour of axially loaded back-to-back cold-formed steel built-up channel sections-Experimental and numerical investigation. In *Structures* (Vol. 16, pp. 327-346). Elsevier.
- [19] Roy, K., Ting, T. C. H., Lau, H. H., and Lim, J. B. (2018). Nonlinear behaviour of back-to-back gapped built-up cold-formed steel channel sections under compression. *Journal of Constructional Steel Research*, 147, 257-276.
- [20] Roy, K., Ting, T. C. H., Lau, H. H., and Lim, J. B. (2018). Experimental investigation into the behavior of back-to-back gapped built-up cold-formed steel channel sections under compression.
- [21] Roy, K., Ting, T.C.H. Lau, H.H. and Lim, J.B.P. (2018, August). “Experimental Investigation into the Behaviour of Axially Loaded Back-to-back Cold-formed Steel Built-up Channel Sections”, *Proceedings of International Conference on the ‘Trends and Recent Advances in Civil Engineering-TRACE- 2018’*, Noida, Uttar Pradesh, India.
- [22] Roy, K., Ting, T.C.H. Lau, H.H. and Lim, J.B.P. (2018, August). “Finite Element Modelling of Back-to-back Built-up Cold-formed Steel Channel Columns under Compression”, *Proceedings of International Conference on the ‘Trends and Recent Advances in Civil Engineering-TRACE-2018’*, Noida, Uttar Pradesh, India.
- [23] Fratamico, D. C., Torabian, S., Rasmussen, K. J., and Schafer, B. W. (2016). Experimental investigation of the effect of screw fastener spacing on the local and distortional buckling behavior of built-up cold-formed steel columns.

- [24] Stone, T. A., and LaBoube, R. A. (2005). Behavior of cold-formed steel built-up I-sections. *Thin-Walled Structures*, 43(12), 1805-1817.
- [25] Zhang, J. H., and Young, B. (2012). Compression tests of cold-formed steel I-shaped open sections with edge and web stiffeners. *Thin-Walled Structures*, 52, 1-11.
- [26] Young, B., and Chen, J. (2008). Design of cold-formed steel built-up closed sections with intermediate stiffeners. *Journal of Structural Engineering*, 134(5), 727-737.
- [27] Anbarasu, M., and Ashraf, M. (2016). Behaviour and design of cold-formed lean duplex stainless steel lipped channel columns. *Thin-walled structures*, 104, 106-115.
- [28] Becque, J., Lecce, M., and Rasmussen, K. J. (2008). The direct strength method for stainless steel compression members. *Journal of Constructional Steel Research*, 64(11), 1231-1238.
- [29] Anwar-Us-Saadat, M., Ahmed, S., and Ashraf, M. (2015, January). Behavior of stainless steel lipped channel sections subjected to eccentric compression. In *ISEC 2015-8th International Structural Engineering and Construction Conference: Implementing Innovative Ideas in Structural Engineering and Project Management* (pp. 131-136). ISEC Press.
- [30] Anbarasu, M., Kanagarasu, K., and Sukumar, S. (2015). Investigation on the behaviour and strength of cold-formed steel web stiffened built-up battened columns. *Materials and Structures*, 48(12), 4029-4038.
- [31] Dabaon, M., Ellobody, E., and Ramzy, K. (2015). Nonlinear behaviour of built-up cold-formed steel section battened columns. *Journal of Constructional Steel Research*, 110, 16-28.
- [32] Whittle, J., and Ramseyer, C. (2009). Buckling capacities of axially loaded, cold-formed, built-up C-channels. *Thin-Walled Structures*, 47(2), 190-201.
- [33] Piyawat, K., Ramseyer, C., and Kang, T. H. K. (2013). Development of an axial load capacity equation for doubly symmetric built-up cold-formed sections. *Journal of Structural Engineering*, 139(12), 04013008.
- [34] Aslani, F., and Goel, S. C. (1991). An analytical criterion for buckling strength of built-up compression members. *Eng J*, 28(4), 159-168.
- [35] Reyes, W., and Guzmán, A. (2011). Evaluation of the slenderness ratio in built-up cold-formed box sections. *Journal of Constructional Steel Research*, 67(6), 929-935.

- [36] Biggs, K. A., Ramseyer, C., Ree, S., and Kang, T. H. K. (2015). Experimental testing of cold-formed built-up members in pure compression. *Steel and Composite Structures*, 18(6), 1331-1351.
- [37] BNBC (2020), "Bangladesh National Building Code". Dhaka.
- [38] Anwar-Us-Saadat, M., Ashraf, M., and Ahmed, S. (2016). Behaviour and design of stainless steel slender cross-sections subjected to combined loading. *Thin-Walled Structures*, 104, 225-237.
- [39] Ahmed, S., and Ashraf, M. (2015, January). Compression capacity of slender stainless steel cross-sections. In *ISEC 2015-8th International Structural Engineering and Construction Conference: Implementing Innovative Ideas in Structural Engineering and Project Management* (pp. 119-124). ISEC Press.
- [40] CEN, E. (2006). 1-5: 2006-Eurocode 3: Design of steel structures-Part 1-5: Plated structural elements. *Brussels: European Committee for Standardization*.
- [41] Ahmed, S., Ashraf, M., and Anwar-Us-Saadat, M. (2016). The continuous strength method for slender stainless steel cross-sections. *Thin-Walled Structures*, 107, 362-376.
- [42] Roy, K., Ting, T. C. H., Lau, H. H., and Lim, J. B. (2018). Nonlinear behavior of axially loaded back-to-back built-up cold-formed steel un-lipped channel sections. *Steel and Composite Structures*, 28(2), 233-250.
- [43] Gardner, L., and Yun, X. (2018). Description of stress-strain curves for cold-formed steels. *Construction and Building Materials*, 189, 527-538.
- [44] Gardner, L., and Ashraf, M. (2006). Structural design for non-linear metallic materials. *Engineering structures*, 28(6), 926-934.
- [45] Gardner, L., and Nethercot, D. A. (2004). Numerical modeling of stainless steel structural components—a consistent approach. *Journal of Structural Engineering*, 130(10), 1586-1601.
- [46] Ashraf, M., Gardner, L., and Nethercot, D. A. (2004). Numerical modelling of the static response of stainless steel sections. *stainless steel*, 1, 1-4401.
- [47] Ashraf, M., Gardner, L., and Nethercot, D. A. (2006). Finite element modelling of structural stainless steel cross-sections. *Thin-walled structures*, 44(10), 1048-1062.
- [48] Cruise, R. B., and Gardner, L. (2008). Strength enhancements induced during cold forming of stainless steel sections. *Journal of constructional steel research*, 64(11), 1310-1316.

- [49] Kechidi, S., Fratamico, D. C., Schafer, B. W., Castro, J. M., and Bourahla, N. (2020). Simulation of screw connected built-up cold-formed steel back-to-back lipped channels under axial compression. *Engineering Structures*, 206, 110109.